

KU, PEIJIA, Ph.D. Effects of Forest Fires on Mercury Biogeochemical Cycling in Terrestrial and Aquatic Ecosystems (2020)
Directed by Dr. Martin Tsz-Ki Tsui. 144 pp.

Mercury (Hg), a persistent and toxic element, is largely stored in forests including forest canopy and surface soils. Therefore, forest disturbances such as wildfires (natural) and prescribed fires (anthropogenic, forest management practice) would interfere with Hg storage in forests and its export to downstream aquatic environment where is a hotspot for methylmercury (MeHg) production by the anaerobic bacteria. Although the two types of forest fires are different in intensity, frequency and duration, earlier studies have shown both forest fires increased Hg emissions from the vegetation and surface soils, shifting forests from “Hg sinks” to “Hg sources”. However, little is known about the Hg reactivity and bioavailability in the burned materials on the forest floor, and its transport pattern to the downstream watersheds.

Part I of this dissertation work (chapter II) examined Hg content, origin, reactivity, bioavailability in wildfire ash and potential effects of ash on Hg fate in the downstream aquatic ecosystems. It has been demonstrated that ash samples generated from two recent northern California wildfires contained measurable but highly variable Hg, most of which were shown by stable Hg isotopic compositions to be derived from vegetation, not from the atmospheric Hg deposition. Ash samples had a highly variable fraction of Hg in recalcitrant forms (0-75 %), and this recalcitrant Hg pool appeared to be associated with the black carbon fraction in ash. Importantly, ash could strongly sequester aqueous inorganic Hg and result in low methylation potential in the aquatic environment.

Part II of this dissertation work (chapter III) showed Hg dynamic export in three controlled-field-observation studies, including wildfire-burned watersheds and prescribed-fire-burned watersheds. During the two-year monitoring study in the wildfire-burned watersheds in northern California, highly elevated total Hg (THg) input, mainly driven by total suspended solids (TSS), was observed in the burned watersheds compared to the unburned watershed, especially in the first year following the wildfire, with rapid recovery in the second year. In contrast, much less Hg and TSS exports were observed in stream water in both the prescribed-fire-burned (pile burning) watersheds in northern California (Sagehen Experimental Forest) and the prescribed-fire-burned (broadcast burning) watersheds (Santee Experimental Forest) in South Carolina following the prescribed fires. Particulate Hg (PHg) dominated in the wildfire-burned watersheds Hg export while dissolved Hg (DHg) dominated in the prescribed-burned watersheds. Dissolved organic carbon (DOC), other than TSS, was the main driver carrying DHg contributing to the THg export in the prescribed-fire-burned watersheds in the present study.

This dissertation work showed alterations in the biogeochemical pool of Hg in wildfire ash materials in post-burn landscapes, as well as the post-burn hydrological responses of Hg transport by wildfires and prescribed fires. Regarding the Hg export to the downstream environment, prescribed fires result in lower input than the wildfires. This work increases our understanding of Hg biogeochemical cycling by natural and anthropogenic forest fires and provided evidence and suggestions to resources managers in forest management agencies and fishery consumption advisories.

EFFECTS OF FOREST FIRES ON MERCURY BIOGEOCHEMICAL CYCLING IN
TERRESTRIAL AND AQUATIC ECOSYSTEMS

by

Peijia Ku

A Dissertation Submitted to
the Faculty of The Graduate School at
The University of North Carolina at Greensboro
in Partial Fulfillment
of the Requirements for the Degree
Doctor of Philosophy

Greensboro
2020

Approved by

Committee Chair

© 2020 Peijia Ku

APPROVAL PAGE

This dissertation written by Peijia Ku has been approved by the following committee of the Faculty of The Graduate School at The University of North Carolina at Greensboro.

Committee Chair _____

Committee Members _____

Date of Acceptance by Committee

Date of Final Oral Examination

ACKNOWLEDGEMENTS

I would like to express my whole-heart gratitude to my advisor Dr. Martin Tsz-Ki Tsui for his patience and considerate help during my Ph.D. study at UNCG. He trained me all the lab techniques and also gave me numerous guidance on the study and life in the United States when I first came here. He always gave tremendous patience to solve the problems and tried his best to help. I am so grateful to have him as my advisor. I would also like to thank my committee members, Drs. Anne E. Hershey and Gideon Wasserberg in the Department of Biology and Dr. Dan Royall in the Department of Geography for their consistent guidance and support over the past 5 years, for their time and help in the meetings and classes.

There is no way to finish all the projects without our collaborators in the different projects, including Dr. Alex Chow, Dr. Huan Chen, Dr. Hamed Majidzadeh, Dr. Mahmut Selim Ersan, Dr. Troy Mason Farmer, Mr. Hunter Robinson *et al.* at Clemson University, Dr. Randy Dahlgren at UC Davis, Dr. Joel Blum at the University of Michigan, Dr. Tham C. Hoang at Loyola University Chicago, Dr. Carl Trettin, Dr. Devendra Amatya, Mr. Charles A. Harrison at U.S. Forest Service for providing the resources and help to do the sampling and analyses. I also want to thank the people at Sagehen Creek Field Station for providing us the site information and access to the field. I appreciate Ms. Julie A. Arnold at U.S. Forest Service for her consistent help in field sampling at Santee Experimental Forest watersheds, and Dr. Troy Farmer as well as his undergraduate research group (Clemson University) for biota sampling. I thank Mr. Marcus Johnson (University of Michigan) for his expert assistance in stable mercury isotope analysis in the present study.

Moreover, thanks to my dear labmates, Yener Ulus, Kristina Morales, Hanhan Li, you're my great help in the lab. Also many thanks to my previous labmates Glenn Woerndle, Chris Hylton, Dr. Songnian Liu and Dr. Xiangping Nie for their help and training in my early lab working time. Many thanks to UNC-Greensboro Biology family for your help and support during the past 5 years.

I am grateful for the financial support for my Ph.D. study including fundings from the National Science Foundation, National Institute of Food and Agriculture, ICMGP travel award, AGU travel award, UNC-Greensboro O'Brien Field award, UNC-Greensboro Biology Graduate Research awards, and the Teaching Assistantship from UNC-Greensboro Graduate School and Department of Biology.

Last but not the least, great thanks to my dear friends and all my family members for your supporting and accompanying me during my Ph.D. study. Thank you very much for bringing me so much happiness, warmness, and love in my life and helping me go through so many difficult times during my Ph.D. study abroad.

TABLE OF CONTENTS

	Page
LIST OF TABLES	vii
LIST OF FIGURES	viii
CHAPTER	
I. INTRODUCTION	1
1.1 Background	1
1.1.1 Forest Fires.....	1
1.1.2 Mercury Biogeochemical Cycling in Forest Ecosystems	4
1.2 Research Focus	8
1.3 Significance of this Research.....	11
1.4 Research Objectives.....	12
1.5 References.....	13
II. ORIGIN, REACTIVITY, AND BIOAVAILABILITY OF MERCURY IN WILDFIRE-BURNED MATERIALS.....	19
2.1 Introduction.....	19
2.2 Materials and Methods.....	22
2.2.1 Sample Collection.....	22
2.2.2 Ash Characterization and Organic Carbon Composition.....	23
2.2.3 Total Hg and Recalcitrant Hg Analyses.....	25
2.2.4 Estimation of Hg Volatilization in Ash Samples	28
2.2.5 Stabl Hg Isotope Analysis.....	29
2.2.6 Testing Sorption Capability of Hg by Wildfire Ash	32
2.2.7 Examining Bioavailability of Hg in Ash during Incubation	33
2.2.8 Statistical Analysis.....	36
2.3 Results and Discussion	36
2.3.1 Chemical Properties and Hg Content of Ash.....	36
2.3.2 Extent of Hg Volatilization upon Burning.....	38
2.3.3 Isotopic Composition and Source Analysis of Hg in Ash.....	39
2.3.4 Experimental Investigation of Hg Sorption by Wildfire Ash	41

2.3.5 Bioavailability of Ash-associated Hg under Sealed Incubation	42
2.3.6 Implications for Hg Biogeochemical Cycles	44
2.4 References	46
2.5 Figures	54
2.6 Tables	67
III. HYDROLOGICAL TRANSPORT OF MERCURY FROM WILDFIRE- BURNED AND PRESCRIBED FIRE-BURNED FORESTS	75
3.1 Introduction	75
3.2 Materials and Methods	80
3.2.1 Site Description and Sample Collection	80
3.2.2 Sample Processing and Analyses	85
3.2.3 Stream Discharge	88
3.2.4 Hg Loading Calculations	89
3.2.5 Statistical Analysis	90
3.3 Results and Discussion	90
3.3.1 Impacts of Wildfires on Hg Export	90
3.3.2 Impacts of Prescribed Fire (Pile Burning) on Hg Export	99
3.3.3 Impacts of Prescribed Fire (Broadcast Burning) on Hg Export	102
3.3.4 Comparison of the Impacts by Wildfires and Prescribed Fires on Hg Export	108
3.4 References	112
3.5 Figures	117
3.6 Tables	134
IV. GENERAL DISCUSSION	137
4.1 References	142
4.2 Figures	144

LIST OF TABLES

	Page
Table S2.1. Summary of Wildfire Site Characteristics and Sampling Information	67
Table S2.2. Physicochemical Properties of the Samples	68
Table S2.3. Estimated Hg Volatilization	70
Table S2.4. Stable Hg Isotope Compositions	71
Table S2.5. Sorption of Ash towards Aqueous and Gaseous Hg.....	72
Table S2.6. Results of Sealed Incubation Experiment after 4-weeks	73
Table S2.7. Results of Sealed Incubation Experiment after 12-weeks	74
Table 3.1. Reference and Wildfire-burned Watersheds Information.....	134
Table 3.2. Groundwater and Surface Water at WS80 and WS77	135
Table S3.1. Analytical Methods and Minimum Reporting Levels	136

LIST OF FIGURES

	Page
Figure 2.1. Properties and Hg in Ash and Unburned Litter	54
Figure 2.2. Relationships between LOI, ArH and Recalcitrant Hg	55
Figure 2.3. Estimation of Hg Volatilization.....	56
Figure 2.4. Isotopic Composition of Hg in Unburned Forest Litter and Ash	57
Figure 2.5. Ash Sorption Properties towards Aqueous and Gaseous Hg.....	58
Figure 2.6. Dissolved Hg and MeHg in the Incubation Experiment	59
Figure S2.1. Picture of Ash Samples	60
Figure S2.2. Relationship between LOI and ArH.....	61
Figure S2.3. Relationship between Hg Isotopic Compositions and LOI, ArH Content	62
Figure S2.4. Physicochemical Properties Data in the Incubation Experiment	63
Figure S2.5. Variations of Dissolved Hg and MeHg in the Incubation Experiment	64
Figure S2.6. Role of Ash-ArH in Hg Release in the Incubation Experiment.....	65
Figure S2.7. Role of LOI in Dissolved Hg and MeHg in the Incubation Experiment	66
Figure 3.1. Site Map of the Wildfire-burned Watersheds.....	117
Figure 3.2. Site Map of Sagehen Experimental Forest by Pile Burning.....	118
Figure 3.3. Site Map of Santee Experimental Forest by Broadcast Burning.....	119
Figure 3.4. Variations of TSS and Hg in the Unburned and Burned Watersheds	120
Figure 3.5. Variations of DOC, SUVA ₂₅₄ , and DHg in the Unburned and Burned Watersheds.....	121

Figure 3.6. Relationship between Hg Speciation and TSS, DOC.....	122
Figure 3.7. Hg Sources from Upland Materials.....	123
Figure 3.8. Recovery of TSS, DOC, and THg for the Two Years Following Wildfires	124
Figure 3.9. Linear Regressions between TSS and THg in the Two Years Following Wildfires	125
Figure 3.10. Discharge and Water Quality at Sagehen Creek	126
Figure 3.11. Hg Export along with Discharge at Sagehen Creek	127
Figure 3.12. Discharge at WS80, WS77 and WS79	128
Figure 3.13. Levels of TSS, UF-THg, and UF-MeHg in Streamwater.....	129
Figure 3.14. Levels of DOC, SUVA ₂₅₄ , DHg, and DMeHg in Streamwater.....	130
Figure 3.15. Relationships between TSS, DOC and Hg Speciation	131
Figure 3.16. Daily Yields from Wildfire-burned and Prescribed-fire-burned Watersheds	132
Figure S3.1. Comparisons of Pre-burn and Post-burn at WS80, WS77, and WS79	133
Figure 4.1. Illustration of Impacts of Forest Fires on Mercury Biogeochemical Cycling in Terrestrial and Aquatic Ecosystems.....	144

CHAPTER I

INTRODUCTION

1.1 Background

1.1.1 Forest Fires

Wildfires burn about 400 mega hectares (Mha) of land on the globe every year, which is equal to more than 3% of all the vegetated landscape (Giglio *et al.* 2010). In the western United States, increases in fire activity, including the number of fires and burned areas have been observed in the past decades, mainly attributed to climate change (Westerling *et al.* 2006). Human-caused climate change has been estimated to contribute to an additional 4.2 million hectares of wildfire burn area during 1984-2015 in California, doubling the cumulative forest fire area since 1984 (Abatzoglou & Williams 2016). In general, wildfires cause tree mortality, release different chemicals (e.g., carbon dioxide and carbon monoxide) to the atmosphere, change the physical and chemical properties of the forest floor, alter the hydrological processes, and increase nutrients and heavy metals input to downstream environments (Shakesby 2011; Smith *et al.* 2011; Abraham *et al.* 2017). The wildfires destroy large areas of shrublands and forests, remove the vegetation covers, and modify the soil hydrological behavior with a wide variability by removing the forest canopy and litter/duff layers and producing ash thus generating a two-layer system with ash as the top layer and soil as the bottom layer. The ash layer, together with the hydrologic condition, are essential in the post-fire hydrologic runoff generation,

depending on the ash types and depth, soil type, and rainfall intensity/duration (Bodí *et al.* 2014). The post-wildfire runoff was indicated to be predominantly contributed by a saturation-excess mechanism at the ash-soil interface during the first storm event, then predominantly contributed by the infiltration-excess mechanism at the ash surface during the second storm (Ebel *et al.* 2012).

Wildfires can lead to public health concerns to humans and ecological risk due to the smoke exposure and the impacts on water quality in downstream water bodies (e.g., streams and lakes). Higher metal levels such as cadmium, copper, lead, aluminum have been reported in a Southern California watershed after the fire in 2009 (Burke *et al.* 2013). The burning generally results in increased soil pH and base saturation, increased carbonate alkalinity in soil solution, potentially alter the water chemistry in streamwater. Moreover, nutrients and heavy metals in vegetation, litter/duff, and soil can potentially be volatilized or mineralized during the fire (pyrolysis or combustion), or lost by ash convection during a fire, and then they can be redistributed by wind movement of ash or by leaching from the ash layer and soil and transported to the downstream environment along with the runoff (Grier 1975). For example, nutrients leaching from the ash layer in the first year following a wildfire transferred 149 kg Ca/ha, 50 kg Mg/ha, 92 kg K/ha, 33 kg Na to the soil, and most of them were retained in the surface soil (0 to 19-cm) (Grier 1975). Wildfire ash has been found to increase ammonium, nitrate, soluble reactive phosphate, and reduce the macroinvertebrates density in streams (Earl & Blinn 2003). In a Canadian boreal coniferous forest watershed impacted by wildfires, elevated total

phosphorus (TP), inorganic nitrogen (N), and algal biomass were observed (Pinel-Alloul *et al.* 2002).

The use of prescribed fires, a commonly used forest management practice after carefully planning and under controlled conditions, is efficient to control the occurrence of the high intensity wildfire as well as some other forest problems including but not limited to pine beetle infestation, control of weeds, silvicultural improvements, and biodiversity maintenance. In the prescribed fire area, wildfire frequencies have declined sharply when prescribed fire hectares increased (i.e. in west-central Georgia, USA from 1982 to 2012) (Addington *et al.* 2015). Prescribed fires are usually conducted on a short period basis (2-4 years) for its effectiveness because of the fuel accumulation rate limitation (Fernandes & Botelho 2003). Although both wildfires and prescribed fires pose real perturbations in forest ecosystems, the prescribed fires are different with wildfires in intensity, frequency, severity, duration time, and burned area. Compared to wildfires, the easier to be managed prescribed fires are usually carried out with negligible or low severity and of shorter duration. The lower severity of the prescribed fires means that the fires could generate lower amount of ash generally and cause less disturbances on the surface soil either in depth or area, potentially leading to less impacts to the downstream environment. It has also been indicated that prescribed fire caused limited effects on soil physical degradations such as permeability, runoff and soil loss. However, regarding water erosion, it has been suggested that the shallower soils be paid more consideration due to degradation in their capacity to hold sufficient vegetation cover for soil protection (Fonseca *et al.* 2017). The low severity prescribed fire could increase nutrient levels in

the soil due to the addition of the ash leaching, without causing soil degradation thus posing less risk to the downstream environment (Pereira *et al.* 2010). In one coastal plain watershed burned by prescribed fire in Southeastern United States, water chemistry such as nitrogen (i.e. total nitrogen, ammonium and nitrate), potassium, sulfate, phosphate etc. was not significantly changed in a 3.5-year period (Richter *et al.* 1982).

Despite of the differences of wildfires and prescribed fires in severity or impacts to downstream water quality in nutrients and trace elements, both forest fires disturb the mercury (Hg) storage, forms, and mobility in forest ecosystems, which is a persistent and toxic global element largely stored in forests (Engle *et al.* 2006; Wiedinmyer & Friedli, 2007; Melendez-Perez *et al.* 2014). However, due to the differences of the two types of forest fires in the burn area and intensity, impacts on soil degradation, alteration of hydrological process, they could lead to different consequences in the amount of Hg or pathways of Hg transport.

1.1.2 Mercury Biogeochemical Cycling in Forest Ecosystems

Mercury (Hg), can essentially contaminate all types of ecosystems due to its atmospheric emission, long-range transport, and deposition (Fitzgerald *et al.* 1998). Mercury is a concerning pollutant due to its extensive bioaccumulation and biomagnification through the aquatic food webs and its neurotoxicity on animals. Sources of Hg in the environment could be natural or anthropogenic, the latter include human activities such as coal combustion and artisanal gold mining which release Hg to the atmosphere. Forest ecosystems including vegetation and surface soil is a major sink of atmospheric Hg. Despite of wet deposition of Hg contributed by precipitation, in

particular, canopies in forested ecosystems greatly enhance Hg deposition (Louis *et al.* 2001) because foliar surfaces can take up atmospheric gaseous Hg through the stomatal openings (referred to dry deposition) (Ericksen *et al.* 2003), which makes forests become a significant storage of Hg than other open landscapes. It has been estimated that surface soil represents the largest pool of Hg, which accounts for ~77% of the global pool of Hg, vs. ~22% in the open ocean, and < 1% in the atmosphere (Mason & Sheu, 2002).

Forests are “sinks” for Hg in the atmosphere, but the disturbances such as forest fires make forests as “sources” of Hg. The disturbances including wildfires and forestry practice (i.e., prescribed fire) could shift forest ecosystems from “Hg sink” to “Hg source”. There is no doubt that forest fires can release Hg stored in the forests into the atmosphere due to the high temperature (Friedli *et al.* 2001). Thermal combustion of vegetation and surface soil can largely release Hg as in elemental gaseous form because ligands binding to Hg in the soil such as thiol groups can be broken down at prolonged heating at ~300 °C (Biester & Scholz 1996). Therefore, wildfires can substantially mobilize atmospherically sequestered Hg from vegetation and soil in forests and then release it back to the atmosphere as gaseous elemental Hg, with a small proportion of that being in a particulate form as smoke (Friedli *et al.* 2001; Sigler *et al.* 2003). The “re-emission” of Hg from forests through wildfires is an important emission source, representing ~10-40% of all natural and anthropogenic emissions (Biswas *et al.* 2007). It has been estimated that on average 44 metric tons Hg was released annually in the lower 48 states of the United States and Alaska during 2002 to 2006, equivalent to ~30% of the National Emissions Inventory of Hg announced by EPA 2002 (Wiedinmyer & Friedli,

2007). Thus, with more frequent and severe wildfires anticipated in the future, more sequestered Hg in forests across the globe is expected to be released back (or re-emitted) to the atmosphere, which may compromise the benefits of global reduction in Hg emissions including the Minamata Convention on Mercury, a legally binding agreement negotiated by countries under the United Nations Environmental Program (UNEP) intended to protect the human health and environment from Hg and Hg compounds (Gustin *et al.* 2016).

Besides the Hg emission due to the forest fires, there is still a large amount of Hg left on the forest floor. However, studies have neglected or underestimated the Hg content in burned materials, i.e., wildfire ash, because of the high Hg volatilization in laboratory control burning studies (Biester & Scholz 1996; Mailman & Bodaly 2005). In the very few studies investigating Hg in the field, Hg in the burned soils collected in 3 southern California watersheds showed a range from 1 to 349 ng/g varying by sites (Burke *et al.* 2010), and a range of 10.1 ± 8.4 ng/g from a forest wildfire site in western Nevada and 49.4 ng Hg/g (± 11.3 ng Hg/g) in burned soil from a desert wildfire site in north-central Nevada (Engle *et al.* 2006). Nevertheless, the studies mentioned above focused on the Hg content or leaching properties in the left-over burned materials, Hg reactivity and bioavailability in the burned materials is less known, especially in the wildfire ash. The reactivity and bioavailability of Hg would impact the bioaccumulation of Hg in the aquatic food webs, constituting health risk to humans and wildlife.

Forest fires made forests not only the Hg “source” for the atmosphere but also for the downstream environment, which caused larger concern. The atmospheric Hg alone

constituted less public health risk concern because of the inertness of gaseous Hg. The risk to humans and wildlife mainly occurs when Hg is transported to the downstream environment and accumulates in the aquatic food web. Following the forest fires, the left-over Hg on the forest floor could be transported to the downstream by wind or surface runoff, soil creep, rainsplash, subsurface water flows and bioturbations. Aquatic ecosystems are hotspots for producing the neurotoxic and immunotoxic methylmercury (MeHg) by the Hg methylation microbes such as sulfate-reducing bacteria (SRB), iron-reducing bacteria, methanogens, etc. especially in the sediment where the anoxic environment may favor the microbes for producing MeHg (Hsu-Kim *et al.* 2013). The forest floor could receive more precipitation after wildfire than the pre-fire condition due to the complete or partial removal of vegetation cover (Shakesby 2011), thus leading to potential higher overland flow to the downstream. Meanwhile, the alterations of the physicochemical and biogeochemical properties of the surface soil on the forest floor by the fires impact the hydrological process, potentially making the surface soils more vulnerable to erosion and thus increase Hg export to downstream waters (Fonseca *et al.* 2017). Since the aquatic ecosystem is an essential environment for Hg transformations, Hg export to downstream waters after the forest fire is critical to be evaluated because it provides either direct organic MeHg or the divalent Hg (Hg^{2+} , electronic acceptor) and a carbon source to the anoxic Hg methylation bacteria. Kelly *et al.* (2006) observed 5-folds higher fish MeHg in the wildfire-burned watersheds, mainly due to the altered food web structure and increased Hg export (Kelly *et al.* 2006), indicating forest fires would cause ecological risk and public health concerns to wildlife and humans regarding the toxic Hg

exposure. Although increased Hg bioaccumulation has been observed in some wildfire-impacted watersheds, the hydrological Hg export pattern in the wildfire-impacted watersheds is still unclear.

Prescribed fire has been indicated to cause less disturbance to hydrological processes including the erosion, surface runoff, and to the downstream environment in nutrient cycling (Richter *et al.* 1982; Fonseca *et al.* 2017). However, rainfall after the prescribed fire has been indicated to increase Hg concentrations in the burned soils approximately 2.1 times higher and elevate Hg mobilization in burned soils in one Australian burned site (Abraham *et al.* 2018), posing ecological risk to the downstream environment regarding Hg export.

1.2 Research Focus

Given the forest terrestrial ecosystems, compared to the numerous studies of Hg emission during forest fires (Friedli *et al.* 2001; Sigler *et al.* 2003; Wiedinmyer & Friedli 2007; Finley *et al.* 2009), there are fewer studies about the Hg remaining on the forest floor. Forest fires break down the ligands of Hg to organic matter or ions (i.e., sulfur) in vegetation and soil, leading to potential alterations in Hg forms and Hg reactivity. The Hg-ligand formation/speciation and Hg adsorption/desorption on the burned landscape will impact Hg bioaccumulation in the aquatic food webs in the downstream environment (Gabriel & Williamson, 2004). The ash layer has largely been neglected or underestimated in Hg content as well as its role in Hg biogeochemical cycling. It has been found there is very low Hg level in the ash (burned vegetation) burned in controlling burning condition

(3.5-15.6 ng/g) with 92-99% Hg reduction compared to the original unburned litter (Mailman & Bodaly, 2005). Compared to laboratory control burning ash, there are very few studies investigating Hg content in the field ash. In the two studies we found that examined Hg levels in ash, the Hg levels in the field ash was much higher, showing 39.2 ng/g (57% Hg reduction compared to the original litter) in western Nevada burned site, and 64-112 ng/g in the sites in Portugal varying by burn intensities (Engle *et al.* 2006; Campos *et al.* 2015). The contrast of Hg content in wildfire ash and control burning ash indicated the wildfire ash showed different properties with the laboratory-generated ash. However, the origin of the Hg in the wildfire ash is still not understood. Therefore, this dissertation work focuses on the Hg content, reactivity, and bioavailability in the ash layer, and implications of the ash layer in the downstream ecosystems.

Moreover, it has been demonstrated that the ash layer plays an essential role in the post-fire hydrologic runoff generation. However, it is still unclear regarding the ash behavior in the aquatic environment. Although there are numerous studies in nutrients (i.e. carbon and nitrogen) loss in burned soil and nutrients exports to the downstream watersheds after the wildfire (Earl & Blinn 2003; DeLuca *et al.* 2006; Caon *et al.* 2014; Rhoades *et al.* 2018), fewer studies have been conducted to investigate the post-fire Hg transport patterns/levels to downstream environment. Among the limited studies examining the post-wildfire Hg export, it has been more focused on simulating Hg leaching from the soil in a laboratory or short-term tracking studies in the field (Burke *et al.* 2010; Jensen *et al.* 2017). Although minimal Hg fraction (<2%) could leach from the burned soils collected from Southern California watersheds impacted by wildfires (Burke

et al. 2010), leading to potential lower concentrations of dissolved Hg (DHg) export, however, particulate Hg (PHg) has also been observed to be elevated in a wildfire-impacted watershed in the Southeast United States by 20.5 folds higher at the burned watershed (2.66 ng PHg per mg TSS) than the unburned watershed (0.13 ng PHg per mg TSS) in the 8-months following the wildfire (Jensen *et al.* 2017). Due to the limited studies, the hydrological transport of Hg following the fire and its recovery is largely not understood.

Furthermore, previous studies discussed the Hg content and leaching properties of burned soils and ash generated by wildfires, which indicated variable Hg in the burned soils, posing an ecological risk to the downstream water environment. Nevertheless, the impacts of prescribed fires on the Hg biogeochemical cycling is less studied. Unlike the high intensive wildfire, the prescribed fire could lead to less Hg disturbance in the surface soils varying by depth (Harden *et al.* 2004). Although prescribed fires have been carried out widely across the United States, most studies focused on hydrological processes, stream chemistry, forest nutrient (nitrogen, phosphorus, carbon) cycling (Richter *et al.* 1982; Fonseca *et al.* 2017), or Hg emission (Melendez-Perez *et al.* 2014), there are less information about the impacts of prescribed fire on the Hg remaining on the burned landscape. In the very limited studies, Abraham *et al.* (2018) indicated that rainfall after the prescribed fire would potentially increase Hg levels and remobilization in the burned soils. Harden *et al.* (2004) indicated minimal Hg reduction in the burned soils compared to the unburned soil. These studies suggested the different impacts of prescribed fire on the Hg content in the post-burn landscape and potentially varied hydrological process

compared to the wildfires. However, to my knowledge, there is no study to date investigating the Hg hydrological transport to the downstream environment. Therefore, another focus of this dissertation work is to evaluate the impacts of both wildfire (natural) and prescribed fire (anthropogenic) on Hg biogeochemical cycling in both the terrestrial ecosystem and the downstream aquatic ecosystems.

1.3 Significance of this Research

Hg levels and bioavailability in streamwater is very important to address because it provides “baseline” concentrations for the toxic MeHg transformation by microbes and bioaccumulation in the aquatic food webs. Forests are critically important to provide many valuable ecosystem services such as supplying clean drinking water and supporting the diversity of wildlife. Mercury storage in forests would be disturbed by natural and anthropogenic disturbances, among which forest fires are substantial perturbations. Natural wildfires are increasing in intensity and frequency due to climate change and burning residuals. Ash generated from wildfires has been essentially neglected for its role in Hg biogeochemical cycling. This dissertation work examines Hg content in ash and the reactivity and bioavailability of Hg contained in ash, as well as the potential ash behaviors/role in Hg transformations in waters.

Prescribed fires, as an effective forestry practice to control wildfires, have been widely conducted across the United States. However, the ecological risk and public concern of prescribed fires regarding Hg is not clear. It is essential to compare the impacts of wildfire and prescribed fires on Hg transport in aquatic ecosystems to provide

models linking natural wildfire (usually higher intensity) and anthropogenic prescribed fire (regular forestry and usually lower intensity) disturbances to downstream environment regarding the toxic Hg. This dissertation research is a relatively complete work about the impacts of forest fires (both natural and anthropogenic fires) on the Hg biogeochemical cycling in the aquatic ecosystems, which is expected to increase our understanding in post-fire Hg storage, reactivity, bioavailability and hydrological transport, and the ecological risk of forest fires regarding Hg. This work will provide evidence to policymakers in forest management agencies and fishery advisories.

1.4 Research Objectives

The objectives of this dissertation work are 1) to examine Hg levels, reactivity and bioavailability of Hg in wildfire-burned materials (ash) and ecological implication of ash to Hg biogeochemical cycling in water environment; 2) to investigate Hg hydrological transport pattern in watersheds affected by natural wildfires, and compare the Hg hydrological transport to anthropogenic prescribed fires (pile burning and broadcast burning) impacts. We hope this dissertation work will provide a better understanding in the ecological risk of forest fires regarding Hg in the burned landscape.

1.5 References

- Abatzoglou, J.T. & Williams, A.P. (2016). Impact of anthropogenic climate change on wildfire across western US forests. *Proceedings of the National Academy of Sciences*, 113, 11770-11775.
- Abraham, J., Dowling, K. & Florentine, S. (2017). Risk of post-fire metal mobilization into surface water resources: A review. *Science of the Total Environment*, 599, 1740-1755.
- Abraham, J., Dowling, K. & Florentine, S. (2018). Effects of prescribed fire and post-fire rainfall on mercury mobilization and subsequent contamination assessment in a legacy mine site in Victoria, Australia. *Chemosphere*, 190, 144-153.
- Biester, H. & Scholz, C. (1996). Determination of mercury binding forms in contaminated soils: mercury pyrolysis versus sequential extractions. *Environmental Science and Technology*, 31, 233-239.
- Biswas, A., Blum, J.D., Klaue, B. & Keeler, G.J. (2007). Release of mercury from Rocky Mountain forest fires. *Global Biogeochemical Cycles*, 21.
- Bodí, M.B., Martin, D.A., Balfour, V.N., Santín, C., Doerr, S.H., Pereira, P. *et al.* (2014). Wildland fire ash: Production, composition and eco-hydro-geomorphic effects. *Earth-Science Reviews*, 130, 103-127.

- Burke, M.P., Hogue, T.S., Ferreira, M., Mendez, C.B., Navarro, B., Lopez, S. *et al.* (2010). The Effect of Wildfire on Soil Mercury Concentrations in Southern California Watersheds. *Water, Air, and Soil Pollution*, 212, 369-385.
- Caon, L., Vallejo, V.R., Ritsema, C.J. & Geissen, V. (2014). Effects of wildfire on soil nutrients in Mediterranean ecosystems. *Earth-Science Reviews*, 139, 47-58.
- DeLuca, T.H., MacKenzie, M.D., Gundale, M.J. & Holben, W.E. (2006). Wildfire-Produced Charcoal Directly Influences Nitrogen Cycling in Ponderosa Pine Forests. *Soil Science Society of America Journal*, 70, 448.
- Earl, S.R. & Blinn, D.W. (2003). Effects of wildfire ash on water chemistry and biota in South-Western USA streams. *Freshwater Biology*, 48, 1015-1030.
- Ebel, B.A., Moody, J.A. & Martin, D.A. (2012). Hydrologic conditions controlling runoff generation immediately after wildfire. *Water Resources Research*, 48.
- Engle, M.A., Sexauer Gustin, M., Johnson, D.W., Murphy, J.F., Miller, W.W., Walker, R.F. *et al.* (2006). Mercury distribution in two Sierran forest and one desert sagebrush steppe ecosystems and the effects of fire. *Science of the total Environment*, 367, 222-233.
- Ericksen, J.A., Gustin, M.S., Schorran, D.E., Johnson, D.W., Lindberg, S.E. & Coleman, J.S. (2003). Accumulation of atmospheric mercury in forest foliage. *Atmospheric Environment*, 37, 1613-1622.
- Fernandes, P.M. & Botelho, H.S. (2003). A review of prescribed burning effectiveness in fire hazard reduction. *International Journal of Wildland Fire*, 12, 117-128.

- Finley, B.D., Swartzendruber, P.C. & Jaffe, D.A. (2009). Particulate mercury emissions in regional wildfire plumes observed at the Mount Bachelor Observatory. *Atmospheric Environment*, 43, 6074-6083.
- Fitzgerald, W.F., Engstrom, D.R., Mason, R.P. & Nater, E.A. (1998). The case for atmospheric mercury contamination in remote areas. *Environmental Science and Technology*, 32, 1-7.
- Fonseca, F., de Figueiredo, T., Nogueira, C. & Queirós, A. (2017). Effect of prescribed fire on soil properties and soil erosion in a Mediterranean mountain area. *Geoderma*, 307, 172-180.
- Friedli, H.R., Radke, L.F. & Lu, J.Y. (2001). Mercury in smoke from biomass fires. *Geophysical Research Letters*, 28, 3223-3226.
- Gabriel, M.C. & Williamson, D.G. (2004). Principal biogeochemical factors affecting the speciation and transport of mercury through the terrestrial environment. *Environmental Geochemistry and Health*, 26(3-4), 421-434.
- Giglio, L., Randerson, J.T., van der Werf, G.R., Kasibhatla, P.S., Collatz, G.J., Morton, D.C. *et al.* (2010). Assessing variability and long-term trends in burned area by merging multiple satellite fire products. *Biogeosciences*, 7, 1171-1186.
- Grier, C.C. (1975). Wildfire effects on nutrient distribution and leaching in a coniferous ecosystem. *Canadian Journal of Forest Research*, 5, 599-607.
- Gustin, M.S., Evers, D.C., Bank, M.S., Hammerschmidt, C.R., Pierce, A., Basu, N. *et al.* (2016). Importance of Integration and Implementation of Emerging and Future

- Mercury Research into the Minamata Convention. *Environmental Science and Technology*, 50, 2767-2770.
- Harden, J.W., Neff, J.C., Sandberg, D.V., Turetsky, M.V., Ottmar, R., Gleixner, G., Fries, T.L. and Manies, K.L. (2004). Chemistry of burning the forest floor during the FROSTFIRE experimental burn, interior Alaska, 1999. *Global Biogeochemical Cycles*, 18 (3).
- Hsu-Kim, H., Kucharzyk, K.H., Zhang, T. & Deshusses, M.A. (2013). Mechanisms regulating mercury bioavailability for methylating microorganisms in the aquatic environment: a critical review. *Environmental Science and Technology*, 47, 2441-2456.
- Jensen, A.M., Scanlon, T.M. & Riscassi, A.L. (2017). Emerging investigator series_the effect of wildfire on streamwater mercury and organic carbon in a forested watershed. *Environmental Science Processes & Impacts*, 2017, 1505-1517.
- Louis, V.L.S., Rudd, J.W.M., Kelly, C.A., Hall, B.D., Rolffhus, K.R., Scott, K.J. *et al.* (2001). Importance of the forest canopy to fluxes of methyl mercury and total mercury to boreal ecosystems. *Environmental Science and Technology*, 35, 3089-3098.
- Mailman, M. & Bodaly, R.A. (2005). Total mercury, methyl mercury, and carbon in fresh and burned plants and soil in Northwestern Ontario. *Environmental Pollution*, 138, 161-166.

- Melendez-Perez, J.J., Fostier, A.H., Carvalho, J.A., Windmüller, C.C., Santos, J.C. & Carpi, A. (2014). Soil and biomass mercury emissions during a prescribed fire in the Amazonian rain forest. *Atmospheric Environment*, 96, 415-422.
- Pereira, P., Ubeda, X., Martin, D., Mataix-Solera, J. & Guerrero, C. (2011). Effects of a low severity prescribed fire on water-soluble elements in ash from a cork oak (*Quercus suber*) forest located in the northeast of the Iberian Peninsula. *Environmental Research*, 111, 237-247.
- Pinel-Alloul, B., Prepas, E., Planas, D., Steedman, R. & Charette, T. (2002). Watershed Impacts of Logging and Wildfire: Case Studies in Canada. *Lake and Reservoir Management*, 18, 307-318.
- Rhoades, C.C., Chow, A.T., Covino, T.P., Fegle, T.S., Pierson, D.N. & Rhea, A.E. (2018). The Legacy of a Severe Wildfire on Stream Nitrogen and Carbon in Headwater Catchments. *Ecosystems*.
- Richter, D., Ralston, C. & Harms, W. (1982). Prescribed fire: effects on water quality and forest nutrient cycling. *Science*, 215, 661-663.
- Shakesby, R.A. (2011). Post-wildfire soil erosion in the Mediterranean: Review and future research directions. *Earth-Science Reviews*, 105, 71-100.
- Sigler, J., Lee, X. & Munger, W. (2003). Emission and long-range transport of gaseous mercury from a large-scale Canadian boreal forest fire. *Environmental Science and Technology*, 37, 4343-4347.

- Smith, H.G., Sheridan, G.J., Lane, P.N.J., Nyman, P. & Haydon, S. (2011). Wildfire effects on water quality in forest catchments: A review with implications for water supply. *Journal of Hydrology*, 396, 170-192.
- Westerling, A.L., Hidalgo, H.G., Cayan, D.R. & Swetnam, T.W. (2006). Warming and earlier spring increase western US forest wildfire activity. *Science*, 313, 940-943.
- Wiedinmyer, C. & Friedli, H. (2007). Mercury emission estimates from fires: an initial inventory for the United States. *Environmental Science and Technology*, 41, 8092-8098.

CHAPTER II

ORIGIN, REACTIVITY, AND BIOAVAILABILITY OF MERCURY IN

WILDFIRE-BURNED MATERIALS

This chapter has been published as: Ku, P., Tsui, M.T.K., Nie, X., Chen, H., Hoang, T.C., Blum, J.D., Dahlgren, R.A. and Chow, A.T., 2018. Origin, reactivity, and bioavailability of mercury in wildfire ash. *Environmental Science and Technology*, 52(24), pp.14149-14157. Reprinted (adapted) with permission from (*Environ. Sci. Technol.* 2018, 52, 24, 14149-14157). Copyright (2018) American Chemical Society.

2.1 Introduction

Wildfire is an important ecosystem perturbation affecting ~3% of the global vegetated land surface each year (Giglio *et al.* 2010). Due to climate change, wildfire is predicted to be more frequent and intense this century in semiarid regions including California, Australia and the Mediterranean region of Europe (Williams *et al.* 2001; Scholze *et al.* 2006; Westerling *et al.* 2006; Marlon *et al.* 2009). Forest ecosystems represent an important sink for atmospheric mercury (Hg) but also are a source of Hg to the environment through biomass burning and runoff (Mason 2009). Wildfire can lead to substantial loss of Hg previously sequestered in vegetation, surficial detritus, and topsoil to the atmosphere, predominantly in the form of gaseous elemental Hg(0) (Friedli *et al.* 2001; Friedli *et al.* 2003; Biswas *et al.* 2007).

Despite the prevalence of studies focusing on Hg loss during wildfires, one aspect of wildfire effects on Hg cycling has received very little attention—the concentrations

and reactivity of Hg in burned biomass residues (i.e., wildfire ash). To our knowledge, there are only two prior studies reporting Hg levels in wildfire ash. Engle *et al.* (2006) found that ash had 39.2 ng/g of Hg (on a dry mass basis) compared to 91.4 ng/g in unburned forest litter in western Nevada (USA) (Engle *et al.* 2006); but it should be noted that ash samples were collected almost a year after the wildfire and the results may have been compromised by subsequent rainfall, runoff, and leaching. Campos *et al.* (2015) collected wildfire ash four weeks after burning from two sites in Portugal that had different burn intensities and found ash with significantly more Hg in areas of moderate burning (112 ng/g) compared to ash in areas with high-intensity burning (64 ng/g) (Campos *et al.* 2015). In contrast, studies using controlled biomass burning under oxygenated conditions consistently found ash with very low Hg content, ranging from 0.4 to 11.1 ng/g (on a dry mass basis) (Friedli *et al.* 2003; Mailman & Bodaly 2005), raising questions regarding the factors controlling the Hg content of wildfire ash.

Based on their colors and percentages of loss-on-ignition (LOI) (Bodí *et al.* 2011; Campos *et al.* 2015), wildfire ash can be operationally divided into two major classes: black ash (BA; low-intensity fire; 200-500 °C) and white ash (WA; high-intensity fire; >500 °C) (Bodí *et al.* 2014). However, it should be noted that within each class, ash may consist of a mixture of materials with contrasting mineral and organic matter contents. In essence, BA is generated by incomplete combustion of biomass while WA is produced by more complete combustion (DeBano *et al.* 1998). BA is known to contain appreciable amounts of charcoal or black carbon (BC), while WA generally contains high mineral concentrations that can be dominated by CaCO₃, CaO and/or aluminosilicates

(Pereira *et al.* 2012; Bodí *et al.* 2014). As related to Hg cycling, it is essentially unknown how BC in wildfire ash mediates Hg levels, reactivity, and bioavailability. The wildfire ash layer is highly susceptible to runoff-leaching and erosional processes due to the lack of soil cover and the fine powdery nature of the ash materials, thereby resulting in a strong potential for transporting Hg in the wildfire ash to aquatic environments including streams, lakes and reservoirs (Caldwell *et al.* 2000; Kelly *et al.* 2006). In particular, one area of concern is whether Hg in ash is available for microbial methylation when ash is deposited in anoxic zones, which can serve as biogeochemical hotspots of Hg methylation (e.g., biofilms (Battin *et al.* 2016)). Methylmercury (MeHg) can form under anoxic conditions (Benoit *et al.* 2003), and is highly bioaccumulative, thus elevating MeHg levels in downstream biota (Tsui *et al.* 2009).

The overall goal of this study was to provide the first rigorous characterization of Hg in ash by collecting and analyzing ash from two wildfires (Wragg and Rocky Fires) in northern California. Specifically, we examined *i*) Hg levels and Hg *reactivity* using two acid digestion methods as an operationally-defined measure of Hg *reactivity* in ash, and compared results with unburned vegetation (i.e., the potential fuel load); *ii*) the isotopic composition of Hg in wildfire ash to provide further insights to the origins of Hg in ash; *iii*) the capability of wildfire ash to adsorb ambient Hg (both aqueous and gaseous Hg) due to the “higher-than-expected” Hg content in many wildfire ash samples compared to lab-generated ash (Friedli *et al.* 2003; Mailman & Bodaly 2005); and *iv*) the bioavailability of Hg released from wildfire ash to methylating microbes, to determine whether wildfires might stimulate Hg methylation in downstream aquatic environments.

2.2 Materials and Methods

2.2.1 Sample Collection

We collected wildfire ash samples 3-5 weeks following two northern California wildfires in the summer of 2015: the Wragg Fire and the Rocky Fire (*see* site characteristics and specific sampling points in **Table S2.1**). No rainfall occurred between the fire and the sampling, and thus the ash samples were not eroded or leached by rainfall or runoff (Engle *et al.* 2006; Bodí *et al.* 2014). Paired ash samples [i.e., black ash (BA) and white ash (WA) were visually distinguished in the field] (Roy *et al.* 2010) were collected at each site (5 pairs for the Wragg Fire, and 9 pairs for the Rocky Fire). Surface ash samples (generally 0-5 cm) were carefully collected to avoid mixing with underlying soil using a stainless-steel hand shovel and were then placed into a clean polyethylene bag. It should be noted that BA and WA characterization represents the dominant materials visually identified in the field, but they should not be considered pure endmembers as there is significant short-range spatial variability in both the horizontal and vertical dimensions of the ash layer (Bodí *et al.* 2014). At the landscape scale for both sites we estimated that ~90% of the surface contained BA and ~10% WA, which was a function of local fuel load distribution (e.g., proximity to tree trunks). In general, we expected that the surface materials would be burned at a higher temperature and at more oxygenated conditions than the deeper ash layers leading to inherent variability within the vertical dimension. Unburned vegetation (twigs and branches) and surface litter were collected as a control from the dominant tree species in unburned areas located adjacent to the fire perimeter (*see* locations in **Table S2.1**). We present the data for each

individual ash sample since there was a large heterogeneity among samples within each ash category (BA or WA; originally considered as replicates).

2.2.2 Ash Characterization and Organic Carbon Composition

All ash samples were dry at the time of collection and therefore did not require further drying in the laboratory. Ash samples were heterogeneous in size, shape and color of materials (especially BA; *see* pictures of pre-sieved and 2-mm sieved ash, **Figure S2.1**), and were therefore sieved through a 2-mm acid-cleaned polypropylene mesh and thoroughly homogenized. Unburned litter and dead woody materials were frozen, freeze-dried and homogenized (<2-mm) using a stainless-steel grinder. All samples were analyzed for color using a Munsell color chart (Munsell 1998) (except unburned vegetation materials) and ash color was assigned according to Bodí et al. (2011). LOI was determined using a muffle furnace, and total calcium (Ca) using an ICP-MS. The chemical composition of organic carbon was characterized using pyrolysis-GC/MS to provide semi-quantitative (relative) levels of BC (De la Rosa *et al.* 2008; Song & Peng 2010; Chen *et al.* 2015) as defined here by the fraction of aromatic hydrocarbon (ArH) (Pereira *et al.* 2012). It should be noted that the combustion temperature of LOI was set at 500°C to prevent the loss of dominant inorganic components such as carbonate (e.g., 600-800°C) (Dlapa *et al.* 2015), and thus we regard LOI as a proxy of organic matter content in the samples.

In detail, loss-on-ignition (LOI) for all samples was measured after being held in a muffle furnace (Thermo Scientific; Thermolyne™) at 500 °C for 4 hours at the University of North Carolina at Greensboro (UNCG; Greensboro, NC). Total carbon (TC) and total

nitrogen (TN) contents were analyzed on a CHN-O elemental analyzer (Thermo Scientific; FLASH 2000) at Baruch Institute of Coastal Ecology, Clemson University (Georgetown, SC). Major cations and trace elements were also analyzed for samples after acid digestion (aqua regia; following Olund et al. (2004) and dilution with Barnstead™ Nanopure™ water (18.2 MΩ/cm) using inductively coupled plasma–mass spectrometry (Perkin Elmer; NeXion 300S) at Institute of Environmental Sustainability, Loyola University Chicago (Chicago, IL).

The organic carbon composition in ash and unburned samples was determined by pyrolysis-gas chromatography-mass spectrometry (Py-GC-MS) at Baruch Institute of Coastal Ecology, Clemson University, following a method described by Song and Peng (2010) and Chen et al. (2018). In brief, individual samples (0.1-30 mg depending on organic matter content) were placed in pre-baked quartz tubes with samples held in place by glass wool. The sample-filled quartz tube was introduced into the CDS Analytical Pyroprobe 2000 “Pyrolyzer” and heated from 250 to 700 °C with a temperature ramping rate of 5 °C/millisecond and then held for 10 s on a pyrolysis injector (CDS Analytical Inc., Oxford, PA) connected to a gas chromatography-mass spectrometer (GC-MS; Agilent 7890A). Helium gas at 1 mL/min was used to flush the pyrolytic compounds into the GC column. The GC injector was operated in split-mode (10:1 to 50:1 depending on the organic matter content in sample) with an inlet temperature of 250 °C. Pyrolysis products were identified and quantified according to their GC retention time and mass spectra with reference to the Wiley/NIST library supplied with the MS workstation software 7.0.1.

The identified and quantified pyrolysis products were classified into nine groups according to their chemical similarity: (i) saturated hydrocarbon (SaH), (ii) unsaturated hydrocarbon (UnSaH), (iii) aromatic hydrocarbon (ArH), (iv) polyaromatic hydrocarbon (PAH), (v) carbohydrate (Carb), (vi) phenolic carbohydrate (PhC), (vii) lignin phenol carbohydrate (LgPhC), (viii) halogen-containing compounds (Hal), and (ix) nitrogen-containing compounds (Ntg). Relative abundance of each group was calculated as the sum of the major ion peak areas in each group divided by the sum of all major ion peak areas. An R-script (R Studio Desktop version 1.0.44; Boston, MA) was developed for automated identification and quantification.

2.2.3 Total Hg and Recalcitrant Hg Analyses

All sample processing and analysis for Hg was performed in a semi-clean analytical laboratory at UNCG. For all samples, we used two acid digestion methods to release Hg in order to assess Hg reactivity based on the differences of Hg concentrations generated by the two digestion methods: *Method 1* (reported as [Hg_{method-1}]; targeting organic matter-bound-Hg) used trace-metal grade HNO₃ and H₂O₂ (4:1, v:v) in a 80 °C water bath overnight, and *Method 2* (reported as [Hg_{method-2}]; targeting all geochemical pools) used aqua regia (freshly mixed trace-metal grade HNO₃ and HCl, 1:3, v:v). In *Method 1* (reported as [Hg_{method-1}]), 0.20±0.01 g of dry samples were weighed into acid-cleaned PFA digestion vessels (Savillex, Eden Prairie, MN), and 5 mL of trace-metal grade HNO₃ and H₂O₂ (4:1, v:v, both from Fisher Scientific) were added and allowed to sit at room temperature overnight with the cap loosely tightened (i.e., cold digestion). On the following day, the digestion vessels were tightly closed and placed in a water bath at

80 °C overnight to complete the digestion (i.e., hot digestion). *Method 2* (reported as [Hg_{method-2}]) followed the procedure of Olund et al. (2004) in which samples were weighed into acid-cleaned 40 mL borosilicate glass vials with PTFE-lined septa (Thermo Scientific), and 8 mL of trace-metal grade HNO₃ and HCl (i.e., aqua regia; 1:3, v:v, both from Fisher Scientific) was added and allowed to sit at room temperature for 24 h (i.e., cold digestion). Then, 22 mL of 5% BrCl was added to the acidic mixtures, and the vials containing sample mixtures were placed in a water bath at 80 °C overnight (i.e., hot digestion). To test the robustness of this approach to assess Hg reactivity in environmental samples, we also analyzed two vegetation standard reference materials (SRMs) (i.e., NIST-1515 Apple Leaves; IAEA-359 Cabbage) and litter samples from three reference forests (Angelo Coast Range Reserve in northern California, University of Michigan Biological Station in northern Michigan, and Hubbard Brook Experimental Forest in New Hampshire).

For both digestion methods, aliquots of digested samples (0.5 to 2 mL, depending on estimated Hg content) were added to 100 mL of Nanopure water (18.2 MΩ/cm) in a glass bubbler with stopper/sparger and 200-600 µL of 30% hydroxylamine (Alfa Aesar) were added to partially reduce the reagent. Gold traps were attached in connection to a soda lime trap to collect gaseous Hg(0) following complete reduction by 200 µL of 20% stannous chloride (Alfa Aesar), and the mixture was purged with Hg-free N₂ gas for 15 minutes. Gold traps loaded with Hg were heat-desorbed at 400-500 °C using the double amalgamation technique, and sample Hg was quantified using a Brooks Rand Model III CVAFS detector.

Throughout sample analyses, random samples were digested in duplicate and run for Hg. A primary calibration standard solution (1 ng/mL) was prepared from SMR-NIST-3133 Hg solution and checked against an in-house secondary calibration standard (1 ng/mL) prepared from SRM-NIST-1641d Hg solution; Hg in the two standards always matched within 3%. For each batch of digestions using both methods, we included reagent blanks and standard reference materials (SRM-NIST-1515 Apple Leaves and SRM-IAEA-359 Cabbage). Hg results were not significantly different ($p>0.05$) based on the two digestion methods for SRM-NIST-1515: $[Hg_{\text{method-1}}]$ was 42.3 ± 0.99 ng/g ($n=7$; mean \pm s.d.) and $[Hg_{\text{method-2}}]$ was 45.1 ± 2.19 ng/g ($n=9$) (**Table S2.3**), while the certified value for SRM-NIST-1515 had a mean of 44.0 ng/g (range = 40.0-48.0 ng/g). Similarly, Hg results were not significantly different ($p>0.05$) based on the two digestion methods for SRM-IAEA-359: $[Hg_{\text{method-1}}]$ was 10.2 ± 0.88 ng/g ($n=3$) and $[Hg_{\text{method-2}}]$ was 10.8 ± 1.29 ng/g ($n=3$) (**Table S2.3**). The certified value for SRM-IAEA-359 has a mean of 13.0 ng/g (range = 11.0-15.0 ng/g). All digested reagent blank had Hg concentrations <1 ng/g (based on the same procedure as in method 2).

Based on previous studies on soils and sediments, digestion methods (e.g., hot HNO_3 and H_2O_2) similar to *Method 1* would not result in digestion of charcoal or BC from environmental samples (Middelburg *et al.* 1999; MacKenzie *et al.* 2008), thus it may potentially allow us to distinguish Hg bound to organic matter *vs.* Hg bound to BC in ash samples, while *Method 2* (aqua regia) is expected to result in digestion of recalcitrant BC from the samples. Based on previous sequential extraction studies on Hg, $[Hg_{\text{method-1}}]$ includes Hg from all pools except recalcitrant geochemical pools which include HgS and

HgSe, while [Hg_{method-2}] should also digest Hg from recalcitrant geochemical pools (Biester et al., 1997; Bloom et al., 2003), but we found no study reporting whether BC-bound Hg belongs to the recalcitrant geochemical pools. Based on the above rationale, we operationally defined the “recalcitrant” pool of Hg as:

$$\text{Recalcitrant Hg (\%)} = [1 - (\text{Hg}_{\text{method-1}} / \text{Hg}_{\text{method-2}})] * 100\%$$

We compared [Hg_{method-2}] and Hg *reactivity* in ash samples to unburned biomass samples (collected post-burn). To assess the robustness of our approach for estimating Hg *reactivity*, we included two standard vegetation reference materials (SRMs) and previously characterized litter samples from three reference forests in northern California Coast Range, northern Michigan, and central New Hampshire.

2.2.4 Estimation of Hg Volatilization in Ash Samples

We estimated the Hg volatilization percentage for each ash sample collected in the field. We assumed the wildfire ash was generated from the combustion of the unburned vegetation components (litter and wood) from each site. We used two mass balance methods to calculate Hg volatilization loss based on either LOI or calcium content of ash samples.

Using LOI of the ash, we assumed that the mineral components in the ash samples were completely “conserved” during combustion from the original vegetation materials. We found that the average LOI of unburned vegetation was 95.9%, which means that 4.1% of the original vegetation materials was retained in the BA and WA samples after wildfire/combustion. Therefore, we calculated the amount of biomass combusted to form

the ash mineral component (total sample weight – loss on ignition) (Mineral content % = 100% - LOI%), using the equation $\% \text{Hg volatilized} = 1 - \text{Hg}_{\text{ash}} / [(1 - \text{LOI}_{\text{ash}} \%) / (1 - \text{LOI}_{\text{unburned}} \%) \times \text{Hg}_{\text{unburned}}] \times 100\%$, in which the average LOI_{unburned} % was 95.7% for Wragg Fire, and 96.0% for Rocky Fire and the average Hg_{unburned} was 26.8 ng/g for Wragg Fire and 21.2 ng/g for Rocky Fire site (LOI and Hg data are shown in **Table S2.2**).

Using Ca content of the ash, we assumed no change in Ca content in the original vegetation of the wildfire conditions (i.e., no loss of Ca). We used this equation: $\% \text{Hg volatilized} = 1 - \text{Hg}_{\text{ash}} / [(1 - \text{Ca}_{\text{ash}} \%) / (1 - \text{Ca}_{\text{unburned}} \%) \times \text{Hg}_{\text{unburned}}] \times 100\%$, in which the average Ca content of unburned vegetation was 14.7 mg/g for Wragg Fire site and 10.5 mg/g for Rocky Fire site, and the average Hg_{unburned} concentration was 26.8 ng/g for Wragg Fire site and 21.2 ng/g for Rocky Fire site (Ca and Hg data are shown in **Table S2.2**).

2.2.5 Stable Hg Isotope Analysis

We performed thermal combustion for stable Hg isotope analysis on unburned litter from three natural, unburned forests in the U.S. (Angelo Coast Range Reserve in northern California, University of Michigan Biological Station in northern Michigan, and Hubbard Brook Experimental Forest in central New Hampshire) and the Wragg Fire ash samples ($n=10$; 5 black ash [BA] and 5 white ash [WA]). Prior to thermal combustion, each dry sample was weighed into two clean ceramic sample boats (~0.5-1.0 g per boat), and packed with layers of pre-baked combustion powders (Nippon Instruments Corporation). Samples with low Hg content required multiple rounds of combustion and

sample Hg was later combined during the purge-and-trap sample purification step in order to have sufficient Hg (> 10 ng) for high-precision isotopic analysis (*see below*).

In brief, samples were thermally combusted in a two-stage furnace (the first furnace ramped from room temperature to 750 °C over 6 hours and the second furnace was held at 1,000 °C for the entire period). The released gaseous Hg(0) was collected into a 24 g trap solution containing 1% KMnO₄ (w/w) in 10% trace-metal grade H₂SO₄ (v/v). Following combustion, the trap solution was transferred into an acid-cleaned 40 mL borosilicate glass vial with PTFE-lined septum. To analyze Hg content, the trap solution was completely neutralized with 30% hydroxylamine, and an aliquot of solution was taken for quantification of Hg using the CVAFS system (Brooks Rand Model III CVAFS; described in section **2.2.3**).

Mercury in the initial trap solution (from combustion) was purged (upon complete reduction by 20% SnCl₂) and trapped into a smaller trap solution (6 to 15 g of 1% KMnO₄ in 10% H₂SO₄, depending on the total amount of sample Hg) in order to (i) separate sample Hg from other combustion products in the initial trap solution, and (ii) concentrate Hg in this final solution for Hg isotope analysis. The final trap solution was neutralized and an aliquot of solution was taken for analyzing Hg to determine the recovery of Hg during the purge-and-trap (typically > 95%). Hg levels in the final trap solution were precisely adjusted to a uniform Hg concentration (± 5%) along with a bracketing Hg isotope standard (SRM-NIST-3133) ranging from 2-5 ng/g to (Blum & Bergquist 2007). Stable Hg isotope ratios were measured using a Nu Instruments multicollector-inductively coupled plasma-mass spectrometer (MC-ICP-MS) following

the methods of Blum and Bergquist in the Biogeochemistry and Environmental Isotope Geochemistry Laboratory at the University of Michigan (Ann Arbor, MI) ((Blum & Bergquist 2007). Mass-dependent fractionation (MDF) of Hg isotopes was reported as $\delta^{202}\text{Hg}$ in permil (‰) referenced to SRM-NIST-3133, while mass-independent fractionation (MIF) of Hg isotopes is the difference between the measured $\delta^{202}\text{Hg}$ value and the value that would be predicted based on mass dependence. The mass-independent Hg isotope composition is reported in ‰ for both odd-mass isotopes $\Delta^{199}\text{Hg}$ and $\Delta^{201}\text{Hg}$ and even-mass isotopes $\Delta^{200}\text{Hg}$ and $\Delta^{204}\text{Hg}$. Isotopic compositions were calculated according Blum & Bergquist (2007) as:

$$\delta^{202}\text{Hg} = \{[(^{202}\text{Hg} / ^{198}\text{Hg})_{\text{sample}} \div (^{202}\text{Hg} / ^{198}\text{Hg})_{\text{NIST 3133}}] - 1\} \times 1000 \quad (1)$$

$$\Delta^{201}\text{Hg} \approx \delta^{201}\text{Hg}_{\text{measured}} - (\delta^{202}\text{Hg}_{\text{measured}} \times 0.752) \quad (2)$$

$$\Delta^{199}\text{Hg} \approx \delta^{199}\text{Hg}_{\text{measured}} - (\delta^{202}\text{Hg}_{\text{measured}} \times 0.2520) \quad (3)$$

$$\Delta^{200}\text{Hg} \approx \delta^{200}\text{Hg}_{\text{measured}} - (\delta^{202}\text{Hg}_{\text{measured}} \times 0.5024) \quad (4)$$

$$\Delta^{204}\text{Hg} \approx \delta^{204}\text{Hg}_{\text{measured}} - (\delta^{202}\text{Hg}_{\text{measured}} \times 1.4930) \quad (5)$$

Analytical uncertainty was determined from replicated analyses of a secondary standard solution (UM-Almadén, mean values: $\delta^{202}\text{Hg} = -0.56$ ‰; $\Delta^{199}\text{Hg} = -0.02$ ‰; $n=11$), and replicate combustions and analyses of SRM-NIST-1515 (Apple Leaves [UNCG lot], mean values: $\delta^{202}\text{Hg} = -2.64$ ‰; $\Delta^{199}\text{Hg} = 0.05$ ‰; $n=6$) along with the field samples. These isotopic compositions are similar to previous studies (e.g., (Demers *et al.* 2013)). External analytical reproducibility of $\delta^{202}\text{Hg}$ measurements was estimated to be

$\pm 0.08\%$ for solutions with 5.0 ng/g and $\pm 0.14\%$ for 1.9 ng/g (2 SD) and for $\Delta^{199}\text{Hg}$ it was estimated to be $\pm 0.07\%$ (2 SD), based on the repeated analyses of SRM-NRCC-TORT-2 analyzed at different final Hg concentrations on MC-ICP-MS (1.9-5.0 ng/g) (Tsui *et al.* 2013; Tsui *et al.* 2014).

2.2.6 Testing Sorption Capability of Hg by Wildfire Ash

To determine if wildfire ash can adsorb ambient Hg, we used wildfire ash samples from the Wragg Fire to determine the Hg sorption potential of gaseous Hg [as elemental Hg(0)] and aqueous Hg [as inorganic Hg(II)]. We also used activated carbon as a reference sorbent for comparison to the ash materials. In detail, the ability of wildfire ash to adsorb aqueous Hg(II) was assessed in two sorption experiments that involved adding 1.0 g of ash (4 black ash and 4 white ash from the Wragg Fire, and activated carbon [CAS 7440-44-0; Alfa Aesar] as a positive control) into 100 mL of 18.2 M Ω /cm water spiked with HgCl₂ (Sigma-Aldrich) in 500 mL acid-cleaned borosilicate glass Erlenmeyer flasks. The mean actual Hg concentration in filtered, spiked solution before sorption was 70.3 pg/mL in the first experiment and 74.8 pg/mL in the second experiment. The ash as a solid slurry was shaken for 24 h on a shaker table at room temperature. The slurry was filtered through a pre-baked glass fiber filter (Whatman GF/B, 1.0- μ m pore size). Filtered aqueous samples were treated with an acidic mixture of permanganate/persulfate and heated at 80 °C overnight to complete sample digestion (Woerndle *et al.* 2018). Digested samples were neutralized, and weighed aliquots were analyzed for Hg as previously described. To test the capability of ash at adsorbing gaseous elemental Hg(0), we set up a sorption experiment using the purge-and-trap setup

we routinely used for purging large volumes of stream water for Hg isotopic analysis (*see setup and detailed procedures in Woerndle et al. (2018)*). The Hg(0) gas is slowly released by this method as SnCl₂ is slowly added to the reservoir of aqueous sample with Hg, as opposed to the situation for Hg analysis described above. In brief, we prepared 500 mL of acidic solution spiked with 15.0 ng of Hg from our SRM-NIST-3133 standard solution. We purged this solution by adding 10% SnCl₂ at a rate of ~1 mL/min. Reduced Hg(0) was sparged with 0.45- μ m filtered Hg-free ambient air (produced by a vacuum pump and passed through a Teflon filter and a gold-coated glass trap), and transferred through a soda lime trap (to remove moisture and neutralize acidic fumes) and a Teflon trap with only glass wool (as a negative control) or filled with an ash sample (Wragg Fire BA and WA) or activated carbon (CAS 7440-44-0; Alfa Aesar) as a positive control. The length of packed material inside the Teflon trap was 4.2 cm with an average mass of materials of 1.22 \pm 0.14 g (mean \pm s.d.). Any Hg(0) not removed by the ash or activated carbon trap was collected by the final, downstream gold trap. The gold trap was dried with Hg-free N₂ gas for 20 minutes, and analyzed for Hg as described above.

2.2.7 Examining Bioavailability of Hg in Ash during Incubation

To determine the release and potential bioavailability of Hg associated with wildfire ash for microbial methylation, we conducted a sealed incubation experiment similar to Tsui et al. (2008) by incubating an unburned litter sample from the reference forest in the northern California coast range and BA and WA from both wildfires in natural stream water for 4 and 12 weeks (Tsui *et al.* 2008). We conducted 4- and 12-week incubation experiments of ash and an unburned litter sample from a northern California

forest (Angelo Coast Range Reserve, Branscomb, CA) using sealed bottles. Previous studies have demonstrated that sealed bottle incubation with fresh litter and freshly collected stream water quickly turned anoxic (<1 week) and active microbial Hg methylation quickly proceeded with inorganic Hg(II) released from the decomposing litter (Balogh *et al.* 2002; Tsui *et al.* 2008). This study inoculated samples with the microbial community in freshly collected surface water from an urban stream near UNCG (South Buffalo Creek at Greensboro, NC; GPS location: 36.050563, -79.748731). A preliminary experiment using “aged” stream water (>3 months stored at 4 °C) from the catchment burned by the Wragg Fire in California did not result in detectable levels of MeHg even in the litter-incubated treatment (*data not shown*). This suggests that the anaerobic, methylating microbes needed to be derived from water freshly collected from the ambient environment.

In brief, the incubation experiments used 250 mL air-tight, sterile PETG bottles (Nalgene), and each bottle received 2.80 ± 0.01 g of 2-mm sieved ash or homogenized litter sample. A 280 ± 1.21 mL of unfiltered stream water (with resultant minimal head space in the container) was added to achieve a solid-to-water ratio of 10 g/L, which was 5 times higher than our previous incubation experiments using similar methods (Tsui *et al.* 2008). The bottle was tightly capped and further wrapped with layers of Parafilm to secure the closing. We did not flush the ash slurry with N₂ gas as anoxia was expected to develop quickly over the course of incubation. Each treatment was performed in triplicate. Sealed bottles were placed in the dark at room temperature (20-22 °C) for 4 weeks or 12

weeks. Each bottle was shaken daily to mix the contents (Tsui *et al.* 2008; Blum *et al.* 2018).

At the end of the incubation, bottles were opened and the "rotten egg" odor (i.e., hydrogen sulfide) was noted if it was present or absent to indicate the existence of sulfate-reduction during incubation (Balogh *et al.* 2002; Tsui *et al.* 2008). The aqueous solution was immediately filtered through a pre-baked Whatman GF/B filter (1.0- μm pore size) in an acid- and BrCl-cleaned glass filtration apparatus (Kimble™ Kontes™). Filtered samples were analyzed separately for pH, specific conductivity (12-week samples only), total-dissolved nitrogen (TDN), dissolved organic carbon (DOC), SUVA₂₅₄ (proxy for aromaticity of DOC), Hg and methylmercury (MeHg).

Hg in filtered water samples was analyzed after digestion using an acidic mixture of KMnO₄ and K₂S₂O₈, and heated at 80 °C overnight (Woerndle *et al.* 2018). Filtered water samples were preserved with 0.4 % HCl (Parker & Bloom 2005) and kept in the dark at 4 °C prior to distillation for matrix removal and MeHg analysis (Brooks Rand Model III CVAFS with GC/pyrolysis module). Procedures for MeHg analysis in aqueous samples at the UNCG laboratory are fully described in Woerndle *et al.* (2018). Percent of Hg as MeHg (i.e., %MeHg) in the filtered solution was used to evaluate Hg methylation potential, or conversely, the bioavailability of Hg for microbial methylation (Mitchell *et al.* 2008; Tsui *et al.* 2008).

Measured physiochemical properties of the filtered solution included pH (Mettler Toledo pH meter), specific conductivity (Fisher Scientific conductivity meter), dissolved organic carbon (DOC) and total-dissolved nitrogen (TDN) (Shimadzu TOC analyzer).

The UV-absorbance at 254 nm (UV_{254}) was measured using a diode array spectrophotometer (Hewlett Packard P8452A) and then used to calculate specific UV absorbance at 254 nm ($SUVA_{254}$; in L/mg-C/m) as a proxy for DOC aromaticity (Weishaar *et al.* 2003).

2.2.8 Statistical Analysis

Statistical differences ($p < 0.05$) between two groups were evaluated by student's t-test, and differences between multiple groups were assessed using one-way ANOVA with a post-hoc Tukey's Test. Regression analyses were conducted using SigmaPlot 12.5.

2.3 Results and Discussion

2.3.1 Chemical Properties and Hg Content of Ash

We found that the LOI value decreased in the order: unburned litter/woody materials (~95%) > BA (23-62%) > WA (3-15%) (**Figure 2.1A**) ($p < 0.05$), which was consistent with our expectation of decreasing organic matter content with higher burn intensity (Bodí *et al.*, 2014; Campos *et al.*, 2015). Consistent with other reports,¹⁵ the Ca content in ash was significantly elevated for BA and WA ($p < 0.05$) compared to unburned samples (**Figure 2.1B**) and Ca was significantly higher in WA than BA ($p < 0.05$). Black carbon (BC), defined here as the aromatic hydrocarbon (ArH) fraction, decreased in the order: WA > BA > unburned samples ($p < 0.05$; **Figure 2.1C**). In general, ArH was negatively and significantly correlated with LOI among ash samples ($p = 0.0013$; **Figure S2.2**). These results suggest that increasing burn intensity resulted in ash with a higher

proportion of BC, which is consistent with studies that examined water extracts of ash materials (Wang *et al.* 2015).

We report Hg concentrations of samples digested with aqua regia (i.e., [Hg_{method-2}]), as this digestion method releases the most Hg from different biogeochemical pools (Biester & Scholz 1996; Bloom *et al.* 2003; Olund *et al.* 2004). Similar to vegetation samples across a large geographic gradient in the United States (Obrist *et al.* 2011), we found only a narrow range of [Hg_{method-2}] for litter (20.3-40.1 ng/g in study sites; 35.0-57.8 ng/g in reference forests) and dead woody materials (14.6-57.0 ng/g in study sites) (**Figure 2.1D**). The [Hg_{method-2}] among all ashes ranged from 3.9-124.6 ng/g ($n=58$) (**Figure 2.1D**), with many samples having [Hg_{method-2}] higher than ash generated in lab studies (Friedli *et al.*, 2003; Mailman and Bodaly, 2005). We detected no significant differences in [Hg_{method-2}] among unburned samples, BA, and WA ($p>0.05$) (**Figure 2.1D**). We found that the pool of “% recalcitrant Hg” averaged 7.6% among all unburned samples tested (**Figure 2.1E**) (**Table 2.2**). In contrast, BA samples had highly variable, but significantly higher, “% recalcitrant Hg” than both unburned and WA samples ($p<0.05$), while WA samples (Rocky Fire only) had an intermediate-sized pool of “recalcitrant Hg%” (**Figure 2.1E**).

The negative relationship (significant for Rocky Fire samples only; $p<0.05$) between LOI and “% recalcitrant Hg” in BA from both the Wragg and Rocky Fires (**Figure 2.2A**) may help explain some variations of Hg *reactivity* in ash samples. Such relationships between LOI and “% recalcitrant Hg” were absent among WA samples (**Figure 2.2B**). For BA samples, we posit that increased burn intensity lowered LOI, and

thus potentially more BC was generated due to limited oxygen availability. It is intriguing that we find a positive linear correlation between ArH and “recalcitrant Hg” among all BA and unburned samples (i.e., $r^2 = 0.896$, $p < 0.001$) (**Figure 2.2C**). However, we found no such relationship for WA samples ($p > 0.05$) (**Figure 2.2D**).

Apparently, wildfire increased the occurrence of benzene-ring containing organic compounds in burned biomass, such as the aromatic hydrocarbon (ArH) fraction determined in this study. Aromatic hydrocarbons are known to have a high affinity for trace metals (Harrison *et al.* 2003) as a result of stable pi-complexes between aromatic hydrocarbon ligands and metals (Howell *et al.* 1984). Meanwhile, the lack of a relationship between ArH and recalcitrant Hg in WA may be attributed to the fact that the absolute abundance of OC in WA is very low (e.g., assuming half of the LOI is OC). Thus even WA has a high fraction of ArH (**Figure 2.1C**) and the absolute abundance of ArH is still low and has a narrow range of absolute ArH abundance (inferred by small range of LOI) among WA samples, which may weaken the regression relationship between %ArH and “% recalcitrant Hg” (**Figure 2.4D**).

2.3.2 Extent of Hg Volatilization upon Burning

Since Ca was significantly elevated ($p < 0.05$) in BA and WA compared to unburned samples from the Wragg and Rocky Fires, we performed a simple mass balance calculation to estimate Hg volatilization losses from the pre-burn fuel loads based on LOI and Ca in ash as compared to their unburned counterparts. We assumed a constant LOI of ~95% for the unburned fuels (based on our measured values of unburned materials) and that Ca was conserved during wildfires regardless of temperature and oxygen conditions

(see equations in section 2.2.4). BA and WA samples from the Wragg Fire (**Figure 2.3** and **Table S2.3**) indicated $\geq 80\%$ Hg loss compared to the fuel samples. WA in the Rocky Fire had estimated Hg losses of $\geq 90\%$, but interestingly, BA from the Rocky Fire had a wide range of Hg loss estimates from 34-83%. As previously noted, BA samples may contain materials originating from a wide range of fire conditions (temperature and oxygen levels) resulting in a mixture of highly contrasting ash materials in the horizontal and vertical dimensions. These results suggest that fire intensity and burning conditions (i.e., temperature, oxygen availability and duration) are important in determining Hg volatilization. Although we estimated Hg volatilization in individual samples in the present study, it should be noted that Hg volatilization/emission can be estimated in the field at the landscape level, but this would require the estimation of the total amount of fuel loss (Homann *et al.* 2015).

2.3.3 Isotopic Composition and Source Analysis of Hg in Ash

Forest litter in the unburned reference forests for this study and foliage from another study (Zheng *et al.* 2016) along a large geographic gradient in North America all show a relatively narrow range of $\delta^{202}\text{Hg}$ (MDF; mass-dependent fractionation) and $\Delta^{199}\text{Hg}$ (MIF; mass-independent fractionation) (**Figure 2.4; Table S2.4**). Since forests receive Hg predominantly from atmospheric deposition, we expect Hg isotopic compositions in the unburned vegetation materials (foliage, litter and dead wood) to be similar to the MDF and MIF values of our reference sites. Both BA and WA from the Wragg Fire had very different Hg isotopic compositions compared to litter and foliage samples, as well as gaseous Hg samples from other studies (**Figure 2.4**). Mean $\delta^{202}\text{Hg}$

values (MDF) followed the order: unburned (-2.25 ± 0.22 ‰, $n=16$) < BA (-1.74 ± 0.27 ‰, $n=5$) \approx WA (-1.30 ± 0.47 ‰, $n=5$) (**Figure 2.4**). The higher $\delta^{202}\text{Hg}$ values in ash samples are consistent with our expectation that lighter Hg isotopes are preferentially volatilized by fire while the heavier isotopes are concentrated in the residual ash, slightly more so for WA than BA (by an average of 0.44 ‰, **Figure 2.4**). However, it should be noted that there were large variations in $\delta^{202}\text{Hg}$, even within each ash sample type (WA vs. BA), suggesting mixing of partially burned and unburned materials in BA. Importantly, $\delta^{202}\text{Hg}$ was significantly correlated with LOI and ArH content of individual BA and WA samples (**Figure S2.3**). Thus, it appears that higher burning intensity leads to higher $\delta^{202}\text{Hg}$ in the residual ash.

There was a narrow range of $\Delta^{199}\text{Hg}$ (MIF) values among litter and foliage samples (-0.47 to -0.06 ‰; **Figure 2.6**) and the majority of the ash samples had slightly elevated $\Delta^{199}\text{Hg}$ values relative to litter and foliage, with one BA sample even having a slightly positive $\Delta^{199}\text{Hg}$ value ($+0.10$ ‰). MIF is not expected to occur as a result of combustion (at least in the dark), and is mainly caused by photochemical reactions (Bergquist & Blum 2007). Given the very small magnitude of differences among ash and the unburned materials, there is no compelling evidence for significant MIF during burning of biomass in wildfires. However, we cannot fully exclude the possibility that a small amount of MIF may have occurred during the post-burn period prior to sampling (3-5 weeks) when a surface layer of ash material was exposed to sunlight in the field. We also cannot rule out a small amount of dark microbial reduction in the soils leading to a very small magnitude of MIF through the nuclear volume mechanism (Jiskra *et al.* 2015).

2.3.4 Experimental Investigation of Hg Sorption by Wildfire Ash

To assess if the ash, once released into the environment, may interact with ambient forms of Hg, we conducted a controlled experiment to examine how wildfire ash may adsorb “ambient” Hg. We found that activated carbon ($n=1$) essentially removed all of the Hg(0) (15 ng per 1.22 g of dry material), consistent with its application to remove Hg(0) from flue gas (Korpiel & Vidic 1997; Diamantopoulou *et al.* 2010). In contrast, BA ($n=4$) and WA ($n=2$) removed little Hg(0), averaging $2.0\pm 0.65\%$ and $2.9\pm 3.6\%$ of Hg(0), respectively (**Figure 2.5** and **Table S2.5**). In contrast to the “weak” sorption of gaseous Hg(0) by ash, very strong sorption of aqueous Hg(II) (at 70.3 ng/L in 100 mL solution, per 1 g of materials) was measured using both BA (final Hg(II): 5.3 ± 3.1 ng/L; removal: $92.5\pm 4.4\%$; $n=4$) and WA (final Hg(II): 5.2 ± 4.9 ng/L; $92.7\pm 7.0\%$; $n=4$) (**Figure 2.5**), compared to the nearly 100% sorption of Hg(II) by activated carbon (0.01 ng/L; removal: $\sim 100\%$), which is similar to previous results (Huang & Blankenship 1984).

These results suggest that wildfire ash would not be expected to accumulate Hg(0) in the field (e.g., Hg evasion from underlying soil) and this corroborates the isotopic results given above that indicate Hg in ash is mainly derived from the original vegetation materials. Further, once deposited in aquatic environments, our sorption data suggests that ash can extensively interact with ambient Hg(II) in the water, potentially sequestering ambient Hg(II) into less reactive forms associated with components such as BC. Thus a higher frequency of wildfire induced by climate change might potentially alter the environmental fate of Hg by producing ash (especially BC) that can sequester Hg(II) in the environment.

2.3.5 Bioavailability of Ash-associated Hg under Sealed Incubation

We assessed the release and bioavailability of ash-associated Hg for methylation during sealed incubations with freshly collected surface water. This approach of prolonged incubation provides useful information but has some limitations as the resultant water chemistry can change considerably during the course of incubation. For example, the pH of water (beginning pH was 8.0) at the end of the incubations was as follows: litter (5.9 ± 0.64 ; $n=2$) < BA (7.7 ± 0.36 ; $n=28$) < WA (10.0 ± 0.91 ; $n=28$) (**Figure S2.4; Table S2.6 and S2.7**). We found that almost all BA or WA samples generated an obvious sulfidic smell, indicating the existence of anaerobic sulfate-reduction across all treatments in addition to the litter-incubated treatment (**Table S2.6 and S2.7**), which are similar to previous studies (Balogh *et al.* 2002; Tsui *et al.* 2008).

Compared to litter incubation ($n=1$ with triplicate incubation), we found much lower dissolved (total-) Hg and MeHg in the majority of BA or WA incubation samples after 4- and 12-weeks of incubation (**Figure 2.6 and Figure S2.5**). After 4 weeks of incubation, the percentage of Hg released from the solid materials (after accounting for all Hg pools from water and solid materials) followed the decreasing order: litter (3.3%; $n=1$) > BA ($0.83 \pm 0.50\%$; $n=14$) \approx WA ($0.70 \pm 0.57\%$; $n=14$). Importantly, Hg release appeared to be negatively and significantly correlated with the ArH content of the materials ($p=0.002$) (**Figure S2.6**), implying that “recalcitrant” Hg potentially associated with BC (especially in BA) may limit Hg release into the aqueous phase. However, our interpretation may be confounded by contrasting water quality properties across treatments, such as pH and dissolved organic carbon (DOC) levels (highest in unburned

materials, followed by BA, and then WA-incubations; **Figure S2.4**), as these parameters may have an influence on Hg release from these solid materials. After Hg is leached from the solid-phase, microbial MeHg production may take place in the aqueous phase during incubation under anoxic conditions (Tsui *et al.* 2008). In this study, we found that [MeHg] in filtered leachates was consistently low and close to our analytical detection limit of MeHg (0.02 ng/L) for the majority of BA and WA incubations.

However, the dissolved MeHg concentrations for the WA-incubations (and some BA-incubations) appeared to increase with prolonged incubation from 4- to 12-weeks, and these temporal increases were negatively related to the LOI (**Figure S2.7**). These results suggest that Hg associated with ligands in WA results in somewhat higher release of Hg from the solid-phase as compared to Hg released from BA during longer incubations. For most BA samples, dissolved Hg, and to a lesser extent MeHg, decreased from 4 to 12 weeks implying that during prolonged exposure aqueous Hg may be “re-adsorbed” onto the ArH pools in BA, or simply accumulate as a solid-phase Hg-sulfide, which has been shown to extensively bind dissolved Hg (Benoit *et al.* 2003). We observed similar patterns for litter-incubated treatments (“Litter”) with temporal decreases in both dissolved Hg and MeHg (**Figure S2.7**), which supports the possibility of sulfidic resorption of Hg.

As demonstrated in our aqueous Hg(II) sorption experiment, both BA and WA had the capability to extensively bind Hg(II) (**Figure 2.5**) and this may explain the low release of Hg from BA and WA in the 4-week treatment. In contrast, the 12-week

incubation data suggested that sorption from the aqueous phase may be “reversed” such that some of the ash-associated Hg was eventually released back to the ambient water.

2.3.6 Implications for Hg Biogeochemical Cycles

This study demonstrates that the Hg content in wildfire ash is different from ash generated from laboratory-controlled burning investigations (Friedli *et al.* 2003; Mailman & Bodaly 2005). We found that the majority of Hg in wildfire ash was derived from Hg that originally resided in vegetation materials (e.g., foliage and litter) based on their Hg isotopic compositions. While the majority (>80%) of the Hg in the litter was volatilized by the fire, considerable concentrations of Hg still existed in the resulting ash. Importantly, pyrolysis appears to generate BC and other constituents that may retain Hg within the residual materials, largely in recalcitrant forms. The recalcitrant forms of Hg in ash appear to sequester additional ambient Hg but inhibit subsequent biogeochemical transformations, such as Hg release into solution. Upon deposition into aquatic environments, a small portion of the ash-laden Hg (<1 %) is expected to be released based on our incubation data. The extent of Hg release and methylation generally decreased with increasing ArH content, suggesting a possible role of Hg sorption to BC in regulating solubility and bioavailability in the field.

Prolonged exposure to water (especially under reducing conditions) resulted in enhanced Hg release from WA, but a decreased release from BA, highlighting contrasting interactions among ash types generated under different burning conditions on the landscape. Thus we find that multiple factors (wildfire severity, BC/ArH, length of exposure to water, presence or absence of oxygen, etc.) interact to affect the fate of Hg

and determine whether ash serves as a sink or source of Hg for downstream aquatic environments. Our current findings suggest that wildfire ash could play an important role in global Hg cycling and the Hg biogeochemistry of terrestrial and aquatic ecosystems. For example, wildfire ash itself may decrease or have little effect on Hg contamination in downstream ecosystems (e.g., fish Hg accumulation) (Riggs *et al.* 2017) due to the less reactive nature of Hg within ash. It should also be recognized that in the unburned watersheds other factors such as post-burn alteration of food web structures in aquatic ecosystems may lead to subsequent changes in Hg accumulation in fish (Kelly *et al.* 2006). These effects are expected to be more pronounced in the future as climate change results in more frequent and intensive wildfires leading to increasing production of wildfire ash at the global scale.

2.4 References

- Balogh, S.J., Huang, Y., Offerman, H.J., Meyer, M.L. & Johnson, D.K. (2002). Episodes of elevated methylmercury concentrations in prairie streams. *Environmental Science and Technology*, 36, 1665-1670.
- Battin, T.J., Besemer, K., Bengtsson, M.M., Romani, A.M. & Packmann, A.I. (2016). The ecology and biogeochemistry of stream biofilms. *Nature Reviews Microbiology*, 14, 251.
- Benoit, J., Gilmour, C.C., Heyes, A., Mason, R. & Miller, C. (2003). Geochemical and biological controls over methylmercury production and degradation in aquatic ecosystems. ACS Publications.
- Bergquist, B.A. & Blum, J.D. (2007). Mass-dependent and-independent fractionation of Hg isotopes by photoreduction in aquatic systems. *Science*, 318, 417-420.
- Biester, H. & Scholz, C. (1996). Determination of mercury binding forms in contaminated soils: mercury pyrolysis versus sequential extractions. *Environmental Science and Technology*, 31, 233-239.
- Biswas, A., Blum, J.D., Klaue, B. & Keeler, G.J. (2007). Release of mercury from Rocky Mountain forest fires. *Global Biogeochemical Cycles*, 21.
- Bloom, N.S., Preus, E., Katon, J. & Hiltner, M. (2003). Selective extractions to assess the biogeochemically relevant fractionation of inorganic mercury in sediments and soils. *Analytica Chimica Acta*, 479, 233-248

- Blum, J.D. & Bergquist, B.A. (2007). Reporting of variations in the natural isotopic composition of mercury. *Analytical and Bioanalytical Chemistry*, 388, 353-359.
- Blum, P., Hershey, A., Tsui, M.-K., Hammerschmidt, C. & Agather, A. (2018). Methylmercury and methane production potentials in North Carolina Piedmont stream sediments. *Biogeochemistry*, 137, 181-195.
- Bodí, M.B., Martin, D.A., Balfour, V.N., Santín, C., Doerr, S.H., Pereira, P. *et al.* (2014). Wildland fire ash: Production, composition and eco-hydro-geomorphic effects. *Earth-Science Reviews*, 130, 103-127.
- Bodí, M.B., Mataix-Solera, J., Doerr, S.H. & Cerdà, A. (2011). The wettability of ash from burned vegetation and its relationship to Mediterranean plant species type, burn severity and total organic carbon content. *Geoderma*, 160, 599-607.
- Caldwell, C., Canavan, C. & Bloom, N. (2000). Potential effects of forest fire and storm flow on total mercury and methylmercury in sediments of an arid-lands reservoir. *Science of the Total Environment*, 260, 125-133.
- Campos, I., Vale, C., Abrantes, N., Keizer, J.J. & Pereira, P. (2015). Effects of wildfire on mercury mobilisation in eucalypt and pine forests. *Catena*, 131, 149-159.
- Chen, H.S., Wang, Z.F., Li, J., Tang, X., Ge, B.Z., Wu, X.L. *et al.* (2015). GNAQPMS-Hg v1.0, a global nested atmospheric mercury transport model: model description, evaluation and application to trans-boundary transport of Chinese anthropogenic emissions. *Geoscientific Model Development*, 8, 2857-2876.
- De la Rosa, J., Knicker, H., López-Capel, E., Manning, D., Gonzalez-Perez, J. & González-Vila, F. (2008). Direct detection of black carbon in soils by Py-GC/MS,

- carbon-13 NMR spectroscopy and thermogravimetric techniques. *Soil Science Society of America Journal*, 72, 258-267.
- DeBano, L.F., Neary, D.G. & Ffolliott, P.F. (1998). *Fire Effects on Ecosystems*. John Wiley & Sons.
- Demers, J.D., Blum, J.D. & Zak, D.R. (2013). Mercury isotopes in a forested ecosystem: Implications for air-surface exchange dynamics and the global mercury cycle. *Global Biogeochemical Cycles*, 27, 222-238.
- Diamantopoulou, I., Skodras, G. & Sakellariopoulos, G. (2010). Sorption of mercury by activated carbon in the presence of flue gas components. *Fuel Processing Technology*, 91, 158-163.
- Dlapa, P., Bodí, M.B., Mataix-Solera, J., Cerdà, A. & Doerr, S.H. (2015). Organic matter and wettability characteristics of wildfire ash from Mediterranean conifer forests. *Catena*, 135, 369-376.
- Engle, M.A., Sexauer Gustin, M., Johnson, D.W., Murphy, J.F., Miller, W.W., Walker, R.F. *et al.* (2006). Mercury distribution in two Sierran forest and one desert sagebrush steppe ecosystems and the effects of fire. *Science of the total Environment*, 367, 222-233.
- Friedli, H., Radke, L., Lu, J., Banic, C., Leitch, W. & MacPherson, J. (2003). Mercury emissions from burning of biomass from temperate North American forests: laboratory and airborne measurements. *Atmospheric Environment*, 37, 253-267.
- Friedli, H.R., Radke, L.F. & Lu, J.Y. (2001). Mercury in smoke from biomass fires. *Geophysical Research Letters*, 28, 3223-3226.

- Giglio, L., Randerson, J.T., van der Werf, G.R., Kasibhatla, P.S., Collatz, G.J., Morton, D.C. *et al.* (2010). Assessing variability and long-term trends in burned area by merging multiple satellite fire products. *Biogeosciences*, 7, 1171-1186.
- Gratz, L. E., Keeler, G. J., Blum, J. D. & Sherman, L. S. (2010). Isotopic composition and fractionation of mercury in Great Lakes precipitation and ambient air. *Environmental Science and Technology*, 44, 7764-7770.
- Harrison, R.M., Tilling, R., Callén Romero, M.a.S., Harrad, S. & Jarvis, K. (2003). A study of trace metals and polycyclic aromatic hydrocarbons in the roadside environment. *Atmospheric Environment*, 37, 2391-2402.
- Homann, P.S., Darbyshire, R.L., Bormann, B.T. & Morrissette, B.A. (2015). Forest Structure Affects Soil Mercury Losses in the Presence and Absence of Wildfire. *Environmental Science and Technology*, 49, 12714-12722.
- Howell, J., Goncalves, J., Amatore, C., Klasinc, L., Wightman, R. & Kochi, J. (1984). Electron transfer from aromatic hydrocarbons and their. pi.-complexes with metals. Comparison of the standard oxidation potentials and vertical ionization potentials. *Journal of the American Chemical Society*, 106, 3968-3976.
- Huang, C. & Blankenship, D. (1984). The removal of mercury (II) from dilute aqueous solution by activated carbon. *Water Research*, 18, 37-46.
- Jiskra, M., Wiederhold, J.G., Skyllberg, U., Kronberg, R.M., Hajdas, I. & Kretzschmar, R. (2015). Mercury deposition and re-emission pathways in boreal forest soils investigated with Hg isotope signatures. *Environmental Science and Technology*, 49, 7188-7196.

- Kelly, E.N., Schindler, D.W., St Louis, V.L., Donald, D.B. & Vladicka, K.E. (2006). Forest fire increases mercury accumulation by fishes via food web restructuring and increased mercury inputs. *Proceedings of the National Academy of Sciences*, 103, 19380-19385.
- Korpiel, J.A. & Vidic, R.D. (1997). Effect of sulfur impregnation method on activated carbon uptake of gas-phase mercury. *Environmental Science and Technology*, 31, 2319-2325.
- MacKenzie, M.D., McIntire, E., Quideau, S. & Graham, R. (2008). Charcoal distribution affects carbon and nitrogen contents in forest soils of California. *Soil Science Society of America Journal*, 72, 1774-1785.
- Mailman, M. & Bodaly, R.A. (2005). Total mercury, methyl mercury, and carbon in fresh and burned plants and soil in Northwestern Ontario. *Environmental Pollution*, 138, 161-166.
- Marlon, J.R., Bartlein, P.J., Walsh, M.K., Harrison, S.P., Brown, K.J., Edwards, M.E. *et al.* (2009). Wildfire responses to abrupt climate change in North America. *Proceedings of the National Academy of Sciences*, 106, 2519-2524.
- Mason, R.P. (2009). Mercury emissions from natural processes and their importance in the global mercury cycle. In: *Mercury Fate and Transport in the Global Atmosphere*. Springer, pp. 173-191.
- Middelburg, J.J., Nieuwenhuize, J. & van Breugel, P. (1999). Black carbon in marine sediments. *Marine Chemistry*, 65, 245-252.

- Mitchell, C.P., Branfireun, B.A. & Kolka, R.K. (2008). Spatial characteristics of net methylmercury production hot spots in peatlands. *Environmental Science and Technology*, 42, 1010-1016.
- Obrist, D., Johnson, D.W., Lindberg, S.E., Luo, Y., Hararuk, O., Bracho, R. *et al.* (2011). Mercury distribution across 14 U.S. Forests. Part I: spatial patterns of concentrations in biomass, litter, and soils. *Environmental Science and Technology*, 45, 3974-3981.
- Olund, S.D., DeWild, J.F., Olson, M.L. & Tate, M.T. (2004). Methods for the preparation and analysis of solids and suspended solids for total mercury. Techniques and Methods 5 A–8. U.S. Geological Survey. 2004. Reston, VA.
- Parker, J.L. & Bloom, N.S. (2005). Preservation and storage techniques for low-level aqueous mercury speciation. *Science of the Total Environment*, 337, 253-263.
- Pereira, P., Úbeda, X. & Martin, D.A. (2012). Fire severity effects on ash chemical composition and water-extractable elements. *Geoderma*, 191, 105-114.
- Riggs, C.E., Kolka, R.K., Nater, E.A., Witt, E.L., Wickman, T.R., Woodruff, L.G. *et al.* (2017). Yellow perch (*Perca flavescens*) mercury unaffected by wildland fires in northern Minnesota. *Journal of Environmental Quality*, 46, 623-631.
- Roy, D.P., Boschetti, L., Maier, S.W. & Smith, A.M. (2010). Field estimation of ash and char colour-lightness using a standard grey scale. *International Journal of Wildland Fire*, 19, 698-704.

- Scholze, M., Knorr, W., Arnell, N.W. & Prentice, I.C. (2006). A climate-change risk analysis for world ecosystems. *Proceedings of the National Academy of Sciences*, 103, 13116-13120.
- Sherman, L. S., Blum, J. D., Johnson, K. P., Keeler, G. J., Barres, J. A. & Douglas, T. A. (2010). Mass-independent fractionation of mercury isotopes in Arctic snow driven by sunlight. *Nature Geoscience*, 3, 173-177.
- Song, J. & Peng, P.a. (2010). Characterisation of black carbon materials by pyrolysis–gas chromatography–mass spectrometry. *Journal of Analytical and Applied Pyrolysis*, 87, 129-137.
- Tsui, M.T., Blum, J.D., Finlay, J.C., Balogh, S.J., Nollet, Y.H., Palen, W.J. *et al.* (2014). Variation in terrestrial and aquatic sources of methylmercury in stream predators as revealed by stable mercury isotopes. *Environmental Science and Technology*, 48, 10128-10135.
- Tsui, M.T.K., Blum, J.D., Finlay, J.C., Balogh, S.J., Kwon, S.Y. & Nollet, Y.H. (2013). Photodegradation of methylmercury in stream ecosystems. *Limnology and Oceanography*, 58, 13-22.
- Tsui, M.T.K., Finlay, J.C. & Nater, E.A. (2008). Effects of stream water chemistry and tree species on release and methylation of mercury during litter decomposition. *Environmental Science and Technology*, 42, 8692-8697.
- Tsui, M.T.K., Finlay, J.C. & Nater, E.A. (2009). Mercury bioaccumulation in a stream network. *Environmental Science and Technology*, 43, 7016-7022.

- Wang, J.J., Dahlgren, R.A. & Chow, A.T. (2015). Controlled Burning of Forest Detritus Altering Spectroscopic Characteristics and Chlorine Reactivity of Dissolved Organic Matter: Effects of Temperature and Oxygen Availability. *Environmental Science and Technology*, 49, 14019-14027.
- Weishaar, J.L., Aiken, G.R., Bergamaschi, B.A., Fram, M.S., Fujii, R. & Mopper, K. (2003). Evaluation of specific ultraviolet absorbance as an indicator of the chemical composition and reactivity of dissolved organic carbon. *Environmental Science and Technology*, 37, 4702-4708.
- Westerling, A.L., Hidalgo, H.G., Cayan, D.R. & Swetnam, T.W. (2006). Warming and earlier spring increase western US forest wildfire activity. *Science*, 313, 940-943.
- Williams, A.A., Karoly, D.J. & Tapper, N. (2001). The sensitivity of Australian fire danger to climate change. *Climatic Change*, 49, 171-191.
- Woerdle, G.E., Tsz-Ki Tsui, M., Sebestyen, S.D., Blum, J.D., Nie, X. & Kolka, R.K. (2018). New Insights on Ecosystem Mercury Cycling Revealed by Stable Isotopes of Mercury in Water Flowing from a Headwater Peatland Catchment. *Environmental Science and Technology*, 52, 1854-1861.
- Zheng, W., Obrist, D., Weis, D. & Bergquist, B.A. (2016). Mercury isotope compositions across North American forests. *Global Biogeochemical Cycles*, 30, 1475-1492.

2.5 Figures

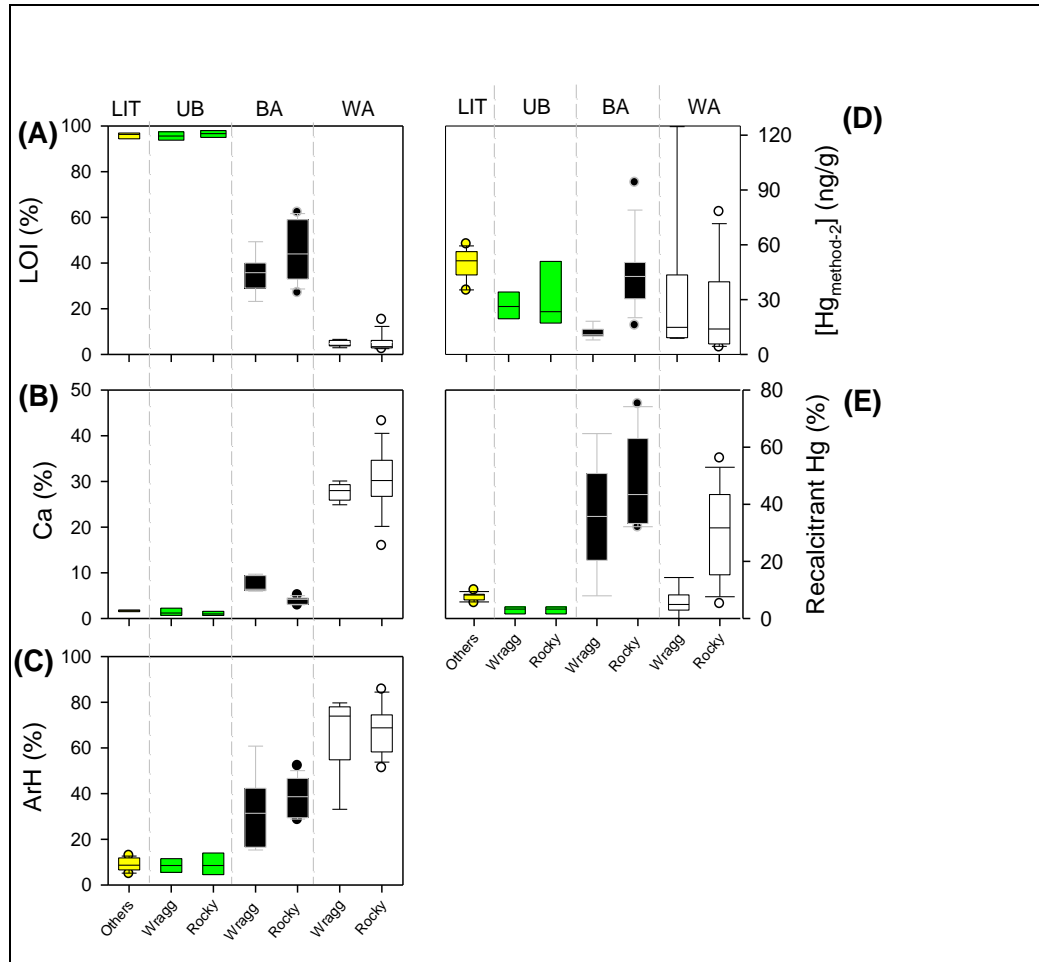


Figure 2.1. Properties and Hg in Ash and Unburned Litter. (A) loss-on-ignition (LOI), (B) calcium (Ca), (C) pyrolysis products (via Py-GC-MS analysis) as fraction of aromatic hydrocarbon (ArH), (D) Hg concentrations based on digestion method 2, aqua regia ($\text{Hg}_{\text{method-2}}$), and (E) percent recalcitrant Hg, in unburned litter (“LIT”) from the three reference forests (“others”) in yellow, litter/wood from the two fire sites (“UB”; in green; $n=2$ of litter and $n=2$ of wood per site), black ash (“BA”; in black; $n=5$ for Wragg, and $n=9$ for Rocky), and white ash (“WA”; in white; $n=5$ for Wragg, and $n=9$ for Rocky).

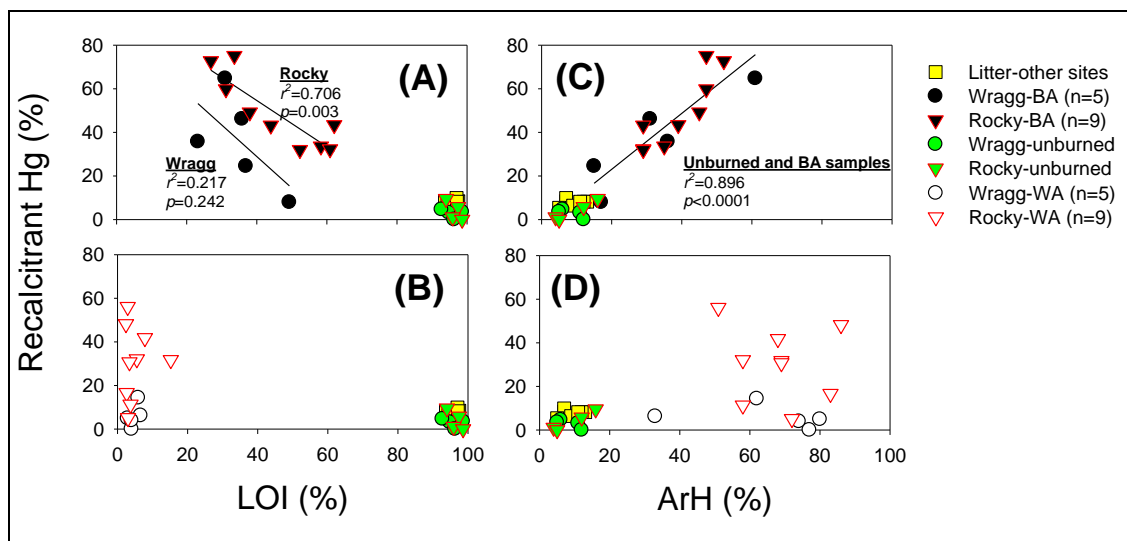


Figure 2.2. Relationships between LOI, ArH and Recalcitrant Hg. In detail, relationships between loss-on-ignition (LOI) and percent recalcitrant Hg in **(A)** unburned materials and black ash (BA), and **(B)** unburned materials and white ash (WA), and relationships between aromatic hydrocarbon (ArH) fraction of pyrolysis products and percent recalcitrant Hg in **(C)** unburned materials and BA, and **(D)** unburned materials and WA. Unburned samples are litter from three reference forests (as “Others”; in yellow), as well as litter/wood from the two fire sites (in green, different symbols).

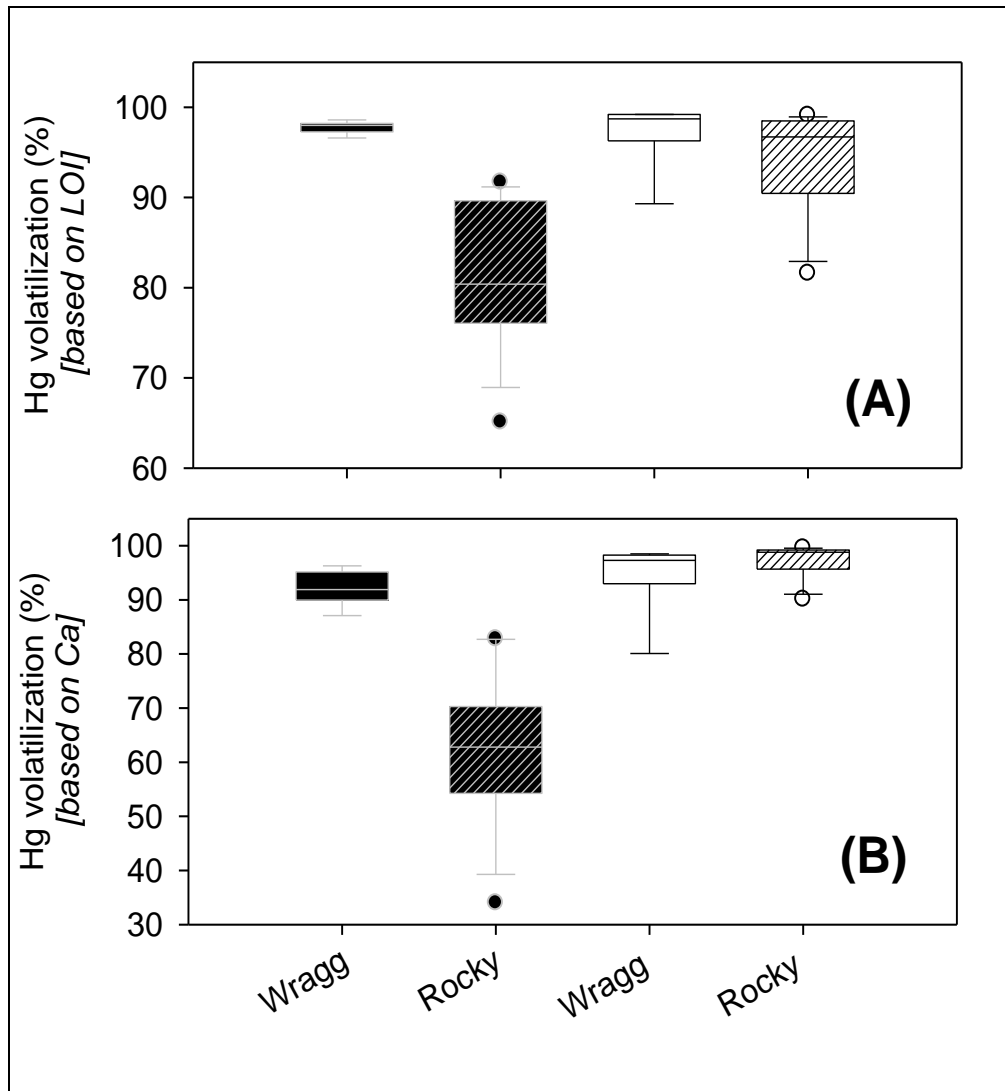


Figure 2.3. Estimation of Hg Volatilization. The original fuel loads were assumed to be a mixture of litter and dead woody materials in the Wragg Fire (2015) and the Rocky Fire (2015), based on (A) loss-on-ignition (LOI) and (B) calcium (Ca) content of ash samples. *Note:* Wragg Fire black ash (in black bars), Wragg Fire white ash (in white bars), Rocky Fire black ash (in hatched black bars), and Rocky Fire white ash (in hatched white bars). See **Table S2.3** for the individual ash data.

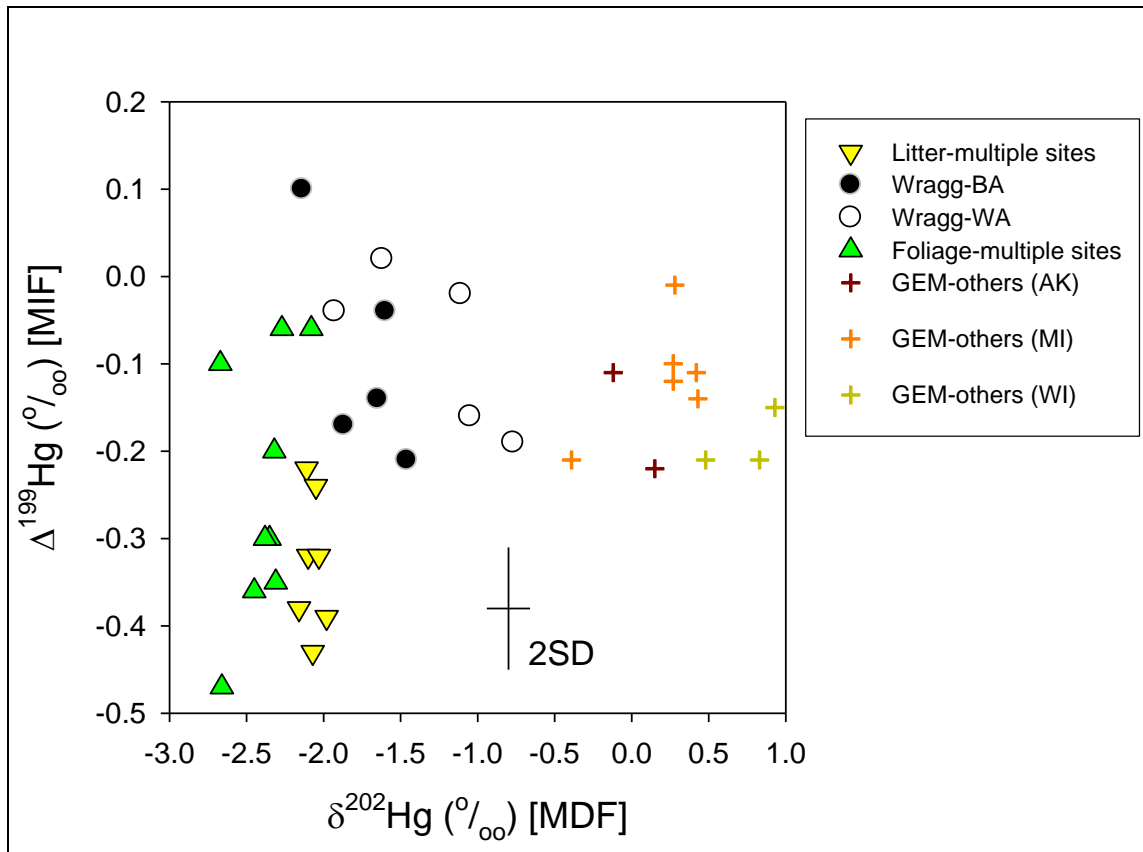


Figure 2.4. Isotopic Composition of Hg in Unburned Forest Litter and Ash. The unburned litter were from three reference forests in this study and foliage from Zheng *et al.* (2016). Ash samples were black ash (BA) and white ash (WA) collected from the Wragg Fire. Data on gaseous elemental mercury (GEM) were obtained from Gratz *et al.* (2010) for Michigan (MI), Sherman *et al.* (2010) for Alaska (AK), and Demers *et al.* (2013) for Wisconsin (WI). Error bars represent the maximum analytical error associated with sample analysis (2SD).

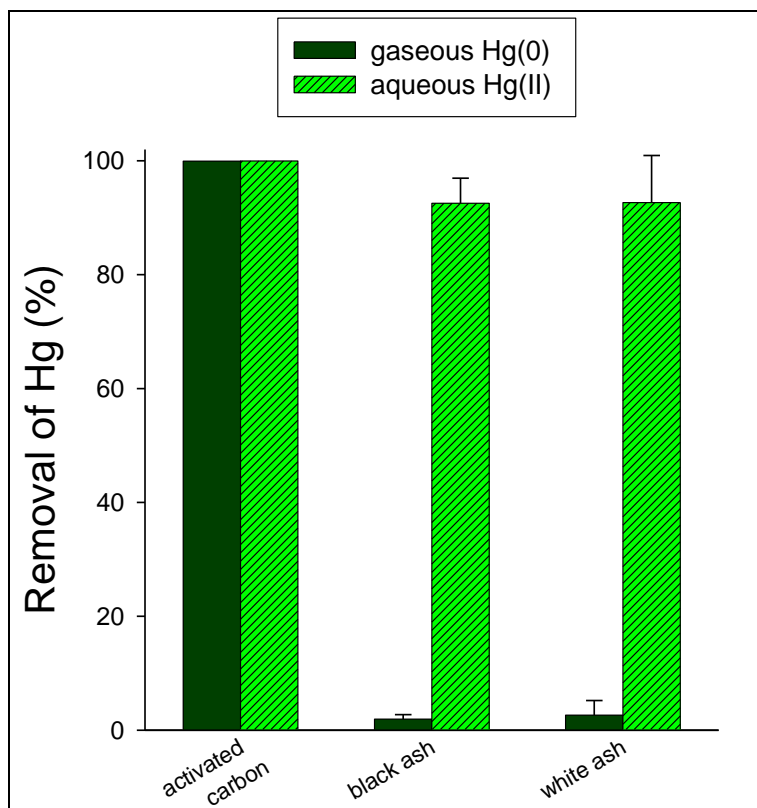


Figure 2.5. Ash Sorption Properties towards Aqueous and Gaseous Hg. Removal of gaseous Hg(0) (at 15 ng per test, passing through an average of 1.22 g of sorbent) and aqueous Hg(II) (at ~7-7.5 ng per test with 1.0 g of sorbent) by activated carbon ($n=1$ for both tests), black ash from the Wragg Fire ($n=4$ for both tests), and white ash from the Wragg Fire ($n=2$ for gaseous Hg(0) test and $n=4$ for aqueous Hg(II) test). Error bars represent standard deviation.

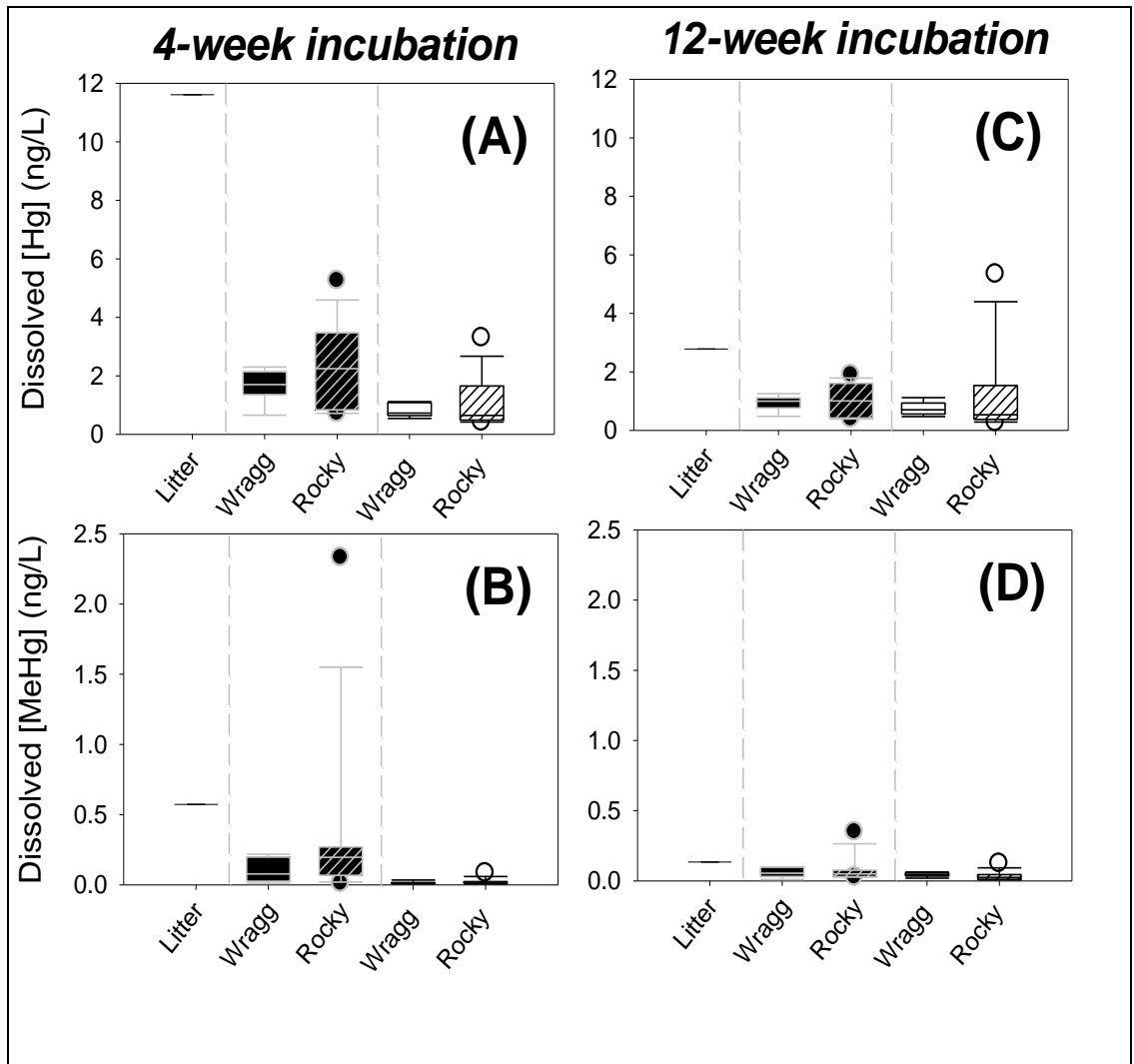


Figure 2.6. Dissolved Hg and MeHg in the Incubation Experiment. Box plots of (A) dissolved mercury concentrations ([Hg]) after 4 weeks of incubation, (B) dissolved methylmercury concentrations ([MeHg]) after 4 weeks of incubation, (C) dissolved [Hg] after 12 weeks of incubation, and (D) dissolved [MeHg] after 12 weeks of incubation, from an unburned northern California coast range forest litter, Wragg Fire black ash (in black bars), Wragg Fire white ash (in white bars), Rocky Fire black ash (in hatched black bars), and Rocky Fire white ash (in hatched white bars). Individual data represents triplicate of incubation. See SI Figure S2.5, SI Table S6, and SI Table S7 for the original data.

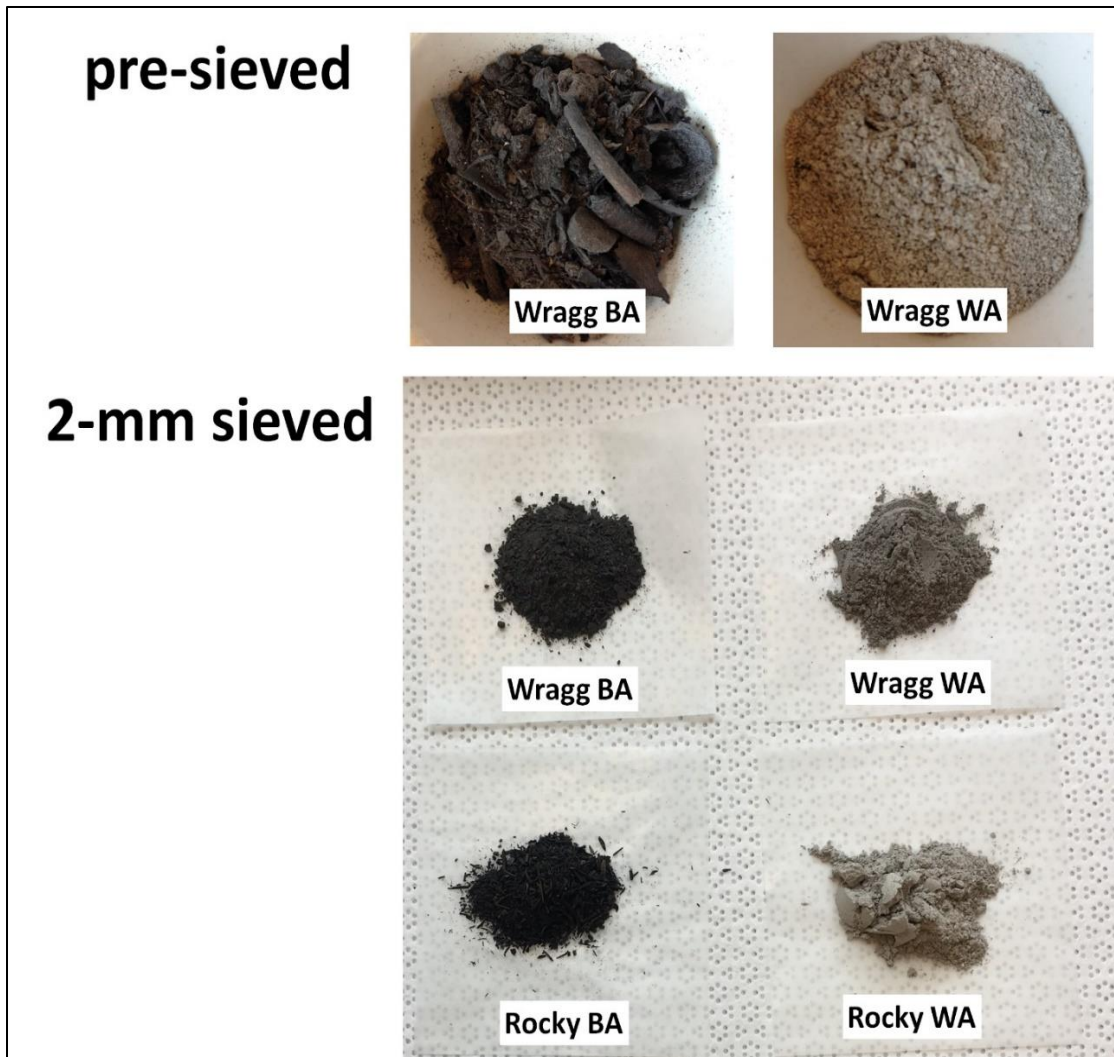


Figure S2.1. Pictures of Ash Samples. Top-pictures of pre-sieved surface (0-5 cm depth) ash samples -- black ash (BA) and white ash (WA) from the Wragg Fire (2015). Bottom-pictures of 2-mm sieved surface (0-5 cm depth) ash samples -- black ash (BA) and white ash (WA) from the Wragg Fire (2015), and the Rocky Fire (2015). Pictures taken by P. Ku and M. Tsui.

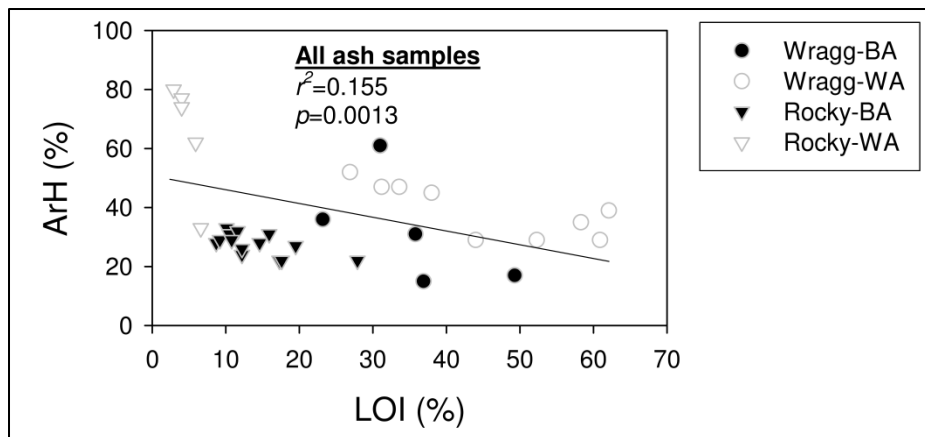


Figure S2.2. Relationship between LOI and ArH. Variation of percent aromatic hydrocarbon (ArH) of pyrolysis products as a function of loss-on-ignition (LOI) of black ash (BA) and white ash (WA) from the Wragg Fire and the Rocky Fire.

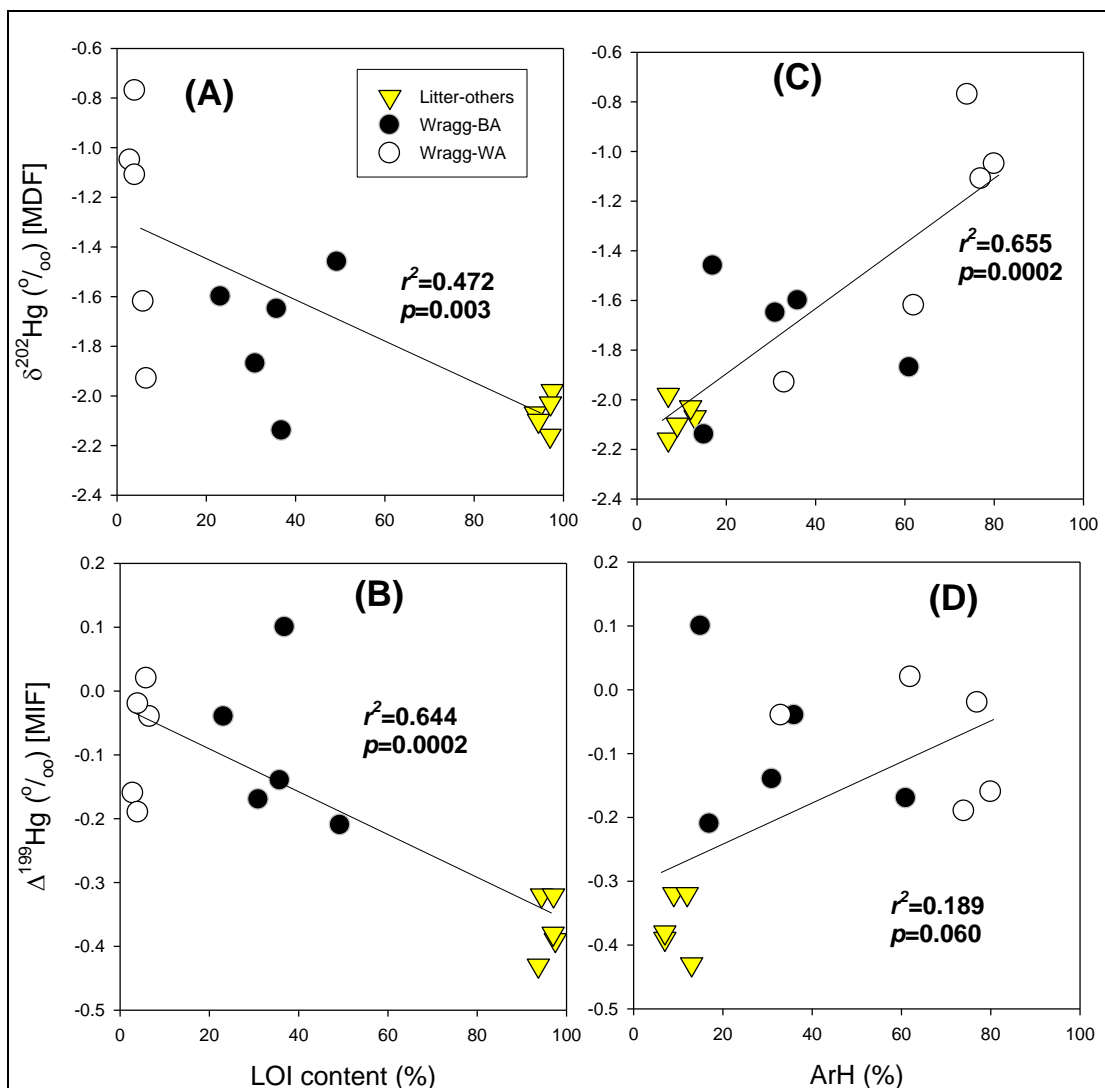


Figure S2.3. Relationship between Hg Isotopic Compositions and LOI, ArH Content. Relationships between loss-on-ignition (LOI) and (A) $\delta^{202}\text{Hg}$ (mass-dependent fractionation [MDF]), and (B) $\Delta^{199}\text{Hg}$ (mass-independent fractionation [MIF]) of Hg isotopes among different unburned litter and ash samples. Relationships between percent of aromatic hydrocarbon (ArH) of pyrolysis products content and (C) $\delta^{202}\text{Hg}$ (mass-dependent fractionation [MDF]), and (D) $\Delta^{199}\text{Hg}$ (mass-independent fractionation [MIF]) of Hg isotopes among different unburned and ash samples. Published isotope data of foliage was not included as that particular study (Zheng *et al.* 2016) did not provide information on LOI and ArH.

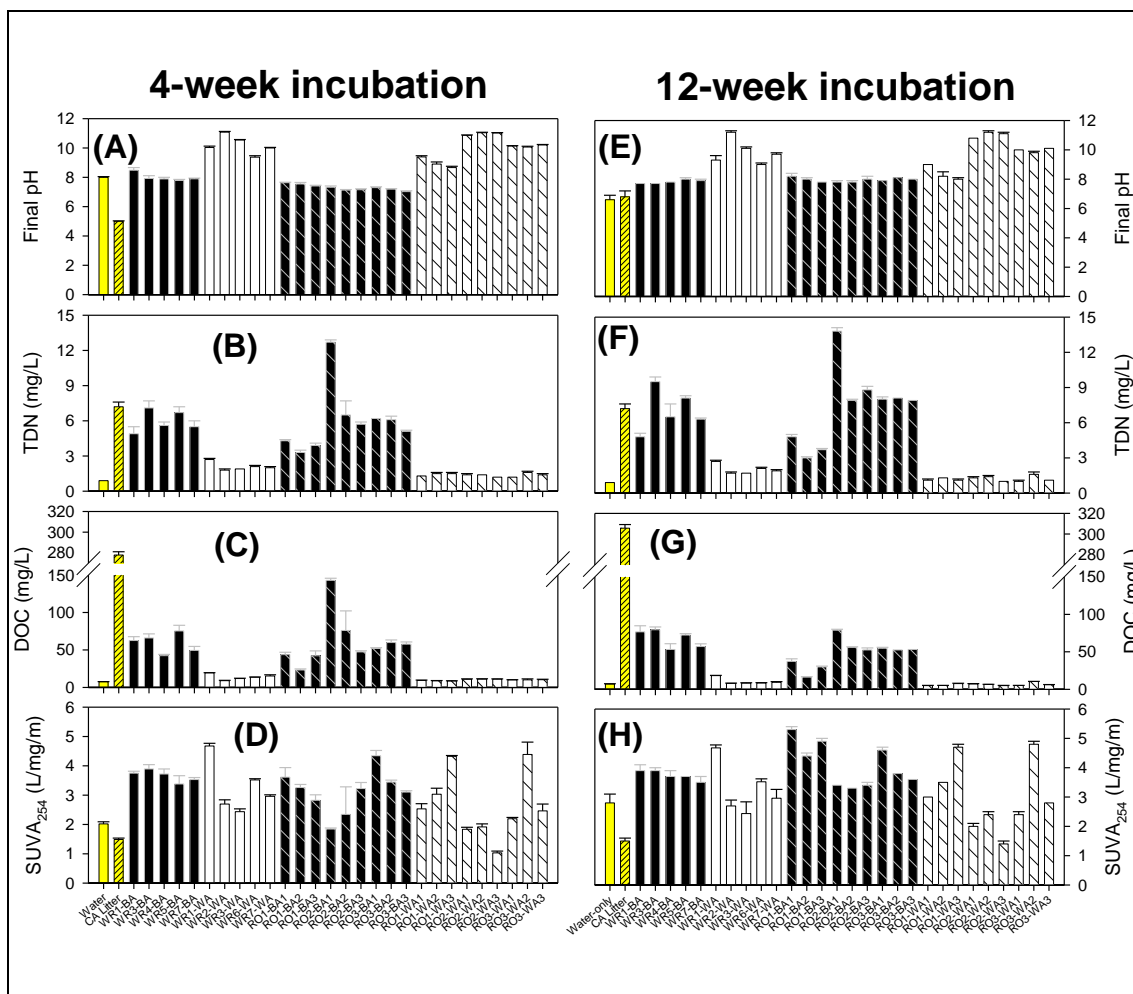


Figure S2.4. Physicochemical Properties Data in the Incubation Experiment. Data are mean \pm s.d. ($n=3$; except RO3-BA2 and RO3-BA3 where $n=1$) for 4-week and 12-week. (A, E) final pH at 4- and 12-week; (B, F) total dissolved nitrogen (TDN) at 4- and 12-week; (C, G) dissolved organic carbon (DOC) at 4- and 12-week; and (D, H) proxy of DOC aromaticity (SUVA₂₅₄) of the aqueous phase at 4- and 12-week. Note: Yellow: water-only; Hatched yellow: unburned litter from a northern California forest (Angelo Reserve); Black: BA from Wragg; White: WA from Wragg; Hatched black: BA from Rocky; Hatched white: WA from Rocky.

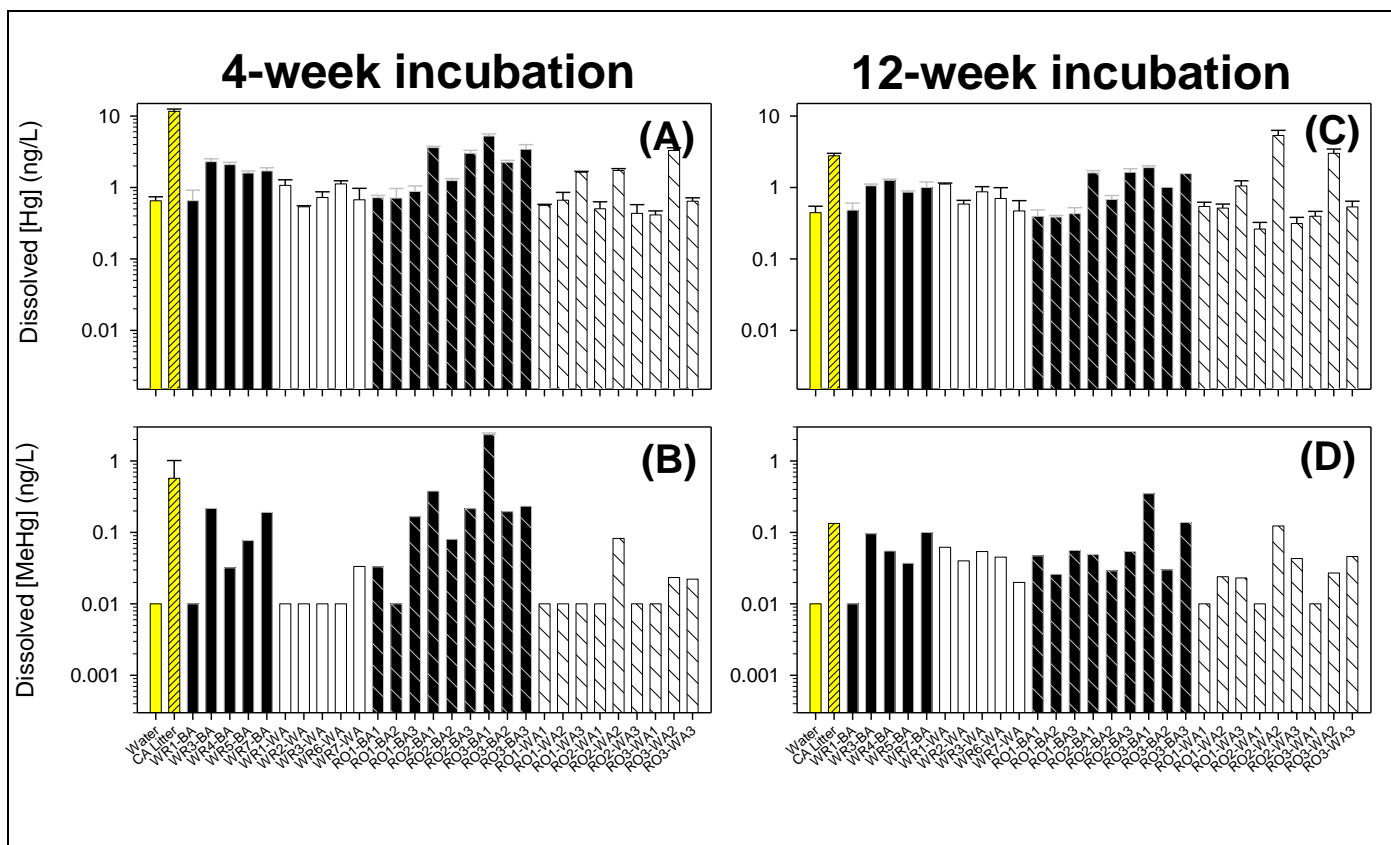


Figure S2.5. Variations of Dissolved Hg and MeHg in the Incubation Experiment. Individual concentration of dissolved ($<1\text{-}\mu\text{m}$) mercury concentrations ([Hg]; **A** and **C**) and dissolved methylmercury concentrations ([MeHg]; **B** and **D**) after 4- or 12-weeks of sealed incubation from water only (filtered stream water only, no solid materials added), unburned California litter (CA Litter), Wragg Fire black ash (WRX-BA), Wragg Fire white ash (WRX-WA), Rocky Fire black ash (RO#-BA), and Rocky Fire white ash (RO#-WA), where # is the site locations. Data are mean \pm s.d. ($n=3$ for Hg data while $n=1$ for most MeHg data).

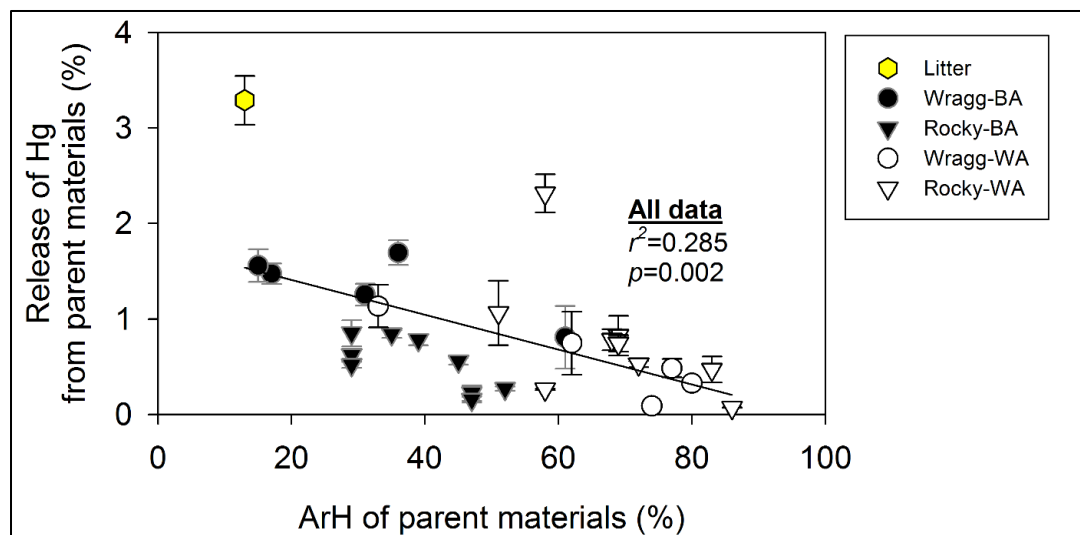


Figure S2.6. Role of Ash-ArH in Hg Release in the Incubation Experiment. Relationships among parameters after 4 weeks of sealed incubation experiment. Release of Hg from parent materials as a function of percent aromatic hydrocarbon (ArH) content of pyrolysis products.

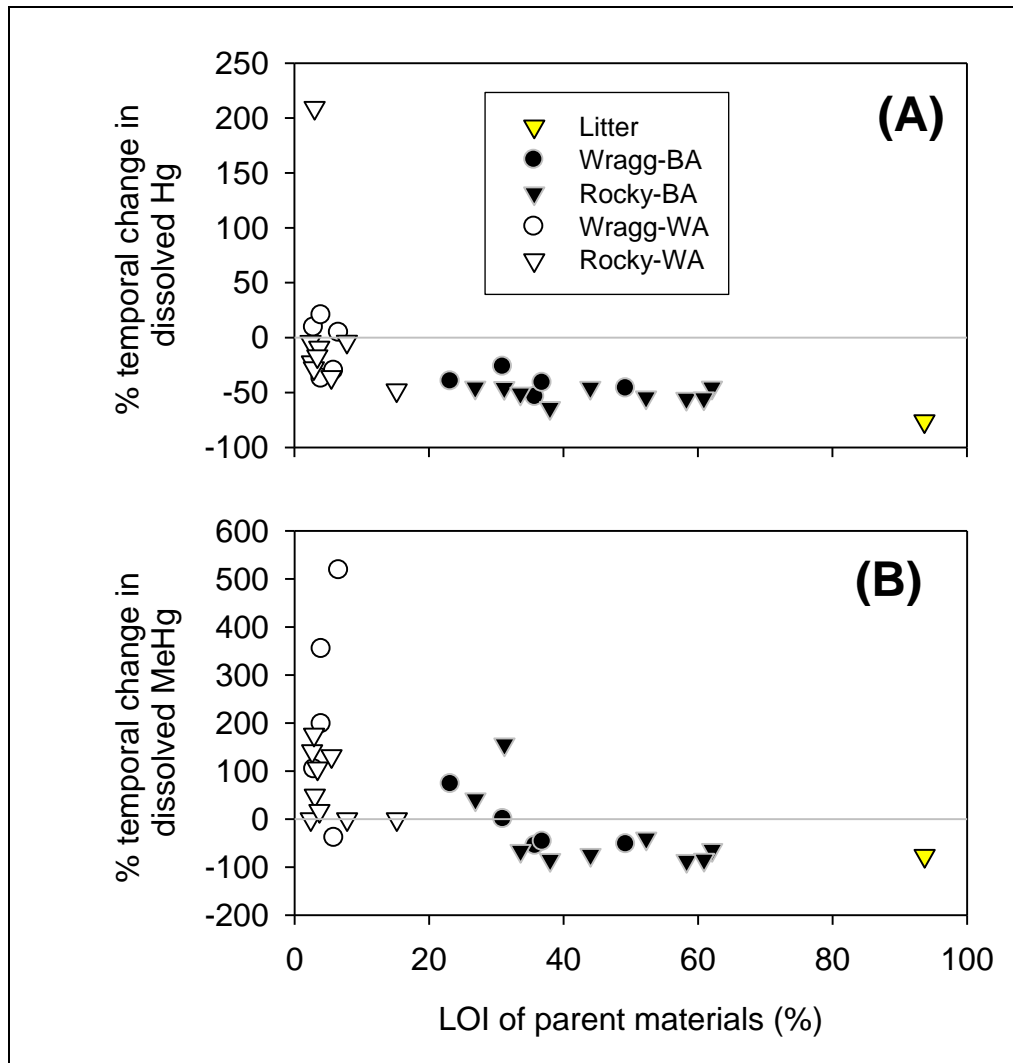


Figure S2.7. Role of LOI in Dissolved Hg and MeHg in the Incubation Experiment. Temporal percent changes of dissolved (A) mercury (Hg) and (B) methylmercury (MeHg) concentrations in incubation bottles from 4-weeks to 12-weeks among incubation materials of different loss-on-ignition (LOI).

2.6 Tables

Table S2.1. Summary of Wildfire Site Characteristics and Sampling Information.



	Wragg Fire	Rocky Fire
Dates	July 22 to August 5, 2015	July 29 to August 14, 2015
Locations	Lake Berryessa, CA	Clearlake, CA
Coordinates	38°29'12.98"N, 122° 4'30.29"W	38°57'48.29"N, 122°29'10.91"W
Burned area	33 km ²	281 km ²
Soil parent material	Mixed sedimentary: shale, mudstone & sandstone	Mixed sedimentary: shale, mudstone & sandstone
Dominant soils	Lithic Haploxerepts & Typic Dystroxerepts	Typic Dystroxerepts & <i>Mollic Haploxeralfs</i>
Dominant vegetation	Blue oak, live oak, scrub oak, chamise, manzanita, ceonothus	Blue oak, live oak, scrub oak, chamise, manzanita, ceonothus
Date of sampling	August 25, 2015	September 19, 2015
Rainfall prior to sampling	No	No
Sampling points	<i>~ 0.5 km transect / trail</i>	<i>~ 10-11 km between sites, along fire perimeter</i>
	 <p>WR1: 1xWA, 1xBA WR2: 1xWA WR3: 1xWA, 1xBA WR4: 1xBA WR5: 1xBA WR6: 1xWA WR7: 1xWA, 1xBA</p>	 <p>RO1: 3xWA, 3xBA RO2: 3xWA, 3xBA RO3: 3xWA, 3xBA</p>

Table S2.2. Physicochemical Properties of the Samples. The table showed the data of standard reference materials (SRMs), litter samples from reference forests, ash and unburned samples from the Wragg Fire (2015), and ash and unburned samples from the Rocky Fire (2015). *Note:* SRM-NIST-1515: apple leaves ($n=9$); SRM-IAEA-359: cabbage ($n=3$); CA-Litter: Angelo Coast Range Reserve ($n=1$); NH-Litter: Hubbard Brook Experimental Forest ($n=3$); MI-Litter: University of Michigan Biological Station ($n=3$). Individual sample data are shown for all ash and unburned samples. ND = not determined.

Category	Sample ID	Munsell color (Hue Value/Chroma)	LOI (%)	TN (%)	Ca (%)	Fe (%)	Hg _{method-1} (ng/g)	Hg _{method-2} (ng/g)	Recalcitrant Hg (%)	Relative abundance of pyrolysis products (%)								
										SaH	UnSaH	ArH	PAH	Carb	PhC	LgPhC	Hal	Ntg
SRMs	NIST-1515	ND	ND	ND	1.7	0.012	42.3	45.1	8.7	ND	ND	ND	ND	ND	ND	ND	ND	ND
	IAEA-359	ND	ND	ND	1.7	0.020	10.2	10.8	6.1	ND	ND	ND	ND	ND	ND	ND	ND	ND
Litter (ref. forests)	CA-Litter	ND	93.7	0.69	2.0	0.048	32.2	35.0	8.2	0	2	13	0	20	50	16	0	0
	NH-Litter	ND	96.3	1.73	ND	ND	53.2	57.8	8.2	4	19	8	4	21	23	17	1	6
	MI-Litter	ND	97.1	0.90	ND	ND	41.7	45.0	7.3	4	19	9	4	21	24	16	0	5
Wragg- unburned	Oak Litter	ND	94.8	1.97	1.4	0.80	27.2	28.1	3.1	1	0	11	0	36	13	8	0	30
	Pine Litter	ND	96.3	1.39	1.0	0.14	42.6	40.1	0	1	0	12	1	33	22	10	1	19
	Oak Wood	ND	92.7	0.69	3.1	0.04	25.4	24.3	4.6	1	1	6	0	25	11	15	0	41
	Pine Wood	ND	98.6	0.44	0.4	0.02	14.1	14.6	3.5	0	0	5	0	21	26	16	5	31
Wragg- black ash	WR1-BA	Gley1 3.5/N	31.0	0.64	9.7	2.3	2.8	7.9	64.7	3	4	61	2	7	5	0	2	15
	WR3-BA	Gley1 3/N	35.8	1.39	6.4	2.7	9.8	18.1	46.1	5	5	31	1	16	20	6	3	12
	WR4-BA	Gley 1 3.5/N	23.2	1.08	6.1	2.8	7.8	12.2	35.7	7	7	36	1	16	13	1	4	15
	WR5-BA	ND	49.3	1.54	9.3	1.4	9.7	10.6	7.9	9	33	17	2	6	26	2	0	6
	WR7-BA	Gley 1 2.75/N	36.9	1.17	6.0	2.9	8.1	10.7	24.5	7	38	15	3	4	14	0	0	20
Wragg- white ash	WR1-WA	Gley1 5.5/N	6.6	0.23	24.9	1.7	8.6	9.2	6.2	7	30	33	3	6	2	0	3	15
	WR2-WA	Gley1 7/N	2.9	0.11	29.0	1.4	15.6	16.4	4.9	0	0	80	5	1	0	0	0	14
	WR3-WA	Gley1 5.5/N	4.0	0.14	26.2	2.1	15.0	14.8	0	0	1	77	5	3	0	0	0	13
	WR6-WA	Gley1 5.5/N	4.0	0.15	30.1	1.6	119.8	124.6	3.9	0	3	74	6	4	0	0	0	14
	WR7-WA	Gley1 5.5/N	5.9	0.17	28.0	1.3	7.5	8.8	14.3	2	12	62	6	1	0	0	0	17
Rocky- unburned	Oak Litter	ND	94.0	1.87	1.3	0.02	18.3	20.3	9.5	1	0	16	0	34	24	6	0	20
	Pine Litter	ND	97.4	0.62	0.7	0.01	28.4	30.1	5.8	0	0	12	2	33	26	8	1	19
	Oak Wood	ND	95.9	0.67	1.8	0.02	16.0	16.2	1.1	1	0	4	0	15	8	24	0	49
	Pine Wood	ND	98.6	0.55	0.6	0.01	73.3	57.0	0.0	0	0	5	0	17	39	15	0	24
Rocky- black ash	RO1-BA1	Gley1 2.5/N	26.9	0.60	5.1	4.8	7.2	26.5	72.7	2	5	52	3	8	18	1	1	9
	RO1-BA2	Gley1 2.5/N	31.2	0.40	2.9	5.2	12.8	31.8	59.8	5	11	47	2	14	13	3	1	4
	RO1-BA3	Gley1 2.75/N	33.6	0.45	4.4	5.2	14.1	56.5	75.1	4	10	47	3	10	12	3	2	9
	RO2-BA1	Gley1 2.5/N	58.3	2.06	4.2	1.8	28.3	42.6	33.6	4	7	35	2	15	19	2	2	13
	RO2-BA2	10YR 2/1	62.1	2.11	3.1	1.2	8.9	15.8	43.4	4	6	39	3	12	16	5	2	14
	RO2-BA3	Gley1 2.5/N	44.0	1.54	3.1	2.6	27.4	48.2	43.2	4	7	29	1	14	21	9	2	12
	RO3-BA1	10YR 2/1	38.0	1.00	4.8	3.4	47.8	94.0	49.2	3	6	45	4	12	18	1	2	11
	RO3-BA2	2.5Y 2.5/1	60.9	1.85	4.2	1.8	29.0	42.9	32.3	4	5	29	1	16	21	11	1	11
	RO3-BA3	5Y 2.5/1	52.3	1.40	3.4	2.3	27.1	39.9	32.0	4	5	29	1	18	21	8	3	12

Rocky- white ash	RO1-WA1	10YR 7.5/1	2.4	0.08	26.5	2.3	40.4	78.0	48.2	0	1	86	4	3	0	0	0	7
	RO1-WA2	10YR 7/1	2.6	0.09	26.8	2.3	11.6	13.9	16.6	0	0	83	5	3	0	0	0	10
	RO1-WA3	2.5Y 7/1	5.5	0.16	27.5	2.1	42.0	61.8	32.1	3	5	58	5	13	1	0	0	16
	RO2-WA1	2.5Y 6.5/1	15.2	0.06	15.9	1.4	4.0	5.9	31.7	6	7	69	4	9	1	0	0	5
	RO2-WA2	Gley1 7.5/N	3.0	0.07	34.0	1.5	30.8	32.4	5.1	2	4	72	7	7	1	0	0	7
	RO2-WA3	WP 8.75/N	2.9	0.00	36.5	1.1	1.7	3.9	56.1	6	16	51	3	22	0	0	0	2
	RO3-WA1	2.5Y 7.5/1	7.8	0.00	33.9	1.0	2.9	5.0	41.8	2	5	68	7	5	0	0	0	14
	RO3-WA2	2.5Y 6/1	3.7	0.07	43.2	0.6	12.4	14.0	11.3	7	10	58	4	12	3	0	2	3
	RO3-WA3	Gley1 7.5/N	3.4	0.05	30.2	1.4	5.8	8.4	30.7	3	5	69	6	7	0	0	0	10

Table S2.3. Estimated Hg Volatilization. The original fuel loads were assumed to be a mixture of litter and dead woody materials) in the Wragg Fire (2015; WR) and the Rocky Fire (2015; RO). The estimations are based on two approaches: loss-on-ignition (LOI) and calcium (Ca) content of ash samples.

Sample ID	Hg volatilization (%) <i>based on LOI</i>	Hg volatilization (%) <i>based on Ca content</i>
WR1-BA	98.6	96.3
WR3-BA	96.6	87.1
WR4-BA	98.1	90.9
WR5-BA	97.5	94.8
WR7-BA	98.0	91.9
WR1-WA	99.2	98.2
WR2-WA	98.6	97.3
WR3-WA	98.7	97.3
WR6-WA	89.3	80.1
WR7-WA	99.2	98.5
RO1-BA1	91.7	82.6
RO1-BA2	89.4	62.8
RO1-BA3	80.4	56.6
RO2-BA1	76.5	66.2
RO2-BA2	90.4	82.8
RO2-BA3	80.2	47.2
RO3-BA1	65.1	34.0
RO3-BA2	74.7	65.4
RO3-BA3	80.7	60.5
RO1-WA1	81.6	90.1
RO1-WA2	96.7	98.3
RO1-WA3	84.9	92.4
RO2-WA1	98.4	98.8
RO2-WA2	92.3	96.8
RO2-WA3	99.1	99.6
RO3-WA1	98.7	99.5
RO3-WA2	96.6	98.9
RO3-WA3	98.0	99.1

Table S2.4. Stable Hg Isotope Compositions. The data below showed the stable Hg isotope compositions of undecomposed litter from reference forests, published data on foliage in other North American forests (Zheng et al., 2016), and black ash (BA) and white ash (WA) samples from Wragg Fire (2015). *Note:* MDF=mass dependent fractionation; MIF=mass independent fractionation.

Sample type and/or sources	Location / Sample ID	$\delta^{202}\text{Hg}$ (‰) [MDF]	$\Delta^{204}\text{Hg}$ (‰) [MIF]	$\Delta^{201}\text{Hg}$ (‰) [MIF]	$\Delta^{200}\text{Hg}$ (‰) [MIF]	$\Delta^{199}\text{Hg}$ (‰) [MIF]
Reference forests	Angelo Forest / CA-Litter	-2.07	0.12	-0.37	-0.04	-0.43
	Hubbard Forest / HB-Litter 1	-1.98	0.01	-0.38	0.03	-0.39
	Hubbard Forest / HB-Litter 2	-2.16	0.00	-0.34	-0.01	-0.38
	Hubbard Forest / HB-Litter 3	-2.10	0.02	-0.28	0.01	-0.32
	U-M Biostation / MI-Litter 1	-2.03	-0.01	-0.30	0.00	-0.32
	U-M Biostation / MI-Litter 2	-2.11	0.05	-0.21	-0.04	-0.22
	U-M Biostation / MI-Litter 3	-2.05	0.03	-0.22	0.00	-0.24
Published data in foliage in other North American forests (Zheng et al., 2016)	Truckee, CA	-2.67	-0.01	-0.04	0.01	-0.10
		-2.27	0.01	-0.04	0.04	-0.06
		-2.08	-0.01	0.00	0.02	-0.06
	Niwot Ridge, CO	-2.31	-0.01	-0.31	-0.04	-0.35
		-2.32	0.01	-0.18	0.00	-0.20
	Howland, ME	-2.35	0.08	-0.24	-0.05	-0.30
		-2.38	0.06	-0.27	-0.02	-0.30
	Thompson Forest, WA	-2.66	0.00	-0.47	0.01	-0.47
		-2.45	0.02	-0.35	-0.01	-0.36
	Black ash (BA)	WR1-BA	-1.87	-0.01	-0.20	0.08
WR3-BA		-1.65	-0.03	-0.20	0.03	-0.14
WR4-BA		-1.60	-0.05	-0.13	0.03	-0.04
WR5-BA		-1.46	0.09	-0.19	0.01	-0.21
WR7-BA		-2.14	0.00	-0.03	0.01	0.10
White ash (WA)	WR1-WA	-1.93	-0.04	-0.05	0.04	-0.04
	WR2-WA	-1.05	-0.12	-0.24	-0.03	-0.16
	WR3-WA	-1.11	-0.14	0.00	-0.02	-0.02
	WR6-WA	-0.77	0.00	-0.23	0.04	-0.19
	WR7-WA	-1.62	-0.07	0.01	0.00	0.02

Table S2.5. Sorption of Ash towards Aqueous and Gaseous Hg. Activated carbon is the control. The ash were from Wragg Fire only. ND=not determined.

	Removal of aqueous Hg(II) (~7.0-7.5 ng per test)	Removal of gaseous Hg(0) (15 ng per test)
Activated carbon	99.9%	99.9%
WR1-BA	97.2%	2.9%
WR3-BA	89.2%	1.6%
WR4-BA	95.3%	ND
WR5-BA	ND	1.4%
WR7-BA	88.3%	2.1%
WR1-WA	95.6%	ND
WR2-WA	98.3%	5.4%
WR3-WA	94.4%	0.4%
WR6-WA	ND	ND
WR7-WA	82.4%	ND

Table S2.6. Results of Sealed Incubation Experiments after 4-weeks. Results are means \pm S.D., except for MeHg in which we pooled the majority of samples from replicates for analysis. All dissolved constituents represent <1.0- μ m fraction. *Note:* smell is sulfide, “rotten” egg smell present (+) or absent (-); DOC=dissolved organic carbon; SUVA₂₅₄=specific ultraviolet absorbance at 254 nm (proxy of DOC aromaticity); TDN=total dissolved nitrogen; Hg=mercury; MeHg=methylmercury; %MeHg=percent of Hg as MeHg.

	Smell	pH	DOC (mg/L)	SUVA ₂₅₄ (L/mg/m)	TDN (mg/L)	Filtered Hg (ng/L)	Filtered MeHg (ng/L)	%Me Hg
Water-only	-	8.0 \pm 0.0	7.6 \pm 0.2	2.0 \pm 0.1	0.9 \pm 0.0	0.7 \pm 0.1	<0.02 \pm 0.0	2.9
CA-Litter	+	5.0 \pm 0.0	277.7 \pm 3.2	1.5 \pm 0.0	7.2 \pm 0.4	11.6 \pm 0.9	0.57 \pm 0.44	4.9
WR1-BA	+	8.5 \pm 0.2	62.6 \pm 5.0	3.7 \pm 0.1	4.9 \pm 0.6	0.7 \pm 0.3	<0.02	2.9
WR3-BA	+	7.9 \pm 0.2	66.0 \pm 5.5	3.9 \pm 0.1	7.1 \pm 0.6	2.3 \pm 0.2	0.22	9.6
WR4-BA	+	7.9 \pm 0.1	42.3 \pm 1.7	3.7 \pm 0.2	5.6 \pm 0.3	2.1 \pm 0.2	<0.02	1.0
WR5-BA	+	7.8 \pm 0.1	75.3 \pm 7.5	3.4 \pm 0.3	6.7 \pm 0.5	1.6 \pm 0.1	0.08	5.0
WR7-BA	+	7.9 \pm 0.1	49.3 \pm 5.4	3.5 \pm 0.1	5.5 \pm 0.5	1.7 \pm 0.2	0.19	11.2
WR1-WA	+	10.0 \pm 0.1	19.5 \pm 0.2	4.7 \pm 0.1	2.7 \pm 0.1	1.1 \pm 0.2	<0.02	1.8
WR2-WA	+	11.1 \pm 0.0	9.0 \pm 0.4	2.7 \pm 0.1	1.8 \pm 0.1	0.5 \pm 0.0	<0.02	4.0
WR3-WA	+	10.5 \pm 0.0	11.9 \pm 0.4	2.4 \pm 0.1	1.9 \pm 0.0	0.7 \pm 0.1	<0.02	2.9
WR6-WA	+	9.4 \pm 0.1	13.7 \pm 0.2	3.5 \pm 0.0	2.1 \pm 0.1	1.1 \pm 0.1	<0.02	1.8
WR7-WA	+	10.0 \pm 0.0	15.3 \pm 1.6	3.0 \pm 0.1	2.0 \pm 0.1	0.7 \pm 0.3	<0.02	2.9
RO1-BA1	+	7.6 \pm 0.0	43.8 \pm 3.1	3.6 \pm 0.3	4.3 \pm 0.1	0.7 \pm 0.1	<0.02	2.9
RO1-BA2	+	7.5 \pm 0.1	23.3 \pm 1.4	3.3 \pm 0.1	3.3 \pm 0.2	0.7 \pm 0.3	<0.02	2.9
RO1-BA3	+	7.4 \pm 0.0	42.1 \pm 6.6	2.8 \pm 0.2	3.9 \pm 0.2	0.9 \pm 0.2	<0.02	18.9
RO2-BA1	+	7.3 \pm 0.1	142.9 \pm 2.9	1.8 \pm 0.0	12.7 \pm 0.2	3.6 \pm 0.2	0.38	10.6
RO2-BA2	+	7.1 \pm 0.0	76.0 \pm 26.2	2.3 \pm 0.9	6.5 \pm 1.2	1.2 \pm 0.1	0.08	6.7
RO2-BA3	+	7.2 \pm 0.1	47.4 \pm 1.6	3.2 \pm 0.2	5.7 \pm 0.2	3.0 \pm 0.3	0.22	7.3
RO3-BA1	+	7.3 \pm 0.1	52.0 \pm 1.1	4.3 \pm 0.2	6.2 \pm 0.0	5.2 \pm 0.4	2.33 \pm 0.14	44.8
RO3-BA2	+	7.2 \pm 0.0	59.9 \pm 3.4	3.4 \pm 0.1	6.1 \pm 0.3	2.2 \pm 0.1	0.20	0.9
RO3-BA3	+	7.0 \pm 0.1	57.6 \pm 3.0	3.1 \pm 0.1	5.1 \pm 0.1	3.4 \pm 0.6	0.23	6.8
RO1-WA1	+	9.4 \pm 0.1	5.9 \pm 0.4	2.5 \pm 0.2	1.3 \pm 0.0	0.6 \pm 0.0	<0.02	3.3
RO1-WA2	+	8.9 \pm 0.2	6.4 \pm 0.3	3.0 \pm 0.2	1.5 \pm 0.1	0.7 \pm 0.2	<0.02	2.9
RO1-WA3	+	8.7 \pm 0.1	8.8 \pm 0.2	4.3 \pm 0.0	1.5 \pm 0.1	1.6 \pm 0.1	<0.02	1.3
RO2-WA1	+	10.9 \pm 0.0	7.6 \pm 0.5	1.8 \pm 0.1	1.4 \pm 0.1	0.5 \pm 0.1	<0.02	4.0
RO2-WA2	+	11.0 \pm 0.0	6.2 \pm 0.4	1.9 \pm 0.1	1.4 \pm 0.0	1.7 \pm 0.1	0.08	4.7
RO2-WA3	+	11.0 \pm 0.0	5.8 \pm 0.4	1.0 \pm 0.1	1.2 \pm 0.0	0.4 \pm 0.1	<0.02	5.0
RO3-WA1	+	10.1 \pm 0.0	5.5 \pm 0.1	2.2 \pm 0.0	1.2 \pm 0.0	0.4 \pm 0.1	<0.02	5.0
RO3-WA2	+	10.1 \pm 0.1	11.3 \pm 1.3	4.4 \pm 0.4	1.6 \pm 0.1	3.3 \pm 0.3	<0.02	0.6
RO3-WA3	+	10.2 \pm 0.0	7.1 \pm 0.7	2.5 \pm 0.2	1.4 \pm 0.1	0.6 \pm 0.1	<0.02	3.3

Table S2.7. Results of Sealed Incubation Experiments after 12-weeks. Results are means \pm S.D., except for MeHg in which we pooled the majority of samples from replicates for analysis. All dissolved constituents represent <1.0- μ m fraction. *Note:* smell is sulfide, “rotten” egg smell present (+) or absent (-); COND=conductivity; DOC=dissolved organic carbon; SUVA₂₅₄=specific ultraviolet absorbance at 254 nm (proxy of DOC aromaticity); TDN=total dissolved nitrogen; Hg=mercury; MeHg=methylmercury; %MeHg=percent of Hg as MeHg.

	Smell	COND (μ S/cm)	pH	DOC (mg/L)	SUVA ₂₅₄ (L/mg/m)	TDN (mg/L)	Filtered Hg (ng/L)	Filtered MeHg (ng/L)	%Me Hg
Water-only	-	124 \pm 3	6.6 \pm 0.3	7.0 \pm 0.5	2.8 \pm 0.3	0.3 \pm 0.0	0.4 \pm 0.1	<0.02	0.0
CA-Litter	+	387 \pm 4	6.8 \pm 0.4	305.6 \pm 3.6	1.5 \pm 0.1	3.6 \pm 0.5	2.8 \pm 0.2	0.13	4.8
WR1-BA	+	645 \pm 17	7.7 \pm 0.0	76.6 \pm 8.2	3.9 \pm 0.2	4.8 \pm 0.3	0.5 \pm 0.1	<0.02	3.3
WR3-BA	+	715 \pm 18	7.7 \pm 0.0	79.5 \pm 3.7	3.9 \pm 0.1	9.5 \pm 0.4	1.1 \pm 0.1	0.10	9.2
WR4-BA	+	540 \pm 38	7.8 \pm 0.0	53.1 \pm 7.8	3.7 \pm 0.2	6.5 \pm 1.1	1.3 \pm 0.1	0.06	4.4
WR5-BA	+	864 \pm 22	8.0 \pm 0.1	72.4 \pm 1.9	3.7 \pm 0.0	8.1 \pm 0.2	0.9 \pm 0.0	0.04	4.3
WR7-BA	+	607 \pm 34	7.9 \pm 0.1	57.1 \pm 3.5	3.5 \pm 0.2	6.3 \pm 0.1	1.0 \pm 0.2	0.10	10.0
WR1-WA	+	258 \pm 1	9.3 \pm 0.3	18.3 \pm 0.3	5.4 \pm 0.1	2.7 \pm 0.1	1.1 \pm 0.0	0.06	5.5
WR2-WA	+	906 \pm 86	11.2 \pm 0.1	7.9 \pm 0.3	3.5 \pm 0.2	1.7 \pm 0.1	0.6 \pm 0.1	0.04	6.9
WR3-WA	+	363 \pm 28	10.1 \pm 0.1	8.2 \pm 0.5	4.1 \pm 0.4	1.7 \pm 0.0	0.9 \pm 0.2	0.05	6.2
WR6-WA	+	432 \pm 6	9.0 \pm 0.1	8.4 \pm 0.4	5.7 \pm 0.1	2.1 \pm 0.1	0.7 \pm 0.3	0.05	6.5
WR7-WA	+	497 \pm 42	9.7 \pm 0.1	9.3 \pm 1.0	5.2 \pm 0.3	1.9 \pm 0.1	0.5 \pm 0.2	<0.02	4.3
RO1-BA1	+	493 \pm 28	8.2 \pm 0.2	37.2 \pm 3.5	5.3 \pm 0.1	4.8 \pm 0.2	0.4 \pm 0.1	0.05	11.8
RO1-BA2	+	391 \pm 29	8.0 \pm 0.1	16.3 \pm 0.5	4.4 \pm 0.1	3.0 \pm 0.1	0.4 \pm 0.0	0.03	6.7
RO1-BA3	+	422 \pm 35	7.8 \pm 0.0	29.9 \pm 1.1	4.9 \pm 0.1	3.7 \pm 0.1	0.4 \pm 0.1	0.06	13.0
RO2-BA1	+	715 \pm 23	7.8 \pm 0.1	78.8 \pm 1.3	3.4 \pm 0.0	13.8 \pm 0.3	1.6 \pm 0.1	0.05	3.1
RO2-BA2	+	641 \pm 10	7.8 \pm 0.1	56.0 \pm 0.7	3.3 \pm 0.0	7.9 \pm 0.1	0.7 \pm 0.1	0.03	4.2
RO2-BA3	+	557 \pm 5	8.0 \pm 0.2	52.6 \pm 2.6	3.4 \pm 0.1	8.8 \pm 0.3	1.6 \pm 0.2	0.05	3.3
RO3-BA1	+	598 \pm 6	7.9 \pm 0.0	54.7 \pm 1.2	4.6 \pm 0.1	8.0 \pm 0.2	1.9 \pm 0.1	0.35	18.4
RO3-BA2	+	621	8.1	52.5	3.8	8.1	1.0	0.03	3.0
RO3-BA3	+	605	8.0	53.2	3.6	7.9	1.6	0.14	8.8
RO1-WA1	+	214 \pm 3	9.0 \pm 0.0	5.0 \pm 0.2	3.0 \pm 0.0	1.1 \pm 0.1	0.5 \pm 0.1	<0.02	3.0
RO1-WA2	+	183 \pm 12	8.2 \pm 0.3	5.1 \pm 0.1	3.5 \pm 0.0	1.3 \pm 0.0	0.5 \pm 0.1	<0.02	4.7
RO1-WA3	-	306 \pm 21	8.0 \pm 0.1	7.6 \pm 0.4	4.7 \pm 0.1	1.1 \pm 0.1	1.0 \pm 0.2	<0.02	2.2
RO2-WA1	-	3,113 \pm 20	10.8 \pm 0.0	7.2 \pm 0.4	2.0 \pm 0.1	1.3 \pm 0.1	0.3 \pm 0.1	<0.02	5.0
RO2-WA2	-	948 \pm 35	11.2 \pm 0.1	6.5 \pm 0.2	2.4 \pm 0.1	1.4 \pm 0.1	5.3 \pm 1.0	0.12	2.3
RO2-WA3	+	664 \pm 50	11.1 \pm 0.1	5.0 \pm 0.2	1.4 \pm 0.1	1.0 \pm 0.0	0.3 \pm 0.1	0.04	13.6
RO3-WA1	+	1,168 \pm 42	10.0 \pm 0.0	5.1 \pm 0.1	2.4 \pm 0.1	1.0 \pm 0.1	0.4 \pm 0.1	<0.02	3.3
RO3-WA2	+	853 \pm 68	9.8 \pm 0.1	10.4 \pm 0.2	4.8 \pm 0.1	1.6 \pm 0.2	3.0 \pm 0.4	0.03	0.9
RO3-WA3	-	711 \pm 31	10.1 \pm 0.0	6.2 \pm 0.1	2.8 \pm 0.0	1.1 \pm 0.0	0.5 \pm 0.1	0.05	8.5

CHAPTER III

**HYDROLOGICAL TRANSPORT OF MERCURY FROM WILDFIRE-BURNED
AND PRESCRIBED FIRE-BURNED FORESTS**

3.1 Introduction

The frequency and intensity of wildfires are expected to increase in the next few decades, especially in regions with prolonged dry summers, such as in the Mediterranean climate of California where forests have accumulated a large fuel load over the past century (Westerling *et al.* 2006). The ash generated by wildfire form a top layer above the burned soil, could be eroded and transported to the aquatic environment together with the burned soils by soil erosion, surface runoff and wind. The post-fire runoff has been known to convey nutrients (i.e. carbon, nitrogen, and phosphorus), organic contaminants (i.e. polyaromatic hydrocarbon), as well as trace elements downstream, leading to potential risks to water supplies and aquatic ecosystems (Smith *et al.* 2011). As indicated in the previous chapter and other studies, Hg in forest ecosystems would be disturbed by wildfires altering its storage, reactivity, and mobility (Ericksen *et al.* 2003; Obrist *et al.* 2011; Ku *et al.* 2018). Besides the substantial amounts of previously sequestered Hg in natural forests released by wildfires (Friedli *et al.* 2001), the residual pools of Hg in the burned vegetation/ash layer and burned soils are still a significant source to downstream water bodies (Burke *et al.* 2010; Campos *et al.* 2015), especially by the hydrological transport process. The Hg export into the downstream water bodies is affected by both

the Hg content in the upland ash/soils and the hydrological transport of the upland materials. Mercury contents in burned soils varies by sites, which have been observed 1 to 349 ng/g in the burned soils in three southern California watersheds, 10.1 ± 8.4 ng/g in the burned soils in western Nevada, and 49.4 ± 11.3 ng/g in burned soil from a desert wildfire site in north-central Nevada (Engle *et al.* 2006; Burke *et al.* 2010). Meanwhile, Hg contained in the ash materials on the forest floor would be eroded and transported to the downstream then contributed to the Hg cycling in aquatic environment (Ku *et al.* 2018).

Wildfires have also been demonstrated to increase Hg bioaccumulation in fish species via food web restructuring (i.e., increase the food chain length) and increased Hg inputs (Kelly *et al.* 2006), although other studies in Canadian boreal shield lakes in Quebec showed no significant elevation in MeHg in zooplankton in burned lakes than the unburned lakes (Garcia & Carignan 1999). This implies that the disturbances of wildfires vary potentially due to the various Hg transport patterns. However, although there have been multiple studies investigating Hg loss in the burned soils (Burke *et al.* 2010; Campos *et al.* 2015), the hydrological transport pattern of Hg to the downstream water bodies and its recovery after wildfires is still unclear.

Mercury transport into the aquatic environment has been demonstrated to be associated with total suspended solids (TSS) (Balogh *et al.* 2006), mainly in particulate form. Meanwhile, dissolved Hg transport has been demonstrated to be associated with dissolved organic matter (DOC) in the water environment (Ravichandran 2004). Ash and burned soils, combining the unburned materials (litter and soil) in the post-fire landscape

lead to the inputs of both TSS and DOC that convey Hg to the downstream waterbodies, through surface runoff, throughflow or groundwater movement. In a lightly/moderately burned watershed in the Southeastern United States, Hg input was found to be associated with TSS, and particulate Hg (PHg) per unit of TSS was 20.5 times higher at the burned site (2.66 ng PHg per mg TSS) than unburned site (0.13 ng PHg per mg TSS) for 8 months following the fire after the “first flush” (Jensen *et al.* 2017). Caldwell *et al.* (2000) examined the effects of fires and storm flow on Hg in sediments of the watersheds of Caballo Reservoir in New Mexico, and they found storm runoff enhanced Hg transport to the reservoir by complexing Hg to organic matter, thus increased MeHg in reservoir sediment. Nevertheless, the role of “first flush” in Hg hydrological transport dynamics and Hg speciation to the watersheds is less understood. The Mediterranean climate in northern California in the present study provided a unique opportunity to track the role of “first flush” due to the long dry summer after wildfires. Moreover, Hg speciation in the stream water would directly affect Hg bioavailability and methylmercury (MeHg) bioaccumulation in food webs. After wildfires, the higher input of Hg to the downstream water bodies could enhance the Hg methylation potential and produce MeHg on site due to the transformation of inorganic Hg by reducing bacteria (i.e. sulfate-reducing bacteria) in watersheds (Hsu-Kim *et al.* 2013). Caldwell *et al.* (2000) discussed the MeHg/THg ratio in the sediment of the burned reservoir to relate to the Hg methylation potential in the burned watershed. However, there is no study to date investigating the direct transport of MeHg to downstream with post-wildfire runoff.

As one of the main drivers in soil degradation and surface runoff, wildfires change the hydrologic regime and dynamics in sediment transport at the burned site (Swanson 1981). Wildfires have been indicated to potentially lead to more erosion by post-fire precipitation and runoff, especially after a sufficient storm event removing some protective ash layer (Andreu *et al.* 2001; Cerdà & Doerr 2008). The wildfires change surface runoff yield and soil erosion rate by affecting several factors including 1) reducing vegetation cover thus reduce evapotranspiration rate, 2) decrease stability of soil aggregates by reducing the soil organic matter, 3) increase water repellency thus decrease infiltration rate due to the high temperature combustion, 4) alter the transport pathway by generation the ash layer cover (Moody *et al.* 2009; Neary *et al.* 2011; Shakesby 2011; Ebel *et al.* 2012). In the fire affected watershed Hg studies mentioned before, all of them were impacted by wildfires, however, the impacts of the anthropogenic prescribed fire on Hg transport to the downstream are poorly known. Compared to wildfires, prescribed fires are less intensive, last for shorter time, and they are conducted regularly every 2-4 years. Two types of prescribed fire are commonly carried out, pile burning and broadcast burning. Pile burning is a type of the prescribed fire that burns vegetation/woods thinned from the forests by piles. Broadcast burning is another type of prescribed fire that burns the vegetation without thinning down the vegetation within determined perimeters. To my knowledge, although there are some studies investigating the Hg content and mobilization in the burned landscape after prescribed fire (Harden *et al.* 2004; Abraham *et al.* 2018), there is no study so far investigating the hydrological transport of Hg following prescribed fire in either type. Abraham *et al.* (2018) examined the impacts of

prescribed fire and post-fire rainfall on Hg in burned soils and its mobilization and they found prescribed fires are able to remobilize the sequestered Hg in vegetation and soils and post-fire rainfall increased the Hg in ~50% of burned soils samples. In another review paper that summarized the post-fire metal mobilization into water environment, it has been indicated most fire-impacted watershed were focused on some other elements and there was very limited information about the prescribed fire impacts on Hg transport (Abraham *et al.* 2017). Since prescribed fires cause less disturbance to forest vegetation (i.e., mortality), and surface soil on the forest floor than wildfires generally, it is expected prescribed fire would lead to less Hg export than the wildfires to the downstream water bodies. However, the Hg transport pattern could be different following the two types of forest fires because of the differed factors involved in the hydrological processes.

The objectives of this work are to understand the long-term dynamic fluvial transport of Hg and Hg speciation in burned watersheds, as well as the long-term Hg transport affected by the burned areas affected by wildfires or prescribed fires. This chapter will discuss and compare the impacts of wildfire (natural) and prescribed fires (anthropogenic) on Hg transport to the downstream water bodies, including three field studies: The first field study was conducted in the wildfire-burned watersheds in northern California, the second was in the prescribed fire (pile burning)-burned watersheds in northern California, the third was in prescribed fire (broadcast burning) in the lower coastal plain of South Carolina. This chapter will provide better understanding on the ecological risk in Hg fluvial transport caused by forest fires including wildfires and the forest management practice-prescribed fires to the downstream water bodies.

3.2 Materials and Methods

3.2.1 Site Description and Sample Collection

3.2.1.1 Wildfire-burned Sites in Northern California

This study investigated the fate and transport of mercury in streamwater following two wildfires in northern California in 2015 (Wragg Fire and Rocky/Jerusalem Fire, hereafter referred to as the Rocky Fire), as same as the wildfires mentioned in the previous chapter (**Figure 3.1**). This investigation builds upon the previous chapter (Ku *et al.* 2018) that examined surficial ash materials (black and white ashes) from two burned sites (Wragg Fire and Rocky Fire) and reported Hg concentrations and reactivity, stable isotope Hg composition, and Hg methylation potential under anaerobic incubation. Here, we report Hg data in streamwater samples collected from two burned watersheds (Wragg Fire and Rocky Fire) over two wet seasons (i.e., first winter and second winter after the summer fire). We included a nearby stream draining an unburned watershed to serve as a reference watershed for the burned watershed by Wragg Fire. Additionally, we report the Hg content of soil samples from the burned areas of the Wragg and Rocky Fires to provide further context for the fluvial transport of Hg.

The Wragg Fire (July 2015) burned 32.58 km², covering more than 90% of the watershed area. We selected Miller Canyon watershed (8.70 km²) as a reference watershed due to the similarity in geology, soils, vegetation, and relief with the watershed affected by Wragg Fire. Two wildfires (Rocky Fire and Jerusalem Fire; hereafter referred to as Rocky Fire) occurred within the Rocky Fire Watershed during the summer of 2015 burning a total area of ~381 km², covering ~15% of the watershed area (total basin area =

3,367 km²). Wang *et al.* (2020) reported high burn severity for the Rocky Fire Watershed area burned by the Rocky Fire, with post-fire tree and vegetation coverage being reduced by 57.6% and 41.4%, respectively, and bare earth increased from 9.2 to 132.6 km².

The diverse geology of the study area includes sedimentary, metamorphic, and volcanic rocks of the Franciscan Complex and Great Valley Sequence, which contain numerous areas of hydrothermal Hg enrichment (Smith *et al.* 2008). The topography is gently-to-steeply sloping low mountains highly dissected by the river systems that drain eastward into the Sacramento River. Pre-fire vegetation was a mixture of oak savanna and woodlands (blue oak [*Quercus douglasii*], interior live oak [*Quercus wislizenii*], California buckeye [*Aesculus californica*]), chaparral (chamise [*Adenostoma fasciculatum*], scrub oak [*Quercus dumosa*], toyon [*Heteromeles arbutifolia*], manzanita [*Arctostaphylos manzanita*], and buck brush [*Ceanothus cuneatus*]), and annual grasslands. The climate in the study area is Mediterranean with mild wet winters and warm dry summers; the majority of rain falls between November and March. The mean annual air temperatures range from about 13.5 to 17.5 °C. Annual precipitation was 623 and 689 mm in the Wragg/Cold Fire areas (Berryessa Station – BER) and 1,206 and 1,298 mm in the Rocky Fire watershed (Knoxville Creek Station - KNO) in the 2015-16 and 2016-17 water years (Oct. 1 to Sept. 30), respectively.

We collected streamwater from the outlet of the respective watersheds following major storm events throughout the winter and spring of 2015 and 2016 (Wragg, Rocky & Reference – 2 years). The Wragg Fire and Reference watersheds have intermittent streams that flow only during the winter/spring period. Water samples were collected

from the onset of streamflow generation (i.e., first flush) through the spring drying of these watersheds. Streamflow generation in the Reference watershed was delayed relative to the burned watersheds due to higher rainfall infiltration and soil recharge resulting in no streamwater samples for the first few sampling events each year in this site compared to other burned sites. In Rocky Fire watershed (Rocky/Jerusalem Fire in 2015), streamflow was persistent throughout the dry summer and fall (U.S.G.S. gaging station at Rumsey, CA) due to water release from Clear Lake for downstream irrigation. Water release from Clear Lake was minimal compared to runoff from the landscape for the majority of the wet season, with winter storm events producing a series of stream hydrograph responses. Based on these hydrograph responses, we were able to collect streamwater samples for the “first flush”, as well as the majority of the subsequent hydrograph responses over the two-year study period.

3.2.1.2 Sagehen Experimental Forest in Northern California burned by Prescribed Fire (Pile Burning)

A two-year planned field study was conducted in Sagehen Experimental Forest in northern California, which is located in the Central Sierra Nevada north of Truckee, California. The major vegetation cover types of the 9000-acre Sagehen Experimental Forest are grass (i.e., fen, wet montane meadow, and dry montane meadow); shrubs dominated primarily by tobacco brush (*Ceanothus velutinus*) with Greenleaf manzanita (*Arctostaphylos patula*), Squaw-carpet (*Ceanothus prostrates*), wax currant (*Ribes cereum*), Bloomer’s goldenbush (*Ericameria bloomer*), dwarf serviceberry (*Amelanchier pumila*), and woolly mule-ears (*Wyethia mollis*); mixed conifer, true fir, and conifer

plantations (mainly ponderosa pine (*Pinus ponderosa*) with some Jeffrey pine (*Pinus jeffreyi*)). The soil of the Sagehen Experimental Forest are dominated by Andic and Ultic Haploxeralfs. Poorly drained soils including Aquolls and Borolls soil types are under the wet montane meadows and fens. Deep and well-drained soil types including various percentages of Fugawee, Tahoma, and Jorge series are under mixed conifer forest and plantations. The annual precipitation is about 847 mm, snowfall accounts for more than 80% of the annual precipitation.

Low-intensity fires (pile burnings) were conducted in Sagehen Experimental Forest in different units (**Figure 3.2**) to suppress the natural wildfire, as well as the native bark beetle infestation. Pile burning was carried out by thinning the local vegetation and woods as fuel and then burning at a low intensity within a specific area to limit the fire spreading. Post-burning ash and surface soil (0-10 cm) samples were collected with a clean shovel in the forest after the burning. The water samples were collected by field technicians of Sagehen Creek Field Station monthly from September 2017 to June 2019, and the sampling frequency increased to weekly when there was pile burning conducted (i.e., May 2019). In winter months the samplings were limited or suspended entirely because of the weather condition (e.g., snow and site access issue). Groundwater (GW) samples were collected for comparison, and surface water samples for the four sites (S1, S2, S3, and S4) were collected to examine the impacts for the burning. The map of the sampling sites (GW, S1, S2, S3, S4) at Sagehen Experimental Forest and the pile burning was shown in **Figure 3.2**. Duplicate samples were collected for each site on some randomly selected dates for quality assurance (QA).

3.2.1.3 Santee Experimental Forest Burned by Prescribed Fire (Broadcast Burning)

This controlled field study was conducted on the two first-order watersheds (WS77 and WS80) and the second-order watershed (WS79) in the Santee Experimental Forest in South Carolina (*see* map in **Figure 3.3**), which was established in 1963, lay on flat, poorly drained soils of lower Atlantic coastal plain developed on a marine terrace of the Pleistocene epoch. WS77 supports a naturally regenerated stand of loblolly pine (*Pinus taeda*) mixed hardwood that has been managed with a prescribed burning program since 2003 (Amatya *et al.* 2019). WS80 is a control watershed and was not salvage-logged after Hurricane Hugo in 1989 (USDA, 2009). WS79 is a second-order watershed and contains both WS77 and WS80. The drainage areas of the two 1st order watersheds are 155 ha for WS77, 160 ha for WS80, respectively, and 500 ha for the 2nd order watershed WS79. The mean annual rainfall for the site is 1,370 mm (2004-2017). The area has low relief with surface elevations ranging from 4 to 10 m above mean sea level. Soils are primarily loams and strongly acidic, infertile Aquults characterized by seasonally high water-tables, argillic horizons at 1.5 meters depth and low base saturation. The U.S. Forest Service - Center for Forested Wetlands Research maintains long-term hydrologic monitoring of watersheds 77, 79, and 80 (USDA, 2009).

WS77 was recently burned by prescribed fire (broadcasting burning) in March 2018 by U.S. Forest Service, but no treatment was conducted at WS80. A post-burn assessment is done to determine the proportion of the upland area burned and a qualitative indication of the severity. This information is developed based on transects that are placed within the watershed, following the protocol developed by Page-

Dumroese *et al.* 2009). The 2018 assessment shows that 66% of the WS77 upland area had a moderate burn, 33% had a light burn and 1% no burn. There was no severe burn in the 2018 prescribed burning at WS77. The streamwater samples were collected biweekly (only monthly for pre-burn samples) at the outlet wire of the gauging station from each watershed (WS77, WS80, and WS79, respectively) from September 2017 to February 2020.

3.2.2 Sample Processing and Analyses

The water samples were collected into acid-cleaned 500-mL Teflon bottle for Hg analyses, and into an acid-clean and baked 1-L amber glass bottle for general water chemistry analyses as mentioned before. Samples were shipped with ice packs within 48 hours to analytical laboratories at UNCG (for Hg) and Clemson University (for general water chemistry). We filtered ~250 mL from the 500-mL Teflon bottle through a pre-baked Whatman GF/F filter paper (nominal pore size: 0.7 μm) in an all-glass filtration apparatus (sequentially cleaned by dilute HNO_3 and BrCl , and rinsed thoroughly). Unfiltered and filtered samples were transferred into acid-cleaned 125 mL Teflon bottles (for THg) or new, Hg-free 125 mL Nalgene PETG bottles (for MeHg). For each water sample, we analyzed four Hg fractions: unfiltered THg, filtered THg, unfiltered MeHg, and filtered MeHg.

For THg analysis, water samples were digested by an acidic mixture of KMnO_4 and $\text{K}_2\text{S}_2\text{O}_8$ in an oven at 60 °C overnight following Woerndle et al. (2018). Digested water samples were cooled, completely neutralized with 30 % $\text{NH}_2\text{OH}\cdot\text{HCl}$, and weighed aliquots of samples (~20 to 120 mL, depending on the expected THg content) were

analyzed by the double amalgamation technique with Hg quantification by cold vapor atomic fluorescence spectrometry (CVAFS; Brooks Rand Model III). A calibration curve (0 to 1 ng) was developed using the NIST-3133 Hg working standard (1 ng/mL) and was verified by a secondary standard prepared from NIST-1641d (1 ng/mL). THg concentrations for water samples were reported in ng Hg per liter (ng/L), and the established method detection limit was 0.10 ng/L. We calculated particulate THg concentration as the difference between unfiltered THg and filtered THg.

For MeHg analysis, water samples were preserved with 0.4 % trace metal grade HCl (Parker and Bloom, 2005) and stored at 4 °C in the dark prior to analysis. Water samples (~50 mL or 100 mL) were distilled to remove matrix interferences, buffered with sodium acetate at pH 4.9, and ethylated by 1 % NaBEt₄ for 25 min. Alkyl Hg species were purged from the bubbler with Hg-free N₂ gas for 12 min. and preconcentrated onto Tenax TA traps. MeHg in water samples was quantified by CVAFS following isothermal gas chromatographic separation and pyrolysis (Bloom, 1989; Horvat et al., 1993). The method detection limit (MDL) for MeHg in water samples was established at 0.04 ng/L for 50 mL of samples analyzed. For water samples having MeHg below the method detection limit (i.e., 0.04 ng/L), we assigned a value of half the detection limit (i.e., 0.02 ng/L) for graphical presentation and calculations (Clark, 1998). A MeHg calibration standard (1 ng/mL stock solution from CEBAM Analytical, Bothell, WA) was used to develop a calibration curve (0 to 0.5 ng), and the MeHg concentration was regularly verified against our in-house THg standard (NIST-3133) following the method outlined by USEPA (2002). For both THg and MeHg analyses, we included multiple field/travel

blanks (n=4) and reagent blanks (n=10), and these blank samples were found to have undetectable MeHg levels (<0.04 ng/L) and very low THg levels (~0.1-0.2 ng/L).

For samples collected in amber glass bottles, an unfiltered subsample was analyzed for TSS (mg/L). A subsample was filtered sequentially through pre-conditioned borosilicate glass filter (pore size: 1.5- μ m; Whatman 934-AH) and pre-washed filter membrane (pore size: 0.45- μ m; Pall Corporation). Filtered samples were analyzed for DOC, specific UV absorbance at 254 nm (to calculate SUVA₂₅₄), and dissolved total nitrogen (DTN). All analyses of general water chemistry were performed at Clemson University (see methods, equipment, and method detection limits (MDLs) in **Table S3.1**).

Ash and soil samples collected from each site, including Wragg and Rocky Fire sites, Sagehen Experimental Forest burned sites, Santee Experimental Forests, were frozen and freeze-dried, and subsequently sieved through acid-cleaned 2-mm polypropylene mesh housed in a PVC-adaptor. THg in ash, soil and suspended sediments was determined following digestion by aqua regia as described in Olund *et al.* (2004). Briefly, ~0.2 g of soil sample was added with freshly mixed 6 mL TMG HCl and 2 mL HNO₃ (aqua regia) in an acid-cleaned 40 mL glass vial, allowed to sit at room temperature for 24 hours (“cold-digestion”), and then heated to 80 °C in a water bath overnight (“hot-digestion”). Next, 22 mL of 5 % BrCl solution was added to the acid digest and an aliquot of the acid digest added into 100 mL of nanopure water in a glass bubbler, which was neutralized by 200 μ L NH₂OH·HCl. The Hg was reduced by adding 200 μ L SnCl₂ to produce gaseous elemental Hg, which was trapped with gold-coated traps and subsequently heat-desorbed for quantification by CVAFS.

3.2.3 Stream Discharge

Stream discharge for the Rocky Fire sampling point was approximated by the Rocky Fire watershed at Rumsey Bridge USGS gaging station located ~12 km downstream. Discharge from the Wragg Fire watershed was approximated by subtracting reservoir outflows from the USGS 11454000 Putah Creek near Winters, CA gauge that was located on Putah Creek downstream of the reservoir and the mouth of the Wragg Fire stream. However, the non-quantified release of water from the overflow spillway in the 2016-17 water year prevented estimates of stream flow contributions from Wragg Fire watershed during part of the second wet season (after 2/17/2017). While no measurements of stream discharge from reference watershed (Miller Canyon Creek) were available, their relative discharge dynamics were expected to be similar to that of the Wragg Fire watershed when we collected samples on the same day (typically within 1-2 hours).

Stream discharge data for Sagehen Experimental Forest watershed were obtained from USGS gaging station at Sagehen C NR Truckee CA (10343500). Since the locations of the gaging stations are close to the sampling sites so we used the discharge data from this gaging station for all the four sites (S1, S2, S3, S4).

Stream discharge data for Santee Experimental Forest were obtained from the gaging station at each site (WS77, WS80 and WS79) from September 2017 to September 2019. Discharge data for 2018 and 2019 have not been published online yet and the data were provided by U.S. Forest Service Southern Research Station thus should be considered as provisional (shown in Figure 3.13).

3.2.4 Hg Loading Calculations

For the wildfire-burned watersheds in northern California, because we collected most of the samples during the storm events, here we only calculate the daily loadings at each event day. Daily loadings of TSS, DOC, and THg on a watershed area basis were calculated for each sampling date at each watershed based on the concentration and discharge. No annual yields were available for these watersheds.

For Sagehen Experimental Forest watersheds (pile burning site) in northern California, daily loadings were not calculated because the sampling sites were from different locations but the same watershed. The pile burning area was limited to a small area, therefore, we will discuss the concentration changes of Hg after each burning event, instead of the loading discussion.

In Santee Experimental Forest watersheds (broadcast burning site), daily loadings of TSS, DOC, and THg were calculated in the same way. Estimations of daily fluxes for the intervening days were made by assuming a linear variation in Hg concentrations from one sampling date to the next. Daily loadings were added up over the entire year to estimate the annual load (g/year) for each watershed. Annual yields (g/km²-year) were calculated by dividing the annual load by the watershed drainage areas. Post-burn annual yields were estimated and compared for the three watersheds for the first year (March 2018 to March 2019). The post-burn 2nd year loadings were not calculated because of the drought from May 2019 to September 2019 (see discharge data).

3.2.5 Statistical Analysis

To compare characteristics among different groups, single-factor ANOVA was followed by a Tukey multiple comparison test at $\alpha = 0.05$. Two-tailed t-tests were used to show the statistical difference between the two groups. However, when the normality test for the two groups was failed, the Mann-Whitney Rank Sum Test was used instead. Linear regression analyses were conducted using SigmaPlot 12.5.

3.3 Results and Discussion

The results are discussed firstly in each individual controlled field study, including the 2-year temporal transport patterns of Hg concentrations and Hg speciation in the wildfire-burned watersheds (section 3.3.1), pile burning affected watershed (section 3.3.2), and broadcast burning affected watershed (section 3.3.3), respectively, then differences between the wildfire and prescribed fire impacts on Hg hydrological transport patterns as well as the assessment of the ecological risk regarding Hg is discussed (section 3.3.4).

3.3.1 Impacts of Wildfires on Hg Export

3.3.1.1 Hg Loadings with Runoff

Since the results showed a more sensitive and varied response in the first year following the fires (Wragg Fire and Rocky Fire), here we will discuss the Hg transport pattern within the first year (2016). The episodes of elevated discharge were along with the precipitation, and the timing of hydrological events in the watersheds was similar in the adjacent watersheds we studied. Since there was little precipitation leading to runoff

between July 2015 (the time the wildfires occurred) and the beginning of January 2016, we were fortunate to collect the first runoff samples in the early January 2016 (1/5/2016). In the reference watershed (Miller Canyon), TSS ranged 1 – 405 mg/L, while the >90% burned watershed Wragg Fire watershed showed 2.5 – 19021 mg/L and the ~15% burned watershed Rocky Fire watershed showed 4.0 – 3177 mg/L in the 1st year following the wildfires (**Figure 3.4**). Compared to reference watershed (Miller Canyon), TSS inputs were much higher with runoff after the wildfire in both watersheds (**Figure 3.4c, 3.4e**), especially in the first precipitation period, with extremely high TSS input even with low discharge in the Wragg Fire watershed (**Figure 3.4c**). Wragg Fire watershed with the higher burned proportion received much more TSS input in the “first flush” than that in Rocky Fire watershed with up to 10301 mg/L in Wragg Fire watershed while 1648.5 mg/L in Rocky Fire watershed in the first sample collection on 1/6/2016, and the maximum TSS levels in streamwater collected in the 1st year following the fires were 19021 mg/L for Wragg Fire watershed and 3177 mg/L for Rocky Fire watershed (**Figure 3.4c, 3.4e**). This suggested that the more burned and smaller watersheds would be more affected by wildfire mainly by erosion.

Meanwhile, high amount of THg was transported to downstream in the first rainy season, similar trend with the high TSS input (**Figure 3.4d**). In Miller Canyon, the reference watershed, THg ranged from 0.5 – 100.4 ng/L, however, in the >90% burned watershed Wragg Fire watershed, THg ranged from 0.9 – 1379 ng/L in the first rainy season. For the latter rainy seasons (i.e., March 2016), both the TSS and THg inputs decreased in the Wragg Fire watershed compared to the first rainy season (1/5/2016 –

1/19/2016) (**Figure 3.4c, 3.4d**). For example, the TSS input range was 106 – 19021 mg/L with THg range 10.1 – 1379.0 ng/L in the first rainy season, but lower TSS range 40–3269 mg/L with THg range 1.1 – 274.4 mg/L were observed in the second rainy season. In watersheds that mainly contributed by diffuse source of Hg, Hg exports were along with discharge due to the strong association of Hg with suspended sediment (Balogh *et al.* 1996). However, in the present study, together with TSS, both THg and MeHg showed high input with low discharge in the “first flush” event, although most of them are inorganic Hg (**Figure 3.4d and 3.4f**). The contrast between TSS or Hg export and discharge in the first rainy season suggested the importance of post-fire “first flush” in the hydrological response of Hg to the wildfire in the highly burned watershed (large burn area). Although there was no information about the role of “first flush” in Hg hydrological transport to date, Jensen *et al.* (2017) showed higher particulate Hg input (2.66 ng PHg/mg TSS compared to 0.13 ng PHg/mg TSS) in the first post-fire period (first 8 months) then returning to non-disturbed condition afterward, indicating that the fire had more impacts on Hg input in the early rainy seasons after the wildfires.

The high TSS and Hg transport in the “first flush” was mainly because the surface layer of the forest floor was physically and chemically altered by the burning, making surface soil and/or covered burning biomass residue vulnerable to precipitation (Moody *et al.* 2013; Campos *et al.* 2015). Precipitation is often the primary driver of post-wildfire runoff and erosion processes (Moody *et al.* 2013), increases the TSS input with surface runoff once the ash and surface soil was saturated, which was demonstrated by the high TSS in the burned watershed in the present study. The runoff generation is impacted by

the thickness of ash layer, reduction of soil organic content which impacts soil water retention, which in turn controls runoff generation following the wildfire (Ebel *et al.* 2012).

The impacts of wildfires on burned watersheds vary from watersheds, mainly because of the different burned areas, burn severity, the slopeness, and post-fire precipitation (Neary *et al.* 2005). The small watershed which was highly affected by wildfire (i.e. Wragg Fire watershed) would potentially have higher TSS input because of the higher burned proportion. We observed highly variable unfiltered THg in streams from both burned watersheds, ranging from 0.9 ng/L (baseflow) to 1379 ng/L (event) for Wragg Fire watershed and from 3.8 ng/L (baseflow) to 688 ng/L (event) for Rocky Fire watershed, indicating the burned proportion of the watershed is likely to be more important than the absolute burn area in erosion and Hg dynamic transport.

3.3.1.2 Dissolved Hg and DOC Transport

Dissolved Hg (DHg) transport was known to be associated with DOC in natural environments due to the strong affinity of to the organic matter especially humic acid. DOC is generally considered as a vector of Hg at the freshwater ecosystem especially for the aromatic fraction of DOC (indicated as SUVA₂₅₄) (Grigal 2002; Ravichandran 2004). Wildfire produced biomass residue, especially charcoal, could leach dissolved carbon and nitrogen to the water (Smith *et al.* 2011), thus being the potential source of organic matter input into streams. Our results showed similar DOC concentrations in the samples collected in 2016 between Miller Canyon and Rocky Fire watershed ($p>0.05$) while DOC input from the Wragg Fire watershed was significantly higher than both the other two

watersheds ($p < 0.001$) (Figure 3.5a). DOC showed highest at the beginning of the first rainy season then decreased in the second and third rainy seasons in the Wragg Fire watershed. The streamwater showed significantly higher $SUVA_{254}$ in the first rainy season than the second rainy season in Wragg Fire watershed ($p < 0.001$) (Figure 3.5b), indicating the increase of DOC aromaticity by wildfire in the small watershed (Weishaar *et al.* 2003). This is consistent with previous wildfire ash leaching experiments, with higher $SUVA_{254}$ in white ash leachate than in unburned vegetation (Wang *et al.* 2015). In the bigger watershed Rocky Fire watershed, no significant increase in DOC amount post-wildfire, but slightly higher $SUVA_{254}$ were observed in the first rainy season than in the latter rainy seasons. The lower DOC concentrations in Rocky Fire Watershed than that in Wragg Fire watershed could be because of the dilution by the higher river discharge from Rocky Fire watershed. In contrast with the present study, DOC was observed to decrease after a wildfire in some previous studies, mainly was attributed to upland biomass burning and carbon reduction (Betts & Jones 2009).

In the Wragg Fire watershed, dissolved form of Hg (DHg) ranged within 0.8-5.6 ng/L (Figure 3.5c), which was a small proportion of THg input (up to 1379 ng/L). This indicated the main contribution of THg in the burned watershed was particulate Hg (PHg). For example, PHg showed up to 265 folds higher than DHg in Wragg Fire watershed (1373.8 ng PHg/L and 5.2 ng DHg/L on 1/19/2016), and 57 folds higher in Rocky Fire watershed (529 ng PHg/L and 9.3 ng DHg/L on 3/6/2016), while PHg/DHg ratio ranged from 0.2-12.4 in the unburned watershed. This contrast indicated that the post-wildfire Hg transport was mainly driven by the particulate Hg form instead of the dissolved Hg

form. Burke *et al.* (2010) showed that the leaching Hg from soil was minimal with only up to 2.07% ($\pm 0.34\%$) Hg leached from the burned soils, suggesting DHg transport to the downstream could be much less compared to the bulk burned soil particles, supporting our results that PHg is the main Hg transport form after wildfire.

In contrast to THg, there were no significant differences in DHg levels between the first rainy season and the second rainy season in either Wragg Fire watershed or Rocky Fire watershed. DOC is involved as carriers in the transport of dissolved THg and MeHg because of the strong interactions between DOC and Hg (Ravichandran 2004), therefore, not surprisingly, we also found a significant linear regression between DOC and DHg in all the three watersheds, including both unburned and burned watersheds ($p < 0.01$) (**Figure 3.6d**). There were also significant linear regressions between DOC and DMeHg in both Wragg Fire watershed ($p = 0.037$, $r^2 = 0.410$, $\text{DMeHg/DOC} = 45.4 \pm 17.7$ ng/g) and Rocky Fire watershed ($p = 0.020$, $r^2 = 0.284$, $\text{DMeHg/DOC} = 15.5 \pm 5.88$ ng/g) for the 2016 sampling, indicating the post-wildfire direct DMeHg input was significantly driven by the DOC.

3.3.1.3 Mercury Speciation Transport Patterns

In watershed contributed by non-point sources, Hg export has been found strongly correlated with TSS in the lower Minnesota river (Balogh *et al.* 1996). In the present study, results showed that PHg is the main form in the post-fire Hg transport in the burned watershed in the first year following the wildfire, by comparing the percentages of PHg and DHg. And PHg was significantly correlated with TSS in all sites ($p < 0.001$), including unburned watershed, and two burned watersheds (**Figure 3.6a**), indicating the

importance of erosion process in the Hg transport in the wildfire-burned watersheds. The relationship is consistent with numerous previous studies between TSS and particulate THg (Balogh *et al.* 1996; Balogh *et al.* 2008), indicating TSS is the main carrier of aqueous THg after wildfire. The PHg/TSS ratios in Rocky Fire watershed (201 ng/g) were higher than the unburned watershed Miller Canyon (96 ng/g), while PHg/TSS in Wragg Fire watershed (71 ng/g) was lower than that in Miller Canyon. The magnitude of PHg/TSS was much lower in our study compared to Jensen and his coworkers' study, in which they observed 2660 ng PHg/g TSS in burned watershed and 130 ng PHg/g TSS in unburned watershed in Virginia (Jensen *et al.* 2017). This could be because of the Hg legacy differences or the geological differences in our California watersheds and the Virginia watersheds.

Moreover, particulate MeHg was significantly correlated with TSS in the Wragg Fire watersheds, while no difference was observed in Rocky Fire watershed and unburned watersheds (**Figure 3.6b**), which indicated the high burned proportion would induce the MeHg transport along with TSS due to runoff. Although DHg was correlated with DOC, DHg percentage became lower with higher TSS input among all watersheds (**Figure 3.6c**), indicating that PHg instead of DHg was the main driver of Hg transport especially when there was high erosion in the burned watersheds.

Mercury source in the watershed may be mainly due to dry deposition (Woerndle *et al.* 2018), which makes the burned biomass and soil being important Hg sources for the downstream water bodies. Therefore, although wildfire would volatilize Hg from the vegetation and forest floor due to the high temperature from the fires, the left-over Hg in

the burned materials could contribute to the Hg transport to the downstream water bodies along with the erosion. To understand the reason of higher Hg/TSS ratio at Rocky Fire Watershed (Hg/TSS: 204 ng/g) than Wragg Fire Watershed (Hg/TSS: 71.4 ng/g), we investigated the Hg levels (by *aqua regia*) in the upland materials including unburned litter, unburned soil, ashes, and burned soils from both sites. The Hg levels in ash have been reported in the previous chapter II, so here in **Figure 3.7** we would like to just summarize the Hg levels at each site regardless of the burn severity. Since TSS is the main driver in the wildfire-burned watersheds as previously discussed, here we showed the relationships between TSS and THg input at each site, which exhibited 204 ng THg per g TSS at Rocky Fire Watershed and 71.4 ng THg per g TSS at Wragg Fire Watershed (**Figure 3.7**). Unburned litter showed no differences in Hg levels between the two sites, but the soils (both unburned and burned) and ash exhibited higher Hg concentrations in the samples collected from Rocky Fire Watershed than those collected from Wragg Fire Watershed, with Rocky Fire burned soil showing 136.1 ± 111.5 ng/g (mean \pm S.D., n=18) and Wragg Fire burned soil 42.2 ± 28.8 ng/g (mean \pm S.D., n=10) regardless of the burn severities (**Figure 3.7**). Specifically, THg levels in the low severity burned soils (under black ash) at Rocky Fire site were 205.0 ± 120.2 ng/g (mean \pm S.D., n=9) and 55.4 ± 29.9 ng/g (n=5) at Wragg Fire site. The THg levels in the high severity burned soils (under white ash) at Rocky Fire site were 67.2 ± 30.2 ng/g (n=9) and 29.0 ± 20.3 ng/g (n=5) at Wragg Fire site. The Hg levels in the surface black ash and white ash on the Wragg Fire burned landscape showed higher values at the Rocky Fire site than that at the Wragg Fire site, especially in black ash, as indicated in Chapter II. The higher THg levels at Rocky

Fire soils were aligned with the higher Hg/TSS in water samples, indicating upland surface floor especially soils as an important source of Hg input in the present study.

3.3.1.5 Recovery of Hg Input in the Burned Watershed

Our results indicated that the input of TSS, DOC and Hg input returned to the lower level in the >90% burned watershed (Wragg Fire watershed), compared to the unburned Miller Canyon and less burned watershed Rocky Fire watershed. As shown in **Figure 3.8**, the TSS input showed no significant difference between Year 1 and Year 2 in Miller Canyon and Rocky Fire watershed ($p=0.174$, Mann-Whitney Rank Sum Test), while TSS levels in Wragg Fire watershed was significantly decreased in Year 2 than Year 1 ($p=0.037$, Mann-Whitney Rank Sum Test). Similarly, DOC concentrations showed no difference in Miller Canyon (two tailed $p=0.083$, $t=1.833$) and Rocky Fire watershed ($p=0.214$, Mann-Whitney Rank Sum Test) and significantly decreased in Year 2 than Year 1 in Wragg Fire watershed ($p=0.002$, Mann-Whitney Rank Sum Test). Moreover, unfiltered THg concentrations showed no difference in Miller Canyon and Rocky Fire watershed ($p>0.05$) and significantly decreased in Year 2 than Year 1 ($p=0.025$, Mann-Whitney Rank Sum Test) (**Figure 3.8**). Moreover, the Hg/TSS slope showed similar trend for the 1st year and 2nd year in the unburned Miller Canyon, while the Hg/TSS ratio decreased in Wragg Fire watershed in the 2nd year (Hg/TSS: 43.8 ng/g, $p<0.001$) than the 1st year (Hg/TSS: 71.1 ng/g, $p<0.001$) but increased in Rocky Fire watershed in the 2nd year (Hg/TSS: 340 ng/g, $p=0.005$) than the 1st year (Hg/TSS: 204 ng/g, $p<0.001$) (**Figure 3.9**).

The difference in the long-term trends in Wragg Fire watershed and Rocky Fire watershed could be due to the very different scales of the watersheds, between which Rocky Fire watershed is a much larger watershed than Wragg Fire watershed. This was supported by the study of Grigal (2002) which has found that THg yield generally decreased with the increasing watershed area, not only because of water yield, but also transport processes. On the other hand, the burn proportion in Wragg Fire watershed was much higher than the Rocky Fire watershed. The burning effect (such as TSS input) in the less burned watershed Rocky Fire watershed was less potentially due to the dilution of other unaffected input from upstream.

3.3.2 Impacts of Prescribed Fire (Pile Burning) on Hg Export

In this part, we will discuss the impacts of one type of prescribed fire-pile burning on Hg export to the downstream water bodies in Sagehen Creek in northern California (*see* map in **Figure 3.2**). We evaluated the concentrations of TSS, DOC, and Hg in streamwater and groundwater from September 2017 to June 2019. Several pile burning events were carried out at different locations along the stream (*see* map in **Figure 3.2**), therefore here we would discuss the impacts of burning on Hg export after each burning event.

In general, the discharge at Sagehen Creek was high in spring/summer months and low in fall/winter months, as shown in **Figure 3.10a**. Despite the small peaks in wintertime, the discharge started to increase from March with snow melting. TSS levels in groundwater and stream water samples at each site were generally low, ranging from 0 to 6.9 mg/L (**Figure 3.10b**). Moreover, DOC levels in groundwater were consistently low

(<1.5 mg/L), but some DOC variations were observed in streamwater, especially right after each pile burning event. For instance, DOC levels at streamwater collected in September/October 2018 and May 2019 were higher after the burning events in June-September 2018 and early May 2019.

Unfiltered total Hg (THg) concentrations in groundwater samples were consistently low, ranging from 0.01- 0.90 ng/L, while THg variations were observed in streamwater from S1-S4. In contrast, the THg levels in streamwater were along with discharge, low concentrations in winter months when discharge was low and higher levels when the discharge increased (**Figure 3.11a**). The changes of THg levels were in accordance with dissolved Hg (DHg) level change (**Figure 3.11c**), indicating the total Hg in stream water was mainly contributed by the dissolved Hg in stream water. The consistently low particulate Hg (PHg) concentrations (<1.0 ng/L) (**Figure 3.11b**) and the high DHg percentage (mostly above 80%) in the water samples also verified the important role of the dissolved Hg in this study (**Figure 3.11d**). Nevertheless, although the trend of DOC was similar to that of dissolved Hg there were no significant linear regressions between DOC and dissolved Hg at all sites ($p>0.05$), which could likely be because of the narrow DOC concentrations range. Notably, compared to the increased DOC after burning, we did not observe the significant changes in THg levels after the burnings in general (**Figure 3.11a**).

The streamwater and groundwater before any pile burning showed low Hg levels (**Figure 3.11a**), mainly dissolved Hg (**Figure 3.11c -d**). Pile burnings seemed to slightly affect TSS or DOC but not THg export significantly in the present study. For instance,

the pile burning events at unit #282 and unit #91 on 6/16/2018 were conducted at a location upstream of S2, thus the burning could potentially affect the downstream sites S2-S4. The streamwater samples after the burning (collected on 6/21/2018) showed higher TSS at the sites S2, S3, S4 than the site S1, but DOC and THg levels did not show differences in the streamwater collected from the four sites (**Figure 3.10b, 3.10c, 3.11a**). Pile burning at unit #100 (next to S3) on 7/16/2018 led the TSS in streamwater from downstream S4 slightly higher but no difference in DOC or THg either. Pile burnings in unit #98, #99 and #61 in August and September 2018 (*see* map in **Figure 3.2**) did not cause THg level change in the streamwater collected in September or October 2018, although the DOC levels increased in these samples. Streamwater in May and June 2019 showed higher THg concentrations in streamwater after the pile burning in unit #76 in late April 2019 (**Figure 9a**). The increase in THg concentrations could be because of the higher THg levels in streamwater along with the higher DOC concentrations in streamwater (**Figure 3.10c and 3.11c, 3.11d**). In this study, our results were consistent with Hg trend in Sagehen Creek from the work of Faïn *et al.* (2011), which showed higher Hg in April and lower in winter (December/January) and the Hg levels range of 0.5-2 ng/L (Faïn *et al.* 2011). We did not observe a significant change in Hg levels in groundwater and streamwater after prescribed burning compared to the pre-burn samples (0.16-1.94 ng/L) in 2018. Therefore, compared to the pre-burn data in their study and There is not sufficient evidence in the present study to differentiate between the wildfire effects and seasonal change in Hg levels.

Compared to the wildfire burned watersheds, there was much less TSS and THg input after the prescribed burning in the present study. For example, doubled streamwater total Hg fluxes were observed in wildfire burned watersheds located in Virginia in a previous study (Jensen *et al.* 2017). The Hg levels ranged from 3.8 to 16 ng/g in upland ash samples and from 2.8 to 55.6 ng/g in burned soils collected from Sagehen Experimental Forest, comparable to the Hg levels in the Wragg Fire watershed mentioned in section 3.3.2. However, the Hg export after the burning was much lower than the Wragg Fire watershed. The high amount of snowmelt leading to high discharge at Sagehen Creek (**Figure 3.10a**) which could be one diluting factor for the Hg export to the downstream aquatic environment.

Although the geological condition and hydrological condition in this Sierra watershed is different from Wragg Fire watershed so we are not able to have a direct comparison, it is still obvious that the pile burning in Sagehen Creek did not cause a significant change in TSS and Hg levels in streamwater by comparing the post-burn data in upstream and downstream. This indicated that prescribed burning could cause less disturbance in TSS and Hg input to watersheds than that burned by wildfires, and the main Hg species transport to the downstream is DHg instead of PHg.

3.3.3 Impacts of Prescribed Fire (Broadcast Burning) on Hg Export

3.3.3.1 Hg Transport by Runoff

In this part, the discussion will focus on the impacts of another type of prescribed fire-broadcast burning on Hg export in Santee Experimental Forest (SEF) watersheds, South Carolina. Compared to pile burning, the broadcast burning burned larger areas and

is not constricted to one specific area. Therefore, broadcast burning could generate more widespread organic matter and affect the forest floor more intensively. The burning at SEF was recently conducted at WS77 in March 2018, and the short-term hydrological Hg export was evaluated in the burned watershed WS77, controlled watershed WS80, and the 2nd order watershed WS79 as indicated in the map of **Figure 3.3**.

Stream discharges at WS80, WS77, and WS79 were indicated in **Figure 3.12**, and the data shown has been normalized by the watershed area for comparison. The discharges at WS80 and WS79 were similar in values and trends (**Figure 3.12a, 3.12c**) but the discharge at WS77 (**Figure 3.12b**) was much higher than WS80 and WS79. Although WS77 and WS80 are paired watersheds with similar vegetation type, similar size, similar soil type, the discharge at WS77 was mostly higher than WS80 (**Figure 3.12d**). The higher discharge at WS77 could lead to higher Hg, TSS or DOC yield than WS80 when the levels in streamwater were similar. Previous studies have shown that the water table at WS77 was deeper than WS80, which could be the reason for the higher discharge at WS77 (Amatya *et al.* 2019).

Forest fires could interfere the physical and chemical properties on the forest floor thus affect the hydrological process of contaminants as previously mentioned. The TSS levels in streamwater from the burned site WS77 after the burning showed significantly higher than the controlled watershed WS80 ($p < 0.05$), especially within the first 1.5 years (from March 2018 to July 2019) (**Figure 3.13**), suggesting the burning likely increased the erosion runoff from the burned forest floor. This burning effect was still obvious in the 2nd order watershed WS79, showing significantly higher TSS than WS80 ($p < 0.05$)

(**Figure 3.13a**). Post-fire TSS export in the first year exhibited a more significant difference between the sites (WS77 vs WS80: $p < 0.05$; WS79 vs WS80: $p < 0.05$) while the difference was not observed in the second year ($p > 0.05$) (Figure 3.14a). However, whether the higher TSS at WS77 was caused by prescribed burn was inconclusive because previous studies found more runoff from the WS77 than WS80 on the same soils before the burning event in 2018 (Jayakaran *et al.* 2014; Amatya *et al.* 2019). Even if it is due to the burning that leads to higher TSS, the elevation in TSS levels was not very high, ranging from -17.9 to 32.7 mg/L when subtracting WS80-TSS from WS77-TSS.

Unfiltered total Hg (indicated as THg below) generally showed the similar trends with TSS, especially in the first year following the prescribed fire (**Figure 3.13b**), although compared to TSS, lower variations of THg in each watershed was observed. There was one sample collected 2 weeks after the burning (3/24/2018) showing extremely high THg (184 ng/L) than all other samples (not shown in the figure), in which we observed ash/soil particles. The TSS level of this sample was 32.8 mg/L, not as high as expected based on the THg level. Therefore, the high THg in this sample could be because of the Hg carried on the lower density in the ash/soil particles (more likely soil particles). The THg levels in ash samples collected at WS77 ranged from 2.7 to 4.3 ng/g in black ash (n=4) and 3.1-7.1 ng/g in white ash (n=3), while THg in the burned soil under black ash ranged from 80.1 ng/g to 127.5 ng/g (n=3). There was barely white ash found after the burning at WS77, so we were not able to collect burned soil under white ash. To avoid messing up the whole statistical analysis, we excluded this outlier for the Hg analyses and discussion below. The THg levels at the three watersheds showed

similar levels in general, with THg in WS80 streamwater ranging from 2.7 to 18.9 ng/L, THg in WS77 streamwater ranging from 2.5 to 13.8 ng/L (excluding that extremely high THg sample), and THg in WS79 streamwater ranging from 2.6 to 18.2 ng/L. There was no significant difference in THg between the three watersheds both before the burning and after the burning ($p>0.05$), either in the 1st year or 2nd year following the prescribed fire, indicating the prescribed burning at WS77 in March 2018 did not cause significant effects on Hg levels in the downstream water. Similarly, MeHg levels in the three watersheds showed narrow range (0-1.0 ng/L), although the MeHg levels in the samples within half-year following the burning (March to October 2018) at WS77 showed higher MeHg than WS80 then went back to similar or lower levels. This indicated that the prescribed burning could increase the direct MeHg in the short term, potentially due to erosion or carbon input.

3.3.3.2 DHg Transport along with DOC

As shown in **Figure 3.14a**, pre-burn DOC in streamwater was similar among the three watersheds ($p>0.05$). However, post-burn DOC at WS77 was significantly lower than that at WS80 ($p=0.005$) and the further downstream WS79 was lower than WS80 ($p=0.028$) (**Figure S3.1**). $SUVA_{254}$ in streamwater before showed no difference among the three watersheds ($p>0.05$), indicating DOC aromaticity in streamwater was similar among the three watersheds. However, post-burn $SUVA_{254}$ was significantly higher at WS77 than WS80 ($p>0.05$), while no significant increase was observed at WS79, indicating the burning increased DOM aromaticity in the watershed. The increased $SUVA_{254}$ value could be because of the leaching from the complete burned ash (white ash),

as indicated in some previous laboratory studies (Wang *et al.* 2015). However, SUVA₂₅₄ value in runoff or streamwater is not always affected by the fire which could be because of the different hydrological processes (i.e. very high discharge diluting the effects) at the burned site (Writer *et al.* 2014). There was no relationship between SUVA₂₅₄ and DHg in all three watersheds ($p>0.05$). DHg and DMeHg levels in streamwater were variable but along with DOC in all the three watersheds (**Figure 3.14**). Although there were no significant differences in DHg among the three watersheds before and after the burning, the median DHg levels at WS77 was higher than WS80 before the burning but lower than WS80 after the burning, mainly due to the more substantial variability of DHg and DOC at WS80 (**Figure 3.14b, 3.14e, Figure S3.1**).

3.3.3.3 Mercury Transport Pattern in the Prescribed Fire-burned Watershed

The THg levels were significant correlated with TSS at both WS80 and WS77 (**Figure 3.15a**), with THg/TSS 229 ng/g at WS80 ($p<0.013$) and 153 ng/g at WS77 ($p<0.001$). The significant differences in THg/TSS ratios between the two 1st order watersheds were mainly because of the DHg part but less because of PHg part since PHg/TSS ratios at WS77 and WS80 were similar (98.5 ng/g at WS77 and 84.4 ng/g at WS80) (**Figure 3.15b**). Compared with the wildfire-burned watersheds, the streamwater in all the three watersheds showed a high proportion of DHg, instead of PHg, indicating DOC is an important driver in Hg transport in the prescribed fire burned watersheds. Although DHg and DMeHg were significantly correlated with DOC at all the three watersheds ($p<0.05$) (**Figure 3.15c and 3.15d**), calculated DHg/DOC ratios showed highest at WS80 (235 ng DHg/g DOC) followed by WS79 (198 ng DHg/g DOC) and

WS77 (99.4 ng DHg/g DOC), indicating DOC at WS80 was more prone to DHg. Interestingly, DMeHg/DOC ratios showed the opposite trends, with WS77 DOC binding highest MeHg (25.8 ng DMeHg/g DOC) and WS80 DOC binding lowest MeHg (10.4 ng DMeHg/g DOC). Therefore, almost 26% of the DHg binding to DOC at the burned WS77 was MeHg, which is a large proportion compared to the 4.4% at WS80. The high percentage of MeHg binding to DOC could be because of the higher aromatic DOC content (indicated as higher $SUVA_{254}$) at WS77 after the burning. Thus, although the THg input did not increase significantly after the burning, DOC at the burned site (WS77) was more sufficient in carrying the more bioavailable MeHg compared to the reference site (WS80), which could be an ecological risk of the prescribed fire to the aquatic food web in a long-term time scale.

After evaluating the contribution of surface runoff to the Hg in streamwater, further investigations have been conducted to understand the contributions of Hg in groundwater to the Hg in streamwater. We found DHg in groundwater collected in the upland wells at each 1st order watershed showed much lower levels than DHg in streamwater as shown in **Table 3.2**. The sample collected in March 2019 showed that DHg in streamwater was 5.14 ng/L, while the groundwater DHg levels ranged from 0.62 ng/L to 4.92 ng/L. The DHg concentrations were significantly correlated with DOC, while the DOC in the groundwater were lower than streamwater. The $SUVA_{254}$ value in groundwater samples were consistently lower than the streamwater samples. The much lower DOC, $SUVA_{254}$ and THg values in groundwater than those in streamwater

indicated the Hg in the groundwater is less likely to be the main source to the streamwater.

3.3.4 Comparison of the Impacts by Wildfires and Prescribed Fires on Hg Export

According to the three controlled-field studies above, it seems that prescribed fires, regardless of pile burning and broadcast burning, induced less Hg export to the downstream, mainly due to less TSS. In wildfire-burned watersheds, particulate Hg contents are the main contents within the THg transport to the downstream water bodies after wildfires. However, prescribed fires introduced Hg were mainly DHg instead of PHg in both pile burning and broadcast burning. More obviously, pile burning in the present study did not increase THg transport significantly, which showed very low PHg and TSS, and the THg levels seemed in accordance with seasonal change and little impacts from the burning event. This could be because of the limited area affected by the burning. In this part, we will focus on the discussion of the relatively more similar broadcast burning and wildfire.

As shown in **Figure 3.16**, the TSS daily yield in the wildfire-impacted watershed (here only shows the more typical Wragg Fire watershed) were very high in the first year following the wildfire (up to $27602 \text{ kg}/(\text{d}\cdot\text{km}^2)$) then decreased in the 2nd year following the wildfire. Daily yields of THg in the Wragg Fire watershed were much lower and similar to the reference watershed in the 2nd year than the 1st year, showing the rapid recovery of THg transport in the 2nd year, which was mainly due to the reduction of TSS input. Wildfire-related high soil erosion rate mainly occurred during the first year after a fire, potentially because of the recovery of the vegetation cover leading to the recovered

evapotranspiration rate (Neary *et al.* 2005; Shakesby 2011). The prescribed fire burned WS77 showed higher TSS yield than WS80 after the burning but the magnitude of TSS yield was much lower than Wragg Fire watershed. The annual TSS yield was 7005 kg/(year*km²) for WS77 and 4167 kg/(year*km²). Notably, the discharge at WS77 was much higher than WS80 (up to 5 times) which could cause a higher yield at WS77. And previous studies also indicated the pre-burn TSS at WS77 was higher than WS80 as previously mentioned (Jayakaran *et al.* 2014; Amatya *et al.* 2019). Considering the factors mentioned above, we should be cautious in evaluating if the broadcast burning would increase TSS substantially.

DOC yield in the Wragg Fire watershed was lower than the reference site in the 1st year following the wildfire, indicating the DOC contributed very little in the wildfire-burned watershed in the present study or the wildfire reduced DOC input to the downstream watershed. Similarly, in the prescribed fire study at SEF, the reference watershed WS80 showed higher DOC yield in most of the days. The annual DOC yield for the 1st year following the prescribed fire was 6639 kg/(year*km²) for WS77 and 9548 kg/(year*km²). We did not have the whole year pre-burn data for calculating the DOC yield, but the September 2017 to March 2018 data indicated DOC loadings at WS77 were 3.1 times higher than WS80. This suggested the burning potentially reduced the DOC input to the downstream or because of the long-term calculation. THg yield in the Wragg Fire watershed was much higher than the reference site in the 1st year following the wildfire, especially when TSS was high, but the prescribed fire impacted watershed WS77 showed similar yield with reference watershed WS80. The annual THg yield for

the 1st year following the prescribed fire was 3217 mg/(year*km²) for WS77 and 3383 mg/(year*km²), not showing significant difference.

Therefore, according to the two controlled field studies burned with prescribed fires, including the pile burning and broadcast burning, we concluded that wildfires were more likely to introduce more Hg into the downstream water bodies than the prescribed burning (including pile burning and broadcast burning). Meanwhile, PHg was dominated in wildfire-burned watersheds, driven by TSS, and DHg was dominated in prescribed-fire watersheds, driven by DOC.

The impacts of wildfires on downstream waters vary from site to site, depending on fire severity, the proportion of watershed burned, steepness of watershed slopes, geology, and post-fire precipitation type, timing, and intensity (Neary *et al.* 2005). And the post-fire transport of Hg was affected by precipitation, infiltration, runoff, and the Hg content in the upland soils (Moody *et al.* 2013). Forest fires especially the wildfires increase the sensitivity of soils to erosive forces, potentially accelerating erosion and sediment delivery to the downstream. The post-wildfire runoff was indicated to be predominantly contributed by a saturation-excess mechanism at the ash-soil interface during the first storm event then predominantly contributed by the infiltration-excess mechanism at the ash surface during the second storm (Ebel *et al.* 2012). In the present study, the wildfire-burned watershed with a large burn proportion (Wragg Fire watershed) showed significantly high sensitivity to the storm, as shown in **Figure 3.16a**. Even a small amount of discharge mobilized a high number of suspended solids. Removal of the vegetation and breaking down topsoil by the burning exposes the relatively lower layer of

impermeable soil thus reduce infiltration rates and enhance storm runoff. Compared to the wildfires, prescribed fires burned with lower severity, causing less interference on the topsoil layer in depth and area, causing less exposure of the deeper mineral soils to the precipitation which is more vulnerable to erosion due to the lower water retention capacity. The larger amount of unburned litter and soil could filter the suspended ash particulate and solutions of DHg before they emerge into the streamflow. Besides Hg, the previous study also found less nutrients input and water quality impair in the Atlantic and Gulf Coastal Plain (Richter *et al.* 1982). Another potential reason that would interfere the conclusion is the slope in the two ecosystems. Topography of Wragg Fire watershed and Miller Canyon watershed is gently-to-steeply sloping low mountains highly dissected by the river systems that drain eastward into the Sacramento River. But Santee Experimental Forest is located in the coastal floodplain and the slope is less than 2% (Amatya *et al.* 2019).

3.4 References

- Abraham, J., Dowling, K. & Florentine, S. (2017). Risk of post-fire metal mobilization into surface water resources: A review. *Science of the Total Environment*, 599, 1740-1755.
- Abraham, J., Dowling, K. & Florentine, S. (2018). Effects of prescribed fire and post-fire rainfall on mercury mobilization and subsequent contamination assessment in a legacy mine site in Victoria, Australia. *Chemosphere*, 190, 144-153.
- Amatya, D., Chescheir, G., Williams, T., Skaggs, R. & Tian, S. (2019). Long-Term water table dynamics of forested wetlands: Drivers and their effects on wetland hydrology in the Southeastern Atlantic Coastal Plain. *Wetlands*, 1-15.
- Andreu, V., Imeson, A.C. & Rubio, J.L. (2001). Temporal changes in soil aggregates and water erosion after a wildfire in a Mediterranean pine forest. *Catena*, 44, 69-84.
- Balogh, S.J., Meyer, M.L. & Johnson, D.K. (1996). Mercury and suspended sediment loadings in the lower Minnesota River. *Environmental Science and Technology*, 31, 198-202.
- Balogh, S.J., Swain, E.B. & Nollet, Y.H. (2006). Elevated methylmercury concentrations and loadings during flooding in Minnesota rivers. *Science of the Total Environment*, 368, 138-148.
- Balogh, S.J., Swain, E.B. & Nollet, Y.H. (2008). Characteristics of mercury speciation in Minnesota rivers and streams. *Environmental Pollution*, 154, 3-11.

- Betts, E.F. & Jones, J.B. (2009). Impact of Wildfire on Stream Nutrient Chemistry and Ecosystem Metabolism in Boreal Forest Catchments of Interior Alaska. *Arctic, Antarctic, and Alpine Research*, 41, 407-417.
- Burke, M.P., Hogue, T.S., Ferreira, M., Mendez, C.B., Navarro, B., Lopez, S. *et al.* (2010). The Effect of Wildfire on Soil Mercury Concentrations in Southern California Watersheds. *Water, Air, and Soil Pollution*, 212, 369-385.
- Caldwell, C., Canavan, C. & Bloom, N. (2000). Potential effects of forest fire and storm flow on total mercury and methylmercury in sediments of an arid-lands reservoir. *Science of the Total Environment*, 260, 125-133.
- Campos, I., Vale, C., Abrantes, N., Keizer, J.J. & Pereira, P. (2015). Effects of wildfire on mercury mobilisation in eucalypt and pine forests. *Catena*, 131, 149-159.
- Cerdà, A. & Doerr, S.H. (2008). The effect of ash and needle cover on surface runoff and erosion in the immediate post-fire period. *Catena*, 74, 256-263.
- Ebel, B.A., Moody, J.A. & Martin, D.A. (2012). Hydrologic conditions controlling runoff generation immediately after wildfire. *Water Resources Research*, 48.
- Ericksen, J.A., Gustin, M.S., Schorran, D.E., Johnson, D.W., Lindberg, S.E. & Coleman, J.S. (2003). Accumulation of atmospheric mercury in forest foliage. *Atmospheric Environment*, 37, 1613-1622.
- Faïn, X., Obrist, D., Pierce, A., Barth, C., Gustin, M.S. & Boyle, D.P. (2011). Whole-watershed mercury balance at Sagehen Creek, Sierra Nevada, CA. *Geochimica et Cosmochimica Acta*, 75, 2379-2392.

- Friedli, H.R., Radke, L.F. & Lu, J.Y. (2001). Mercury in smoke from biomass fires. *Geophysical Research Letters*, 28, 3223-3226.
- Garcia, E. & Carignan, R. (1999). Impact of wildfire and clear-cutting in the boreal forest on methyl mercury in zooplankton. *Canadian Journal of Fisheries and Aquatic Sciences*, 56, 339-345.
- Grigal, D. (2002). Inputs and outputs of mercury from terrestrial watersheds: a review. *Environmental Reviews*, 10, 1-39.
- Hsu-Kim, H., Kucharzyk, K.H., Zhang, T. & Deshusses, M.A. (2013). Mechanisms regulating mercury bioavailability for methylating microorganisms in the aquatic environment: a critical review. *Environmental Science and Technology*, 47, 2441-2456.
- Jayakaran, A., Williams, T., Ssegane, H., Amatya, D., Song, B. & Trettin, C. (2014). Hurricane impacts on a pair of coastal forested watersheds: implications of selective hurricane damage to forest structure and streamflow dynamics. *Hydrology and Earth System Sciences*, 18, 1151-1164.
- Jensen, A.M., Scanlon, T.M. & Riscassi, A.L. (2017). Emerging investigator series_the effect of wildfire on streamwater mercury and organic carbon in a forested watershed. *Environmental Science Processes & Impacts*, 2017, 1505-1517.
- Kelly, E.N., Schindler, D.W., St Louis, V.L., Donald, D.B. & Vladicka, K.E. (2006). Forest fire increases mercury accumulation by fishes via food web restructuring and increased mercury inputs. *Proceedings of the National Academy of Sciences*, 103, 19380-19385.

- Ku, P., Tsui, M.T.-K., Nie, X., Chen, H., Hoang, T.C., Blum, J.D. *et al.* (2018). Origin, reactivity, and bioavailability of mercury in wildfire ash. *Environmental Science and Technology*, 52, 14149-14157.
- Louis, V.L.S., Rudd, J.W.M., Kelly, C.A., Hall, B.D., Rolffhus, K.R., Scott, K.J. *et al.* (2001). Importance of the forest canopy to fluxes of methyl mercury and total mercury to boreal ecosystems. *Environmental Science and Technology*, 35, 3089-3098.
- Moody, J.A., Shakesby, R.A., Robichaud, P.R., Cannon, S.H. & Martin, D.A. (2013). Current research issues related to post-wildfire runoff and erosion processes. *Earth-Science Reviews*, 122, 10-37.
- Neary, D.G., Ryan, K.C. & DeBano, L.F. (2005). Wildland fire in ecosystems: effects of fire on soils and water. *Gen. Tech. Rep. RMRS-GTR-42-vol. 4. Ogden, UT: US Department of Agriculture, Forest Service, Rocky Mountain Research Station.* 250 p., 42.
- Obrist, D., Johnson, D.W., Lindberg, S.E., Luo, Y., Hararuk, O., Bracho, R. *et al.* (2011). Mercury distribution across 14 U.S. Forests. Part I: spatial patterns of concentrations in biomass, litter, and soils. *Environmental Science and Technology*, 45, 3974-3981.
- Ravichandran, M. (2004). Interactions between mercury and dissolved organic matter--a review. *Chemosphere*, 55, 319-331.
- Richter, D., Ralston, C. & Harms, W. (1982). Prescribed fire: effects on water quality and forest nutrient cycling. *Science*, 215, 661-663.

- Smith, H.G., Sheridan, G.J., Lane, P.N.J., Nyman, P. & Haydon, S. (2011). Wildfire effects on water quality in forest catchments: A review with implications for water supply. *Journal of Hydrology*, 396, 170-192.
- Wang, J., Stern, M.A., King, V.M., Alpers, C.N., Quinn, N.W., Flint, A.L. *et al.* (2020). PFHydro: A New Watershed-Scale Model for Post-Fire Runoff Simulation. *Environmental Modelling & Software*, 123, 104555.
- Wang, J.J., Dahlgren, R.A. & Chow, A.T. (2015). Controlled Burning of Forest Detritus Altering Spectroscopic Characteristics and Chlorine Reactivity of Dissolved Organic Matter: Effects of Temperature and Oxygen Availability. *Environmental Science and Technology*, 49, 14019-14027.
- Westerling, A.L., Hidalgo, H.G., Cayan, D.R. & Swetnam, T.W. (2006). Warming and earlier spring increase western US forest wildfire activity. *Science*, 313, 940-943.
- Witt, E.L., Kolka, R.K., Nater, E.A. & Wickman, T.R. (2009). Forest fire effects on mercury deposition in the boreal forest. *Environmental Science and Technology*, 43, 1776-1782.
- Woerndle, G.E., Tsz-Ki Tsui, M., Sebestyen, S.D., Blum, J.D., Nie, X. & Kolka, R.K. (2018). New Insights on Ecosystem Mercury Cycling Revealed by Stable Isotopes of Mercury in Water Flowing from a Headwater Peatland Catchment. *Environmental Science and Technology*, 52, 1854-1861.
- Writer, J.H., Hohner, A., Oropeza, J., Schmidt, A., Cawley, K.M. & Rosario-Ortiz, F.L. (2014). Water treatment implications after the high Park wildfire, Colorado. *Journal-American Water Works Association*, 106, E189-E199.

3.5 Figures

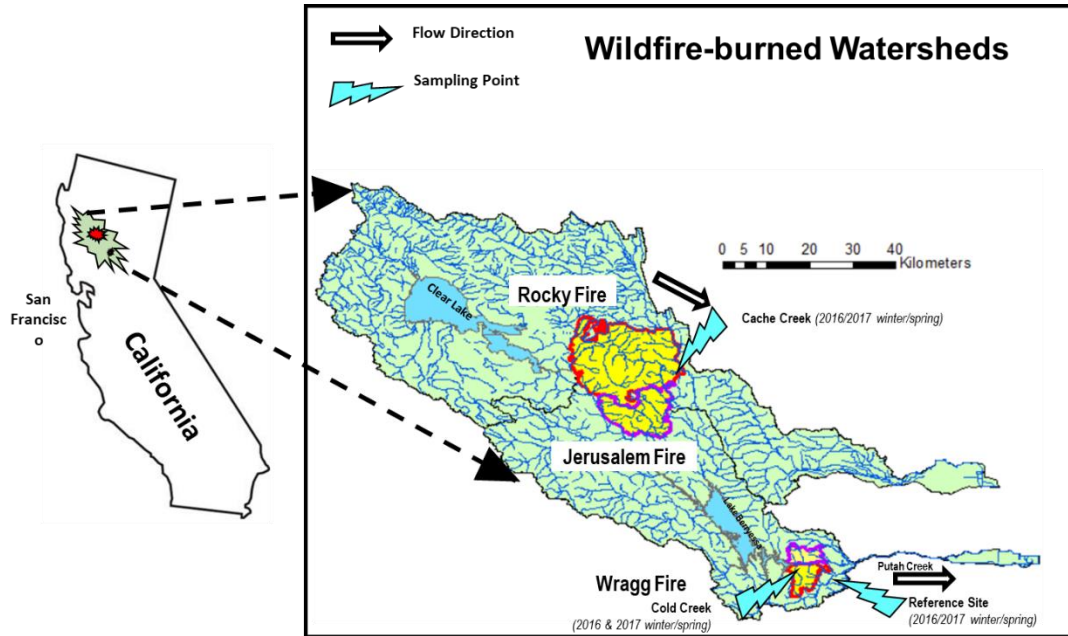


Figure 3.1. Site Map of the Wildfire-burned Watersheds. Locations were shown as in the map. the Wragg Fire within the Putah Creek drainage, Rocky and Jerusalem Fires within the Cache Creek drainage, and reference watershed. Yellow zones are the wildfire perimeters. Streamwater sampling locations are indicated by the blue arrows. Water flow directions were indicated as black arrows.

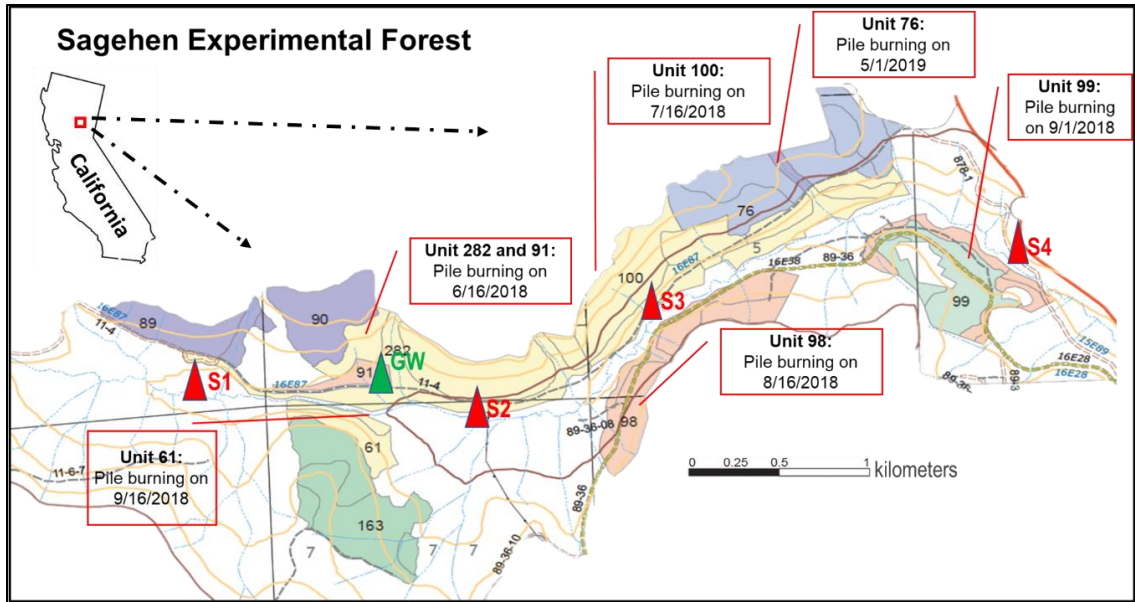


Figure 3.2. Site Map of Sagehen Experimental Forest by Pile Burning. Sagehen Experimental Forest was located in northern California as shown in the above map. Pile burning events were conducted in different units in 2018 and 2019 as indicated in the map. Sampling points were indicated as triangles in red (S1, S2, S3, S4) and green (Groudwater, GW).

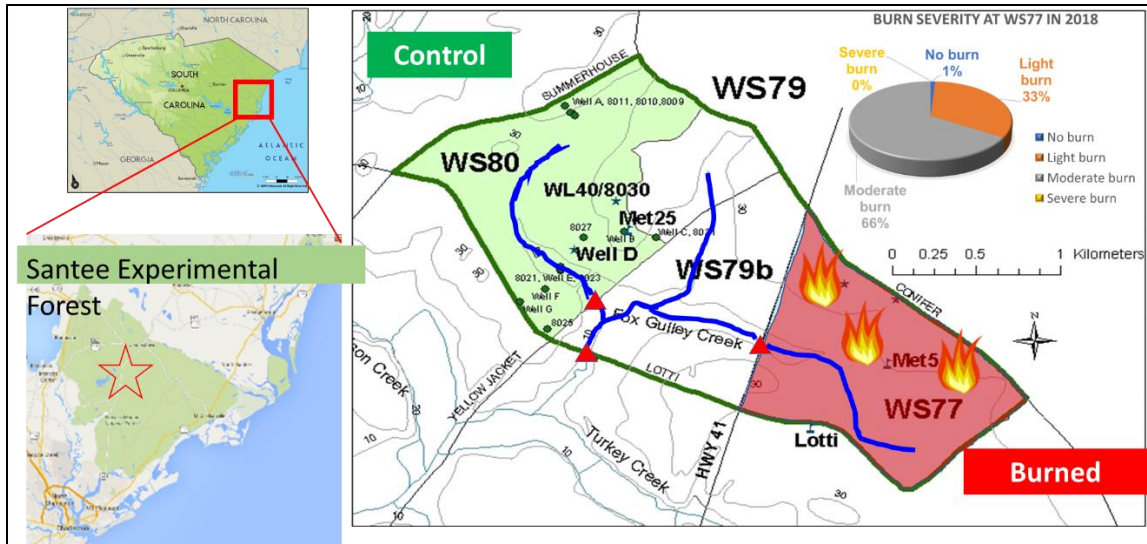


Figure 3.3. Site Map of Santee Experimental Forest by Broadcast Burning. As shown in the map, Santee Experimental Forest was located in South Carolina, southeastern U.S. WS77 (red, recently burned in 2018) and WS80 (green, controlled watershed) are the paired 1st order watersheds, WS79 is the 2nd order watershed in the downstream of WS77 and WS80. Burn severity of the broadcast burning at WS77 was shown in the map, indicating 33% was light burned and 66% was moderate burned, no severe burn.

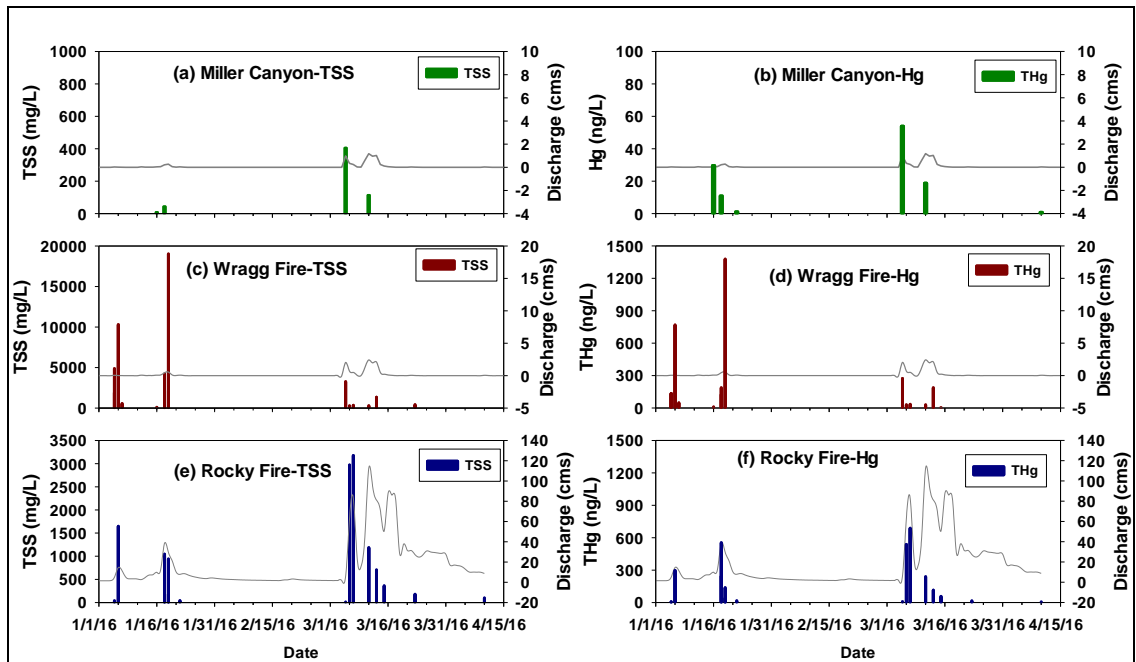


Figure 3.4. Variations of TSS and Hg in the Unburned and Burned Watersheds. The dark gray lines indicated discharges at each watershed. Green bars indicated TSS (a) and Hg (b) in the reference watershed (Miller Canyon); dark red bars indicated TSS (c) and Hg (d) in the Wragg Fire watershed; dark blue bars indicated TSS (e) and Hg (f) in the Rocky Fire watershed.

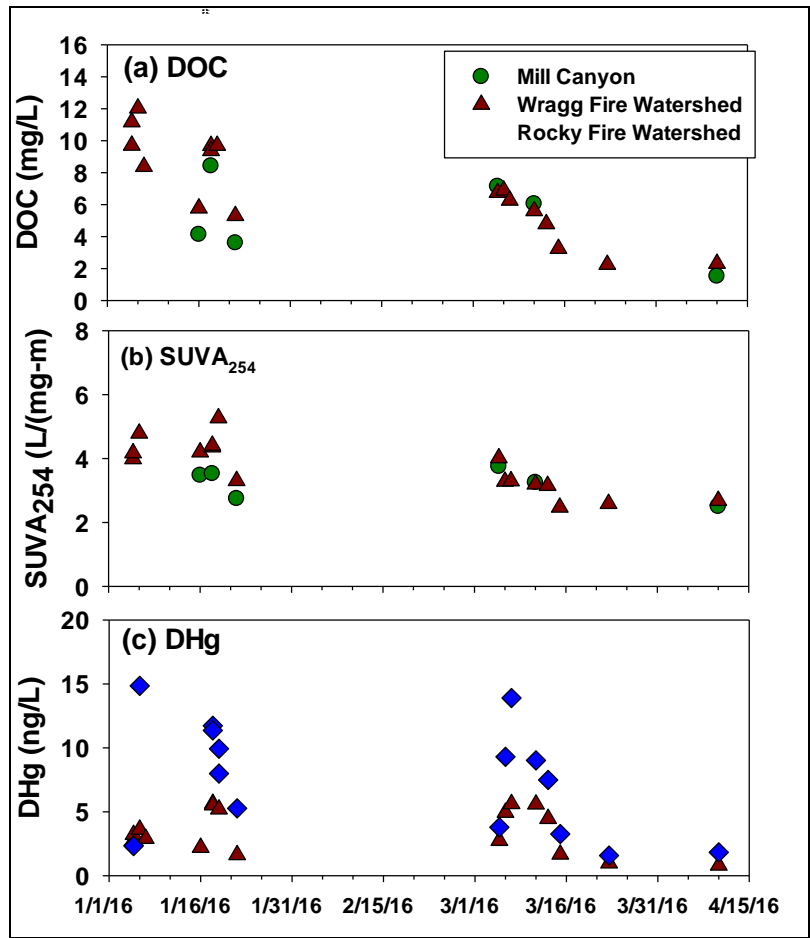


Figure 3.5. Variations of DOC, SUVA₂₅₄, and DHg in the Unburned and Burned Watersheds. DOC (a), SUVA₂₅₄ (b) and DHg (c) were shown in the unburned Mill Canyon watershed (indicated as dark green circles), Wragg Fire watershed (indicated as dark red triangles), Rocky Fire watershed (indicated as dark blue diamonds).

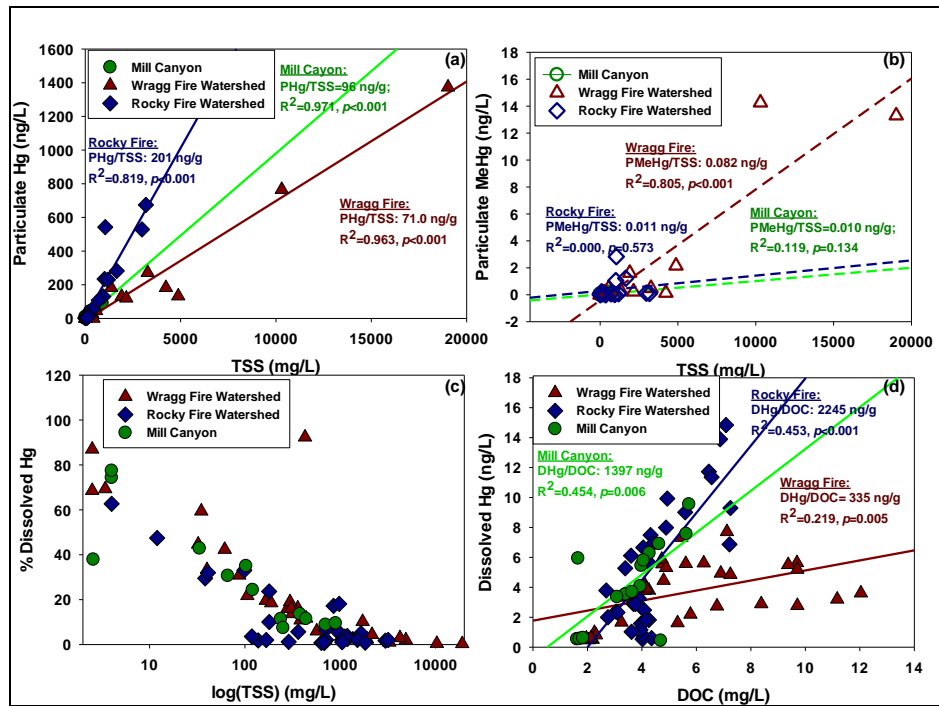


Figure 3.6 Relationship between Hg Speciation and TSS, DOC. Correlations between TSS and Particulate Hg (PHg) (a), TSS and Particulate MeHg (b), the relationship between TSS and %Dissolved Hg (c), and the correlation between DOC and dissolved Hg (d). The solid upside-down triangle represented for particulate Hg; hollow upside-down triangle represented for particulate MeHg; solid triangle represented for dissolved Hg, while green represented for Mill Canyon, dark red represented for Wragg Fire Watershed, dark blue represented for Rocky Fire Watershed.

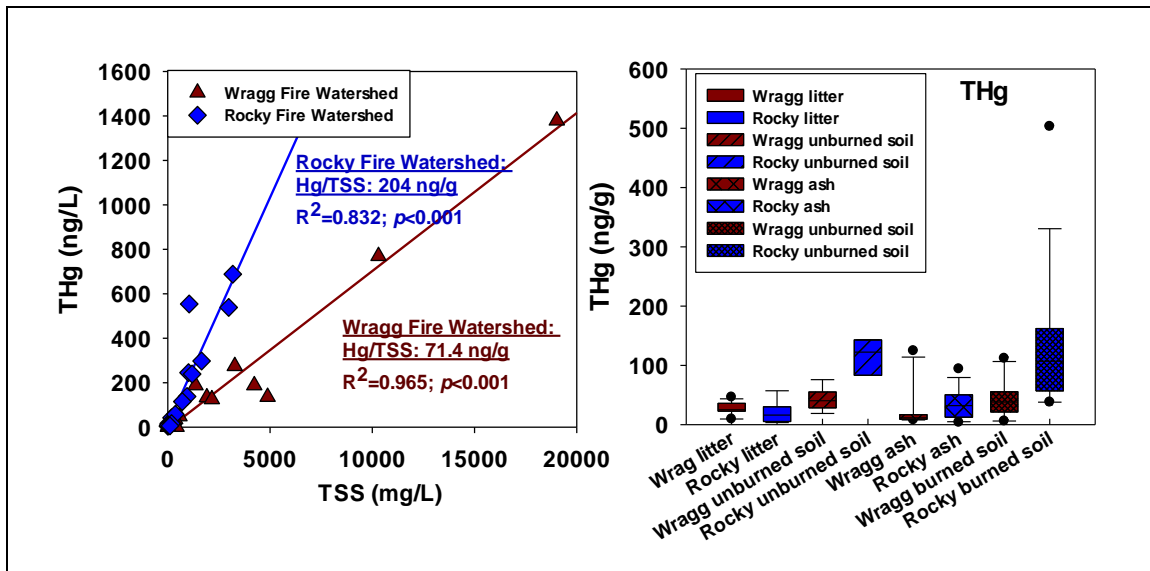


Figure 3.7. Hg Sources from Upland Materials. Relationships of TSS and unfiltered total Hg in Wragg Fire Watershed and Rocky Fire Watershed (left), and total Hg in upland burned soils in both watersheds (right). Dark red represented for Wragg Fire Watershed, dark blue represented for Rocky Fire Watershed.

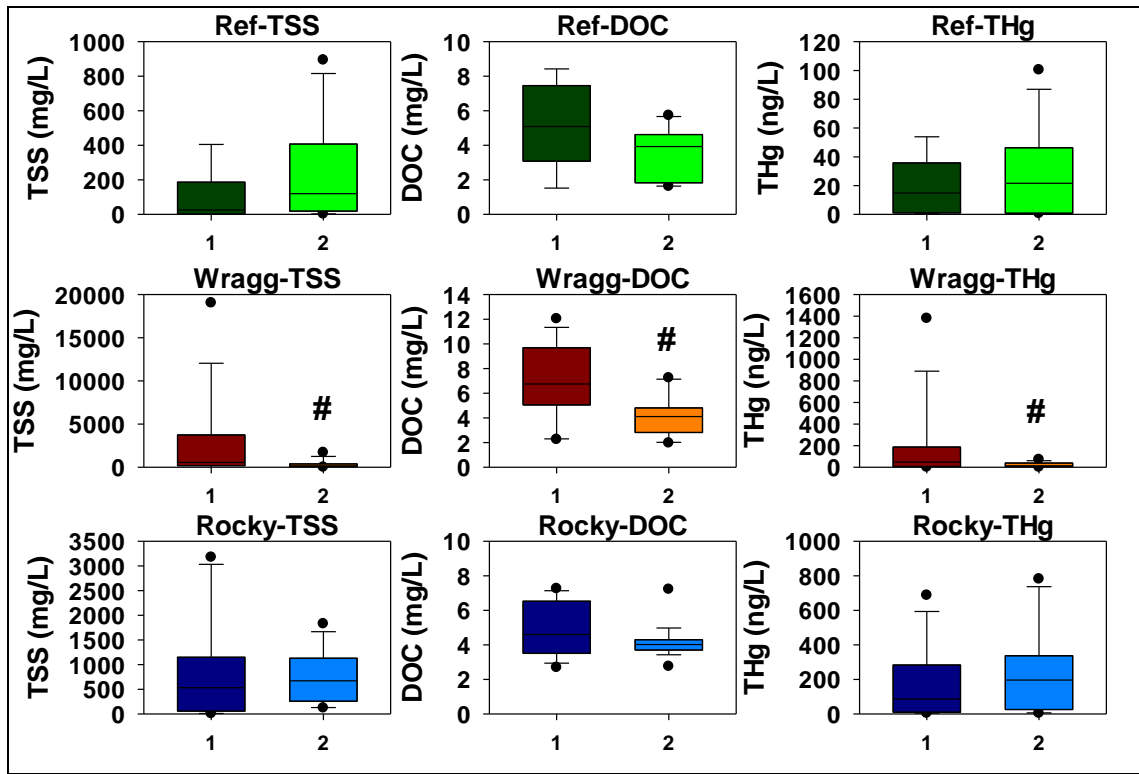


Figure 3.8. Recovery of TSS, DOC, and THg for the Two Years Following Wildfires. Comparison of TSS, DOC and THg for the two years in Mill Canyon (dark green for the 1st year, green for the 2nd year), Wragg Fire Watershed (dark red for the 1st year, orange for the 2nd year), and Rocky Fire watershed (dark blue for the 1st year, blue for 2nd year). Significant differences between Year 1 and Year 2 were indicated with pond (#).

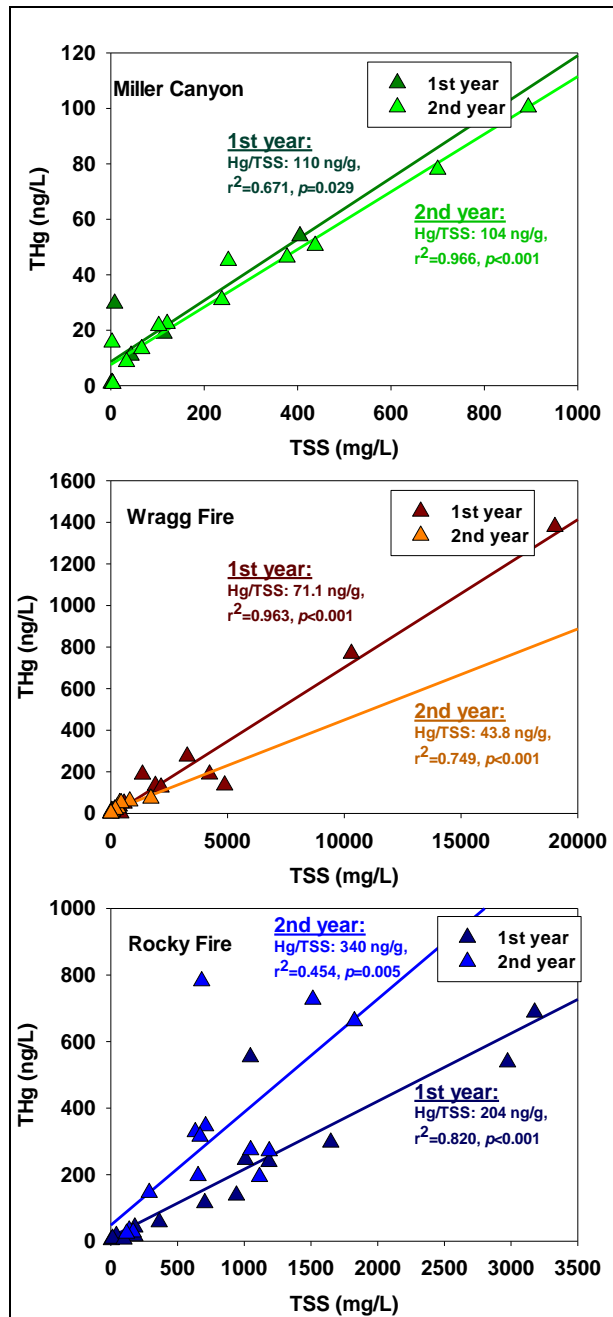


Figure 3.9. Linear Regressions between TSS and THg in the Two Years Following Wildfires. The data from 1st year and 2nd year in Mill Canyon were represented as green symbols, Wragg Fire Watershed as red symbols, Rocky Fire Watershed as blue symbols.

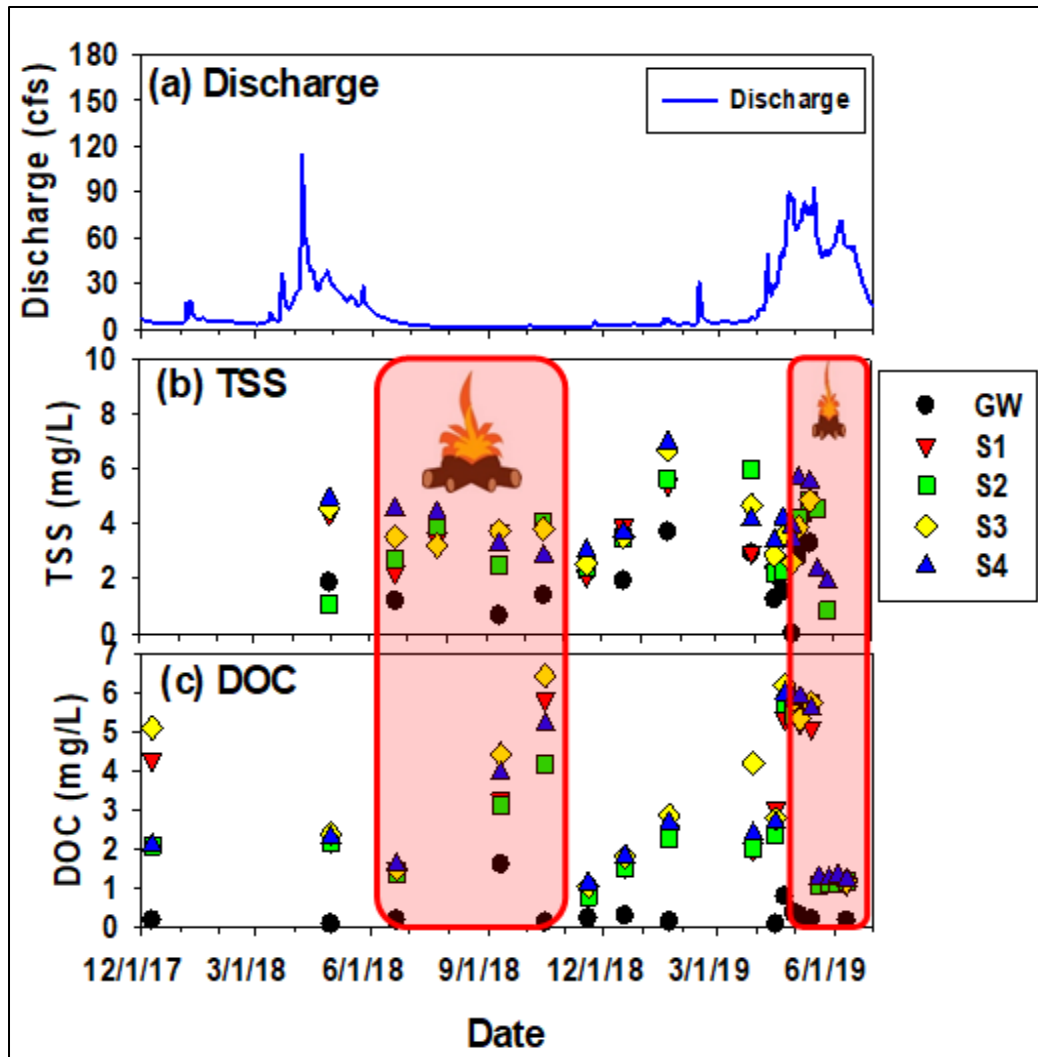


Figure 3.10. Discharge and Water Quality at Sagehen Creek. (a) Discharge, (b)TSS and (c) DOC levels at each site (GW: black circle; S1: red triangle; S2: green rectangle; S3: yellow diamond; S4: blue triangle). The red rectangles indicated the fire events periods (see map in Figure 3.2)

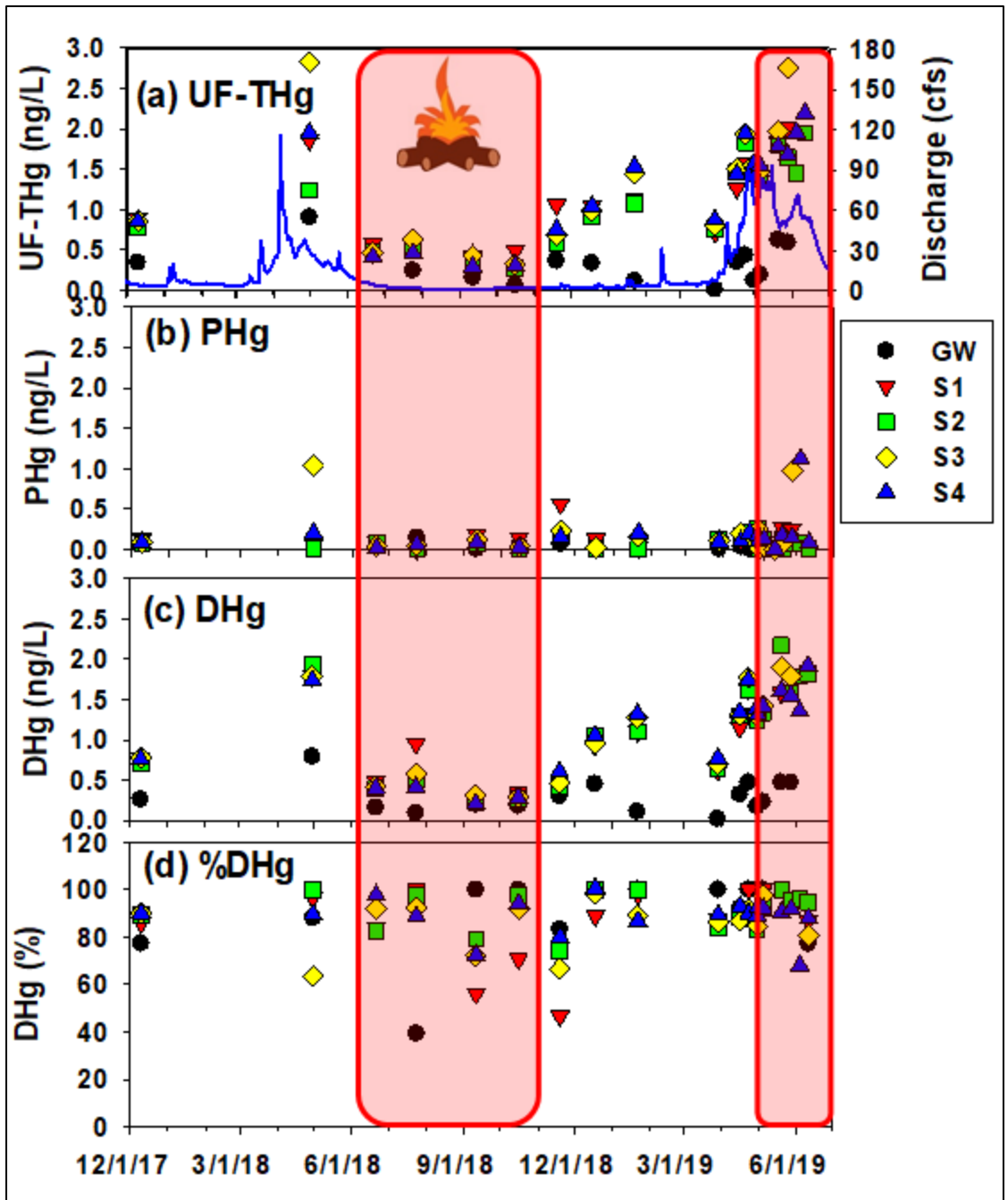


Figure 3.11. Hg Export along with Discharge at Sagehen Creek. Hg species were indicated as a) UF-THg (unfiltered THg); b) PHg (particulate Hg); c) DHg (dissolved Hg); d) %DHg (dissolved Hg percentage) (GW: black circle; S1: red triangle; S2: green rectangle; S3: yellow diamond; S4: blue triangle; discharge indicated as a blue line). The red rectangles indicated the fire events periods (*see* map in Figure 3.2)

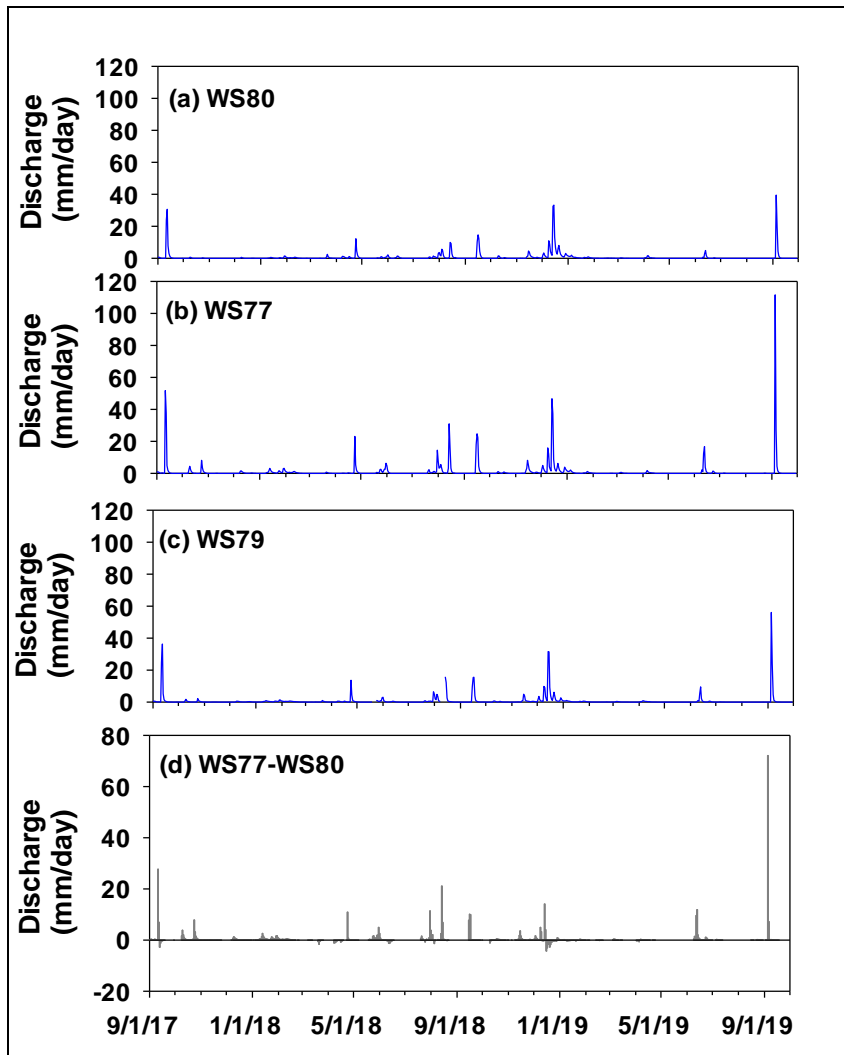


Figure 3.12. Discharge at WS80, WS77 and WS79. Discharges shown in the figure have been normalized by the watershed area (WS80: 160 ha; WS77: 155 ha; WS79: 500 ha), (a) discharge in the 1st order watershed WS80, (b) discharge in the 1st order watershed WS77, (c) discharge in 2nd order watershed WS79, (d) discharge comparison between WS77 and WS80, positive bars showing higher discharge at WS77 than WS80, negative bars showing lower discharge at WS77 than WS80, from 9/1/2017 to 9/30/2019.

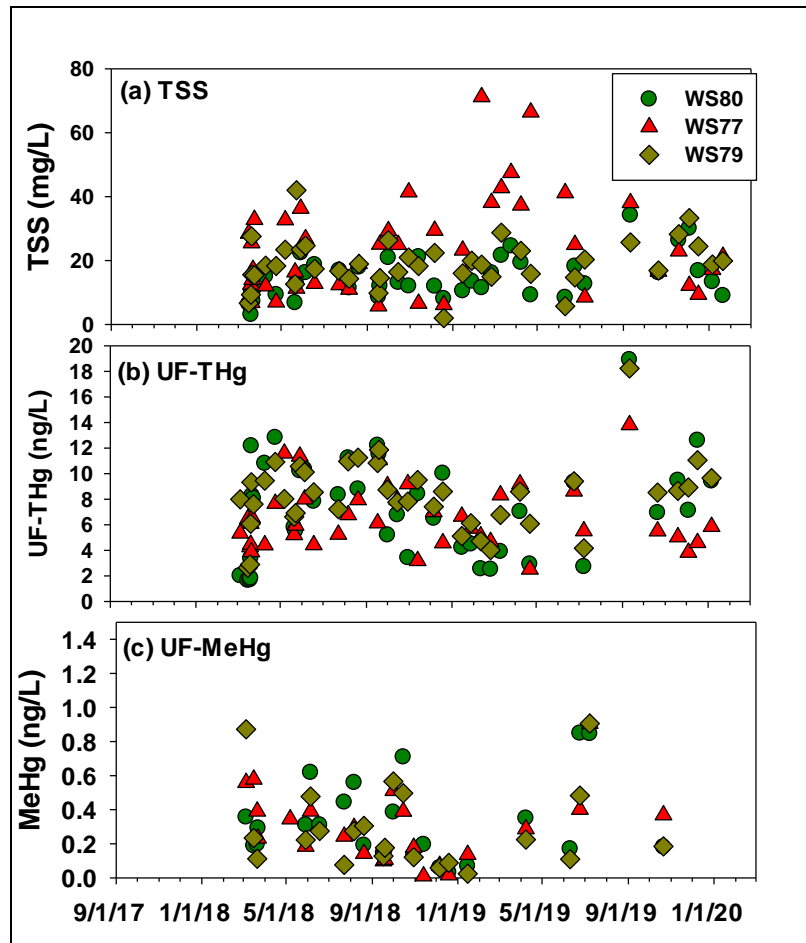


Figure 3.13. Levels of TSS, UF-THg, and UF-MeHg in Streamwater. The 1st order control watershed WS80 was represented as dark green circle symbols, the 1st order prescribed-fire-burned watershed WS77 was represented as red triangles, the 2nd order watershed WS79 was represented as dark yellow diamonds.

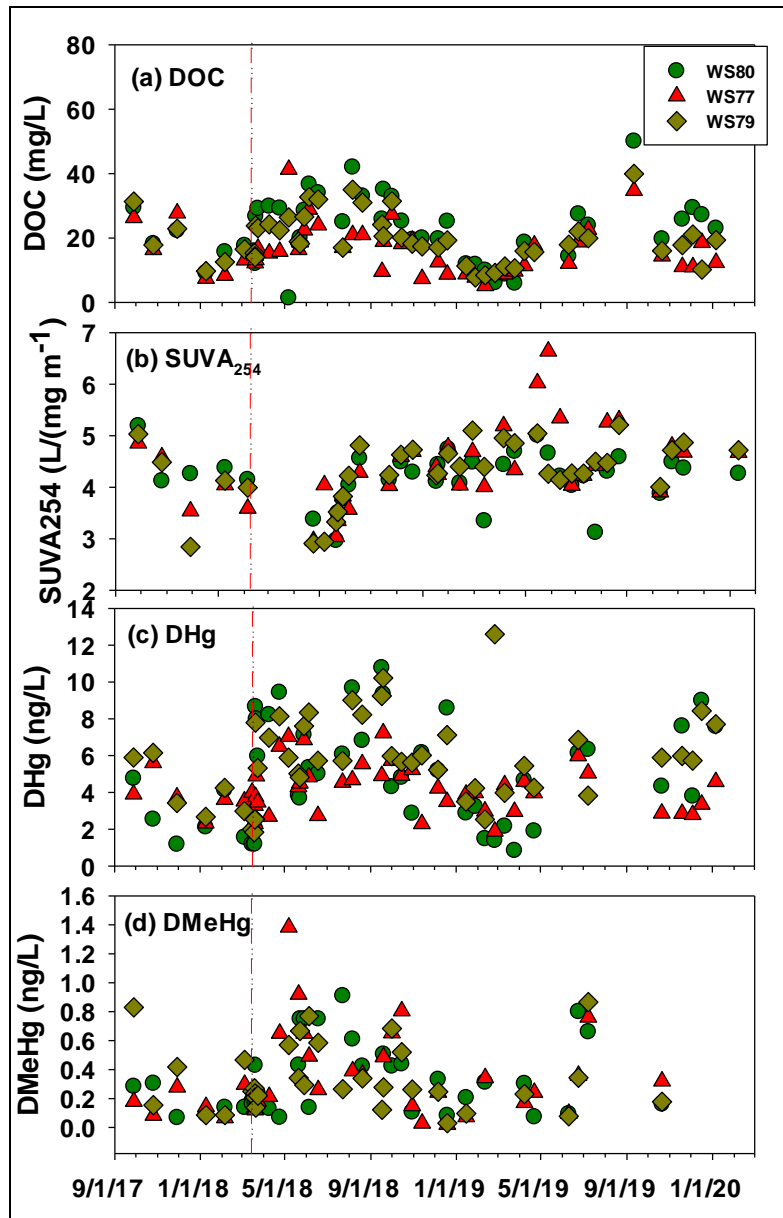


Figure 3.14. Levels of DOC, $SUVA_{254}$, DHg, and DMeHg in Streamwater. The 1st order control watershed WS80 was represented as dark green circle symbols, the 1st order prescribed-fire-burned watershed WS77 was represented as a red triangle, the 2nd order watershed WS79 was represented as a dark yellow diamond. The red dashed line indicated the burning at WS77.

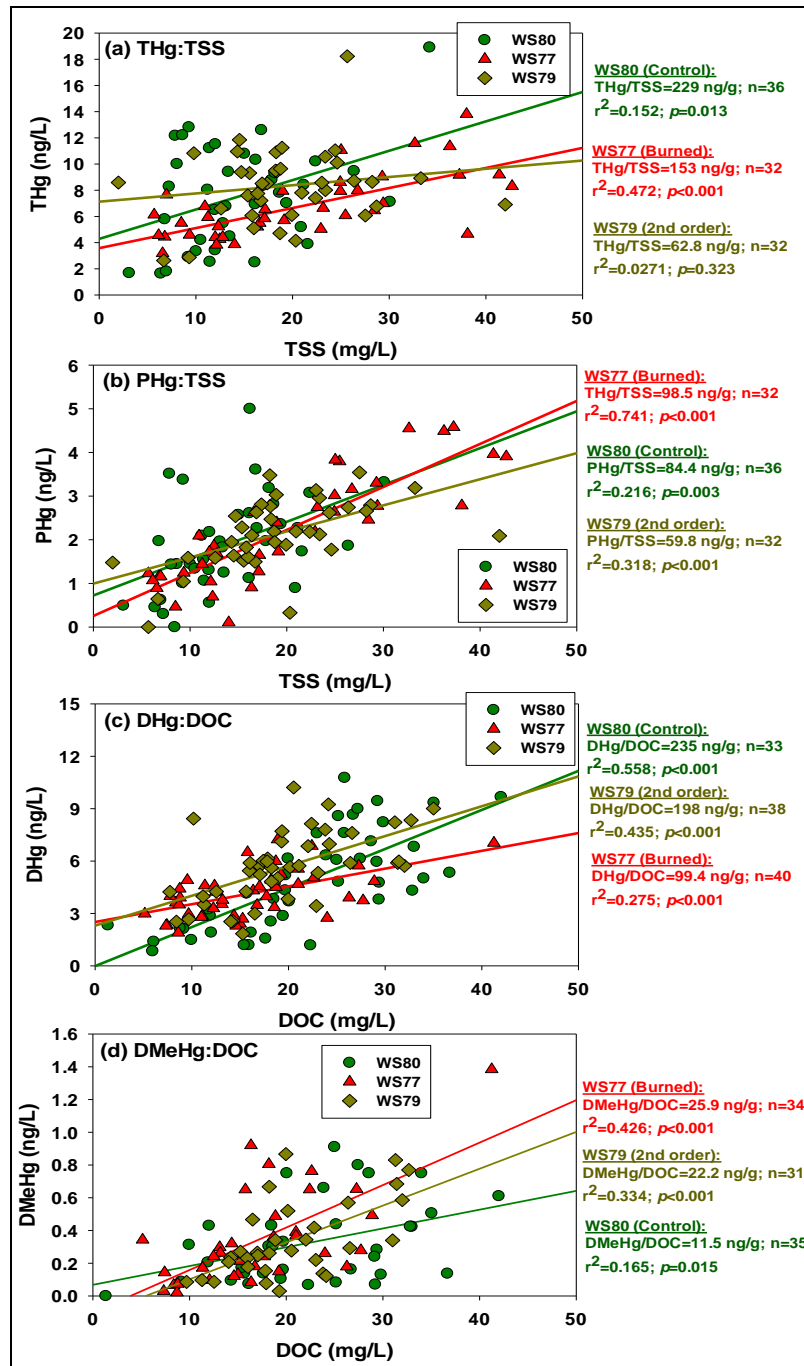


Figure 3.15. Relationships between TSS, DOC and Hg Speciation. Linear Regressions between TSS and THg (a), TSS and PHg (b), DOC and DHg (c), DOC and DMeHg (d) in streamwater at WS80 (dark green circles), WS77 (red triangles), and WS79 (dark yellow diamonds).

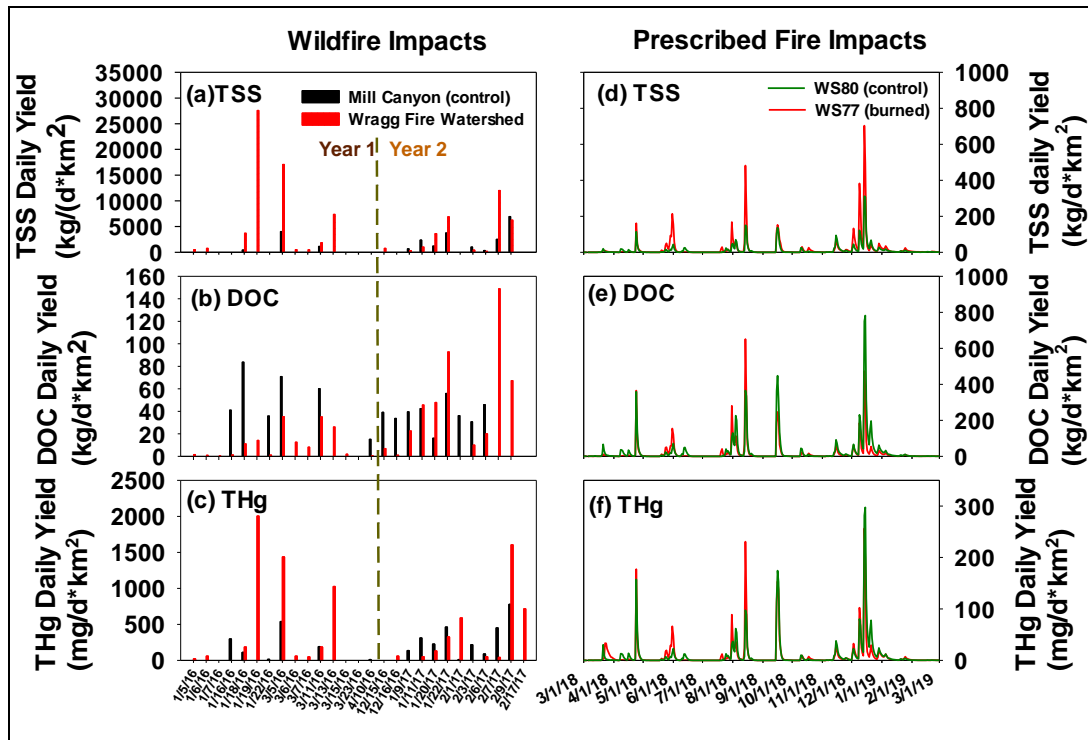


Figure 3.16. Daily Yields from Wildfire-burned and Prescribed-fire-burned Watersheds.

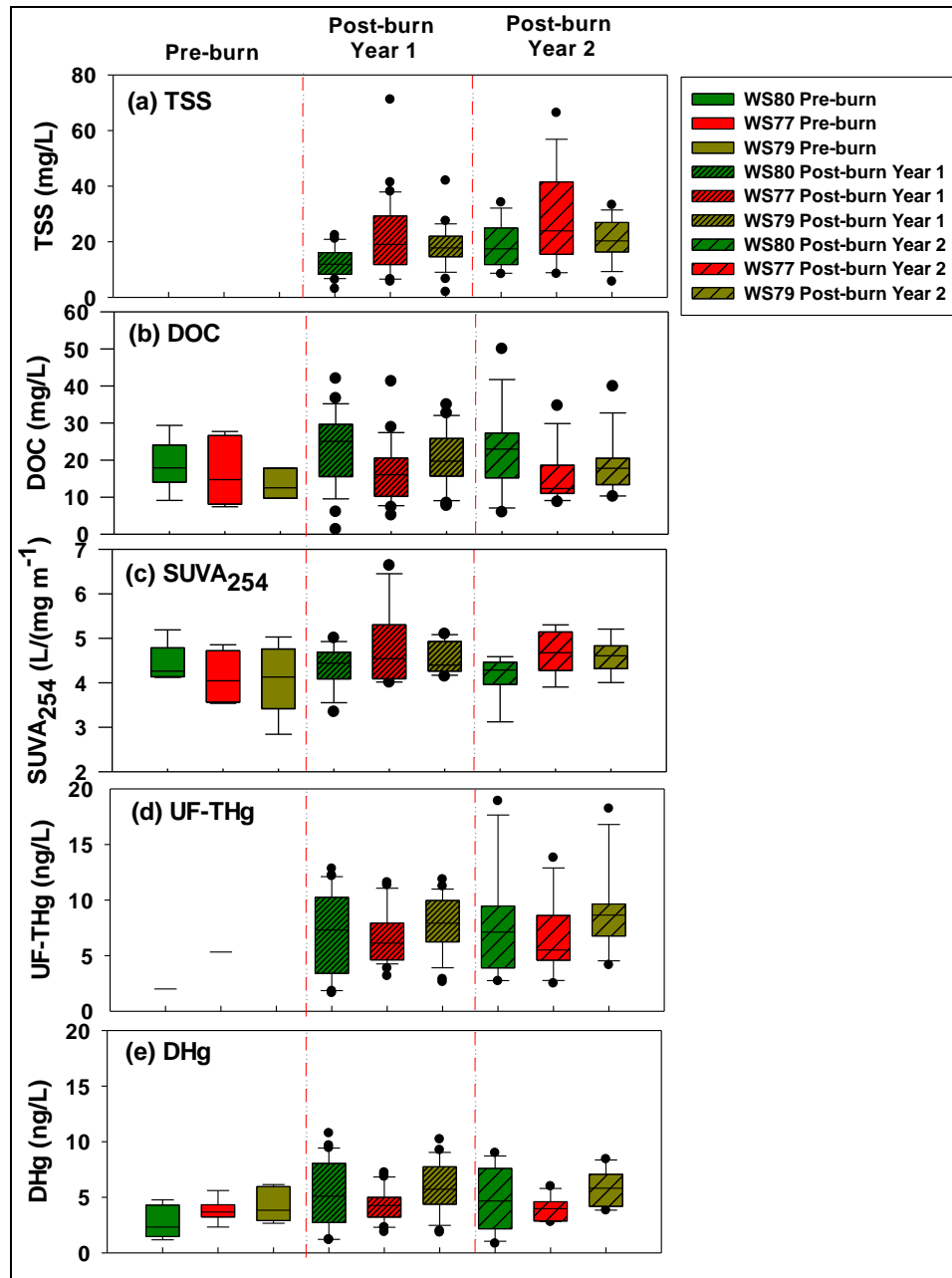


Figure S3.1. Comparisons of Pre-burn and Post-burn at WS80, WS77, and WS79. TSS (a), DOC (b), SUVA₂₅₄ (c), UF-THg (d), DHg (e) were compared pre-burn (pure bars), post-burn Year 1 (fine filled bars), post-burn Year 2 (coarse filled bars). The green bars indicated controlled watershed WS80, the red bars indicated burned watershed WS77, the dark yellow bars indicated the 2nd order watershed WS79.

3.6 Tables

Table 3.1. Reference and Wildfire-burned Watersheds Information.

Watershed	Area (acres)	2015 summer	2016 summer
Mill Canyon	2150	Not burned	Not burned
Wragg Fire Watershed	4448	>90% burned	Not burned
Rocky Fire Watershed	832,000	~15% burned	<1% burned

Table 3.2. Groundwater and Surface Water at WS80 and WS77. DOC, SUVA₂₅₄ and THg in streamwater and groundwater at different dates were shown in the table.

Date	Water type	DOC (mg/L)	SUVA₂₅₄ (L/mg/m)	THg (ng/L)
3/8/2019	WS80 Streamwater	12.94 (n=1)	3.78 9 (n=1)	2.53 (n=1)
	WS80 Groudwater	NA	NA	NA
	WS77 Streamwater	10.78 (n=1)	4.22 (n=1)	5.14 (n=1)
	WS77 Groundwater	5.92 ± 1.74 (n=8)	2.75 ± 0.64 (n=8)	1.92 ± 1.30 (n=8)
5/30/2019	WS80 Streamwater	15.32 (n=1)	3.26 (n=1)	0.90 (n=1)
	WS80 Groudwater	2.41 (n=1)	2.40 (n=1)	0.35 (n=1)
	WS77 Streamwater	20.25 (n=1)	NA	5.24 (n=1)
	WS77 Groundwater	5.50 ± 2.42 (n=4)	2.78	2.50 ± 1.58 (n=4)

Table S3.1. Analytical Methods and Minimum Reporting Levels. a: as reported by the manufacturer. b: reagent grade potassium hydrogen phthalate was used to prepare external standards. Precision ranged from 0.05 to 0.15 mg/L. c: standard methods. d: measured at wavelengths of 254 nm using a 1 cm cell. e: Accuracy (pH units).

Parameter	Unit	Measurement Method	Equipment	Minimum Reporting Level or Accuracy ^a
Dissolved Organic Carbon (DOC) ^b	(mg/L)	SM ^c 5310B	TOC-V _{CHS} , Shimadzu Corp.	0.1
Total Dissolved Nitrogen (TDN)	(mg-N/L)	High Temp. Combustion	Shimadzu TOC-V _{CHS} & TNM-1,	0.1
UV Absorbance ^d		SM 5910	Varian Carry 50	0.004
pH		SM 4500-H ⁺	VWR Symphony	0.01 ^e
Total mercury (total Hg)	(ng/L)	USEPA Method 1631	Brooks Rand CVAFS	0.1
Methylmercury (MeHg)	(ng/L)	USEPA Method 1630	Brooks Rand GC-CVAFS	0.02

CHAPTER IV

GENERAL DISCUSSION

Forest fires disturb Hg biogeochemical cycling in both terrestrial and aquatic ecosystem, however, the information regarding Hg reactivity, bioavailability and transport in the watersheds are less understood. This dissertation work elaborated the post-fire Hg biogeochemical cycling in the critical ash layer, including the origins, concentration, reactivity, and bioavailability of Hg in residual ash materials, as well as the hydrological transport in post-fire landscapes, as illustrated in the conceptual model in Figure 4.1.

In the post-wildfire landscape, all the ash samples have been documented to contain measurable, but highly variable, Hg levels ranging from 4 to 125 ng/g dry wt., after examining Hg levels and reactivity in black ash (BA - low burn intensity) and white ash (WA - high burn intensity) generated from two recent northern California wildfires. Stable Hg isotopic compositions measured in select ash samples suggest that most Hg in wildfire ash is more likely to be derived from vegetation, not from atmospheric deposition. Importantly, this study demonstrated that ash samples had a highly variable fraction of Hg in recalcitrant forms (0-75 %), and this recalcitrant Hg pool appears to be associated with the black carbon fraction in ash. This is the first time to address the association between black carbon and Hg reactivity, and hopefully this mechanism

would be helpful to better understand the post-fire ecological risks provide information for the remediation of Hg-contamination.

Regarding the ecological risk of wildfire ash to the aquatic ecosystem, both BA and WA have been found to strongly sequester aqueous inorganic Hg under controlled conditions. During anoxic ash incubation with natural surface water, we find that Hg in most ash samples had a minimal release and low methylation potential. Thus, the formation of wildfire ash can sequester Hg into relatively non-bioavailable forms, attenuating the potentially adverse effects of Hg erosion and transport to aquatic environments along with eroded wildfire ash. Considering the post-fire Hg transport in the wildfire burned watersheds, we found the Hg transport was highly associated with TSS. The input was extremely high in the “first flush” due to the extensive erosion (high TSS), and then decreased with the following seasons. However, this substantial Hg input was rapidly recovered in the second year after the wildfire, which could be due to the vegetation recovery (Neary *et al.* 2005; Shakesby 2011).

As efficient and commonly used forest management practices, prescribed fires lead to less ecological risk and public health risk than wildfires regarding Hg, mainly due to less suspended sediment yield. The post-fire sediment yields would be enhanced due to the loss of the surface cover on soil (Larsen *et al.* 2009) , therefore, the less severe prescribed fire could potentially lead to less post-fire sediment yields regardless of other factors.

Therefore, prescribed fires is not a big concern regarding Hg input to the aquatic ecosystems according to this dissertation work. On one hand, prescribed fires (both pile

burning and broadcast burning) caused less Hg export than wildfires, compared to wildfire, mainly due to relatively less TSS input, which could be because of smaller interference on the forest floor and less overflow runoff such as less burned area compared to the watershed drainage area, less removal of vegetation cover leading to relatively less rainfall received in the prescribed fire site than wildfire site. Less ash generation and thinner ash layer by prescribed fire would lead to less reduction in water repellency and infiltration rate and further impact the runoff generation immediately following the fire (Ebel *et al.* 2012). On the other hand, compared to wildfire, prescribed fire would be more likely to generate less amount of ash but larger proportions of black ash than the white ash, in which black ash showed higher black carbon content and pose a higher probability to adsorb Hg and inhibit MeHg production in the downstream environment. Therefore, MeHg production could be likely to be inhibited after the ash (especially black ash) input to the downstream environment.

Another major difference in Hg transport between the wildfire-burned watershed and prescribed fire-burned watershed was the Hg speciation, in which PHg was dominated in wildfire-burned watersheds and DHg was dominated in prescribed fire-burned watershed (either by pile burning or by broadcast burning). The difference of Hg speciation input into the water environment would further affect the Hg transformation pathway in the water or the sediment in the downstream environment. PHg carried on TSS would be more likely to be deposited and added to the sediment exposing to the anoxic environment in the sediment which is in favor to the Hg methylation bacteria (i.e. sulfate-reducing bacteria, iron-reducing bacteria, etc.). DHg carried on DOC would be

more likely to exist in the water, transporting with the water flow and expose to the light, which is involved in the MeHg photodegradation.

Notably, this dissertation work only showed the fire impacts (both wildfires and prescribed fires) in around two years following the fires. Practically, prescribed fires especially broadcast burnings were regularly conducted every 2-4 years but for decades. Therefore, attention should be paid after the long-term forest management, since we found the Hg in aquatic macroinvertebrates at the long-term managed site was higher than the unmanaged site. Mercury bioaccumulation in the food web is a more complicated process, which can be related to Hg levels, Hg bioavailability, and food web structure alteration. The impacts and mechanism of the Hg bioaccumulation in the food web at the managed site was not very clear yet. We speculated that the long-term forestry practice could lead to other alterations (i.e. food web structure) gradually that would affect Hg bioaccumulation in the aquatic food web because of the faunal biodiversity alteration in the longleaf pine woodlands (Mitchell *et al.* 2006).

Future research should also address the MeHg production in the downstream sediment, which is a hotspot for inorganic Hg transforming to organic bioaccumulative MeHg, including but not limit to the role of the microbial community in the downstream in MeHg production, which could be affected by the natural DOM input caused by the prescribed fire (Hsu-Kim *et al.* 2013). Hg bioaccumulation in aquatic food web by the forest fires especially by prescribed fires, as well as its mechanisms, should also be documented in the future.

Compared to wildfire, Hg export after prescribed burning to the downstream watersheds was much less, therefore, prescribed burning as an efficient forest management tool to control wildfire can also reduce Hg export, leading to less ecological risk regarding mercury contamination. Previous studies indicated that prescribed fire did not cause water quality problems regarding the nutrients input (Richter *et al.* 1982). Although whether or not do prescribed fires should also consider other regional factors, short-term Hg contamination in downstream aquatic ecosystems by prescribed fire should not be a concern for making the decision if it is necessary to compromise the wildfire frequencies and intensities. However, the possibility of losing control of prescribed burning could lead to big forest fires, which is a big concern to the ecological risk, human safety, and human health. Prescribed fires practice should be considered and compared with other forest management practices, such as thinning, harvesting, for the efficiency, ecological risk, and economic cost before the planning and decision.

4.1 References

- Ebel, B.A., Moody, J.A. & Martin, D.A. (2012). Hydrologic conditions controlling runoff generation immediately after wildfire. *Water Resources Research*, 48.
- Hsu-Kim, H., Kucharzyk, K.H., Zhang, T. & Deshusses, M.A. (2013). Mechanisms regulating mercury bioavailability for methylating microorganisms in the aquatic environment: a critical review. *Environmental Science and Technology*, 47, 2441-2456.
- Ku, P., Tsui, M.T.-K., Nie, X., Chen, H., Hoang, T.C., Blum, J.D. *et al.* (2018). Origin, reactivity, and bioavailability of mercury in wildfire ash. *Environmental Science and Technology*, 52, 14149-14157.
- Larsen, I.J., MacDonald, L.H., Brown, E., Rough, D., Welsh, M.J., Pietraszek, J.H., Libohova, Z., de Dios Benavides-Solorio, J. and Schaffrath, K. (2009). Causes of post-fire runoff and erosion: water repellency, cover, or soil sealing?. *Soil Science Society of America Journal*, 73(4), 1393-1407.
- Mitchell, R.J., Hiers, J.K., O'Brien, J.J., Jack, S.B. and Engstrom, R.T. (2006). Silviculture that sustains: the nexus between silviculture, frequent prescribed fire, and conservation of biodiversity in longleaf pine forests of the southeastern United States. *Canadian Journal of Forest Research*, 36(11), 2724-2736.

Neary, D.G., Ryan, K.C. & DeBano, L.F. (2005). Wildland fire in ecosystems: effects of fire on soils and water. *Gen. Tech. Rep. RMRS-GTR-42-vol. 4. Ogden, UT: US Department of Agriculture, Forest Service, Rocky Mountain Research Station.* 250 p., 42.

Richter, D., Ralston, C. & Harms, W. (1982). Prescribed fire: effects on water quality and forest nutrient cycling. *Science*, 215, 661-663.

Shakesby, R.A. (2011). Post-wildfire soil erosion in the Mediterranean: Review and future research directions. *Earth-Science Reviews*, 105, 71-100.

4.2 Figures

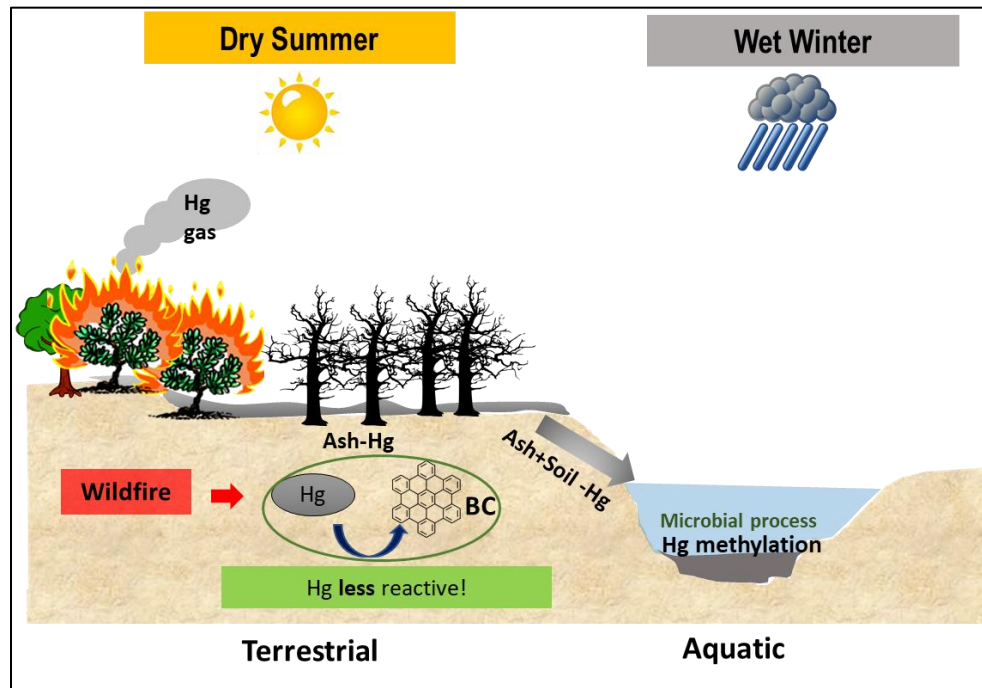


Figure 4.1. Illustration of Impacts of Forest Fires on Mercury Biogeochemical Cycling in Terrestrial and Aquatic Ecosystems. BC in the figure represents for black carbon. (modified from Ku *et al.* 2018).